

1 **Structural architecture and glacitectonic evolution of the Mud** 2 **Buttes cupola hill complex, Southern Alberta, Canada**

3
4 Emrys Phillips^{1*}, David J A Evans², Nigel Atkinson³ and Allison Kendall⁴

5 1. British Geological Survey, The Lyell Centre, Research Avenue South, Edinburgh EH14 4AP,
6 UK

7 2. Department of Geography, University of Durham, South Road, Durham, DH1 3LE, UK

8 3. Alberta Geological Survey, Twin Atria Building Suite 402, 4999 - 98 Avenue, Edmonton,
9 Alberta T6B 2X3, Canada

10 4. Department of Geoscience, University of Calgary ES118, 2500 University Drive Northwest,
11 Calgary, Alberta T2N 1N4, Canada

12 * Corresponding author: e-mail - erp@bgs.ac.uk

13 14 **Abstract**

15 This paper presents the results of a detailed multidisciplinary study of the deformed bedrock
16 and overlying Quaternary sediments exposed at the Mud Buttes in southern Alberta,
17 Canada. This large, arcuate cupola hill is composed of intensely folded and thrust
18 sandstones, siltstones and mudstones of the Cretaceous Belly River Formation.
19 Glacitectonism responsible for the development of this internally complex landform occurred
20 at the margin of the newly defined Prospect Valley lobe of the Laurentide Ice Sheet. Analysis
21 of the deformation structures reveals that construction of this landform occurred in response
22 to at least two phases of south-directed ice sheet advance separated by a period of retreat.
23 The first phase led to the formation of a forward propagating imbricate thrust stack leading to
24 polyphase deformation of the Belly River Formation. D1 thrusting led to the detachment of
25 thrust-bound slices of bedrock which were accreted to the base of the developing imbricate
26 stack. This process resulted in the structurally higher and older thrust-slices being
27 progressively “back-rotated” (tilted), accompanied by D2 thrusting and folding. Further
28 thrusting during D3 was restricted to the core of the Mud Buttes as the deforming sequence
29 accommodated further compression imposed by the advancing ice. Minor oscillations of the
30 ice margin led to localised brittle-ductile shearing (D4) of the bedrock immediately adjacent
31 to the ice contact part of the thrust stack. The second phase of ice advance led to the
32 accretion of a relatively simple thrust and folded sequence seen the northern side of Mud
33 Buttes. The resulting composite thrust moraine was subsequently overridden by ice

34 advancing from the NNW to form a dome-like cupola-hill. This readvance of the Prospect
35 Valley lobe led to the formation of thin carapace of Quaternary sediments mantling the Mud
36 Buttes which include glacitectorite, till and an organic-rich clay-silt (?palaeosol).

37

38 **Introduction**

39 Large-scale glacitectonic deformation caused as a glacier or ice sheet pushes into and
40 overrides a pre-existing sequence of sediments and/or bedrock typically involves folding and
41 thrusting. The range of structures is comparable to that observed within orogenic mountain
42 belts, only at a much smaller scale and with the resultant thrust complexes evolving over
43 significantly shorter timescales; even the largest glacitectonic moraines can develop within
44 tens to hundreds of years and even within a year at surging glacier margins. The
45 compatibility between orogenic and glacial settings has invariably led to the application of a
46 thin-skinned thrust model being applied to deformed glacial sequences, wherein
47 deformation leads to the stacking of detached, thrust-bound slices of sediment and/or
48 bedrock above a prominent basal décollement or sole thrust (e.g. Rotnicki, 1976; Dahlen *et*
49 *al.*, 1984; van der Wateren, 1985; Croot, 1987; Mulugeta and Koyi, 1987; van Gijssel, 1987;
50 Pedersen, 1987; Aber *et al.*, 1989; Harris *et al.*, 1995, 1997; Williams *et al.*, 2001; Andersen
51 *et al.*, 2005; Phillips *et al.*, 2008; Vaughan-Hirsch and Phillips, 2016; Lee *et al.*, 2013, 2016).
52 Experimental data (e.g. sand box experiments) suggest that the structural style and
53 geometric characteristics of proglacial thrusting are strongly controlled by the frictional
54 properties of the sequence beneath this surface (Davis *et al.*, 1984; Nieuwland *et al.*, 2000).
55 Consequently, several studies have suggested that the presence of low-frictional, water-rich
56 sediments within the deforming sequence may assist thrust propagation into the foreland
57 (van Gijssel, 1987; Andersen *et al.*, 2005; Phillips *et al.*, 2008; Vaughan-Hirsch and Phillips,
58 2016).

59 Glacitectonic thickening of the deforming sequence during proglacial thrusting and
60 overriding can lead to the formation of a range of landforms such as hill-hole pairs and
61 glacially overridden cupola hills, as well as a variety of moraines, from small-scale push
62 features to much larger composite ridges and thrust-block moraines, which mark the former
63 positions of ice marginal stillstands or readvances (Bluemle and Clayton, 1984; Aber *et al.*,
64 1989; Aber and Ber, 2007; van der Wateren, 2005; Evans, 2007; Benn and Evans, 2010).
65 The glacitectonised sequences within these landforms often contain a complex array of
66 cross-cutting structures (folds, faults, tectonic fabrics), which record 'multiple' or 'polyphase'
67 deformation histories. Well-documented examples include: the deformed Quaternary
68 glaciofluvial sediments within the composite ridges of the Dammer and Fürstenauer Berge

69 region of Germany (van der Wateren, 1987; 1995); folded and thrust Cretaceous chalk
70 bedrock and associated Pleistocene sediments on the Isle of Rügen, northern Germany
71 (Steinich, 1972; Gehrmann *et al.*, 2016) and at Fur Knudeklint and Møns Klint, Denmark
72 (Pedersen, 2005; 2014); imbricated and folded Quaternary sediments at St. Bees, Cumbria,
73 England (Williams *et al.*, 2001), Dinas Dinlle, northwest Wales (Harris *et al.*, 1997; Thomas
74 and Chiverrell, 2007, 2011) and the Bride Moraine on the Isle of Mann (Slater, 1931;
75 Thomas *et al.*, 2006; Roberts *et al.*, 2006; Thomas and Chiverrell, 2011). High resolution 2D
76 and 3D shallow offshore seismic surveys have also revealed large-scale thrust complexes
77 (up to several hundred metres thick and kilometres across) on the formerly glaciated
78 continental shelf surrounding northern Europe (e.g. Huuse and Lykke-Andersen, 2000;
79 Vaughan-Hirsch and Phillips, 2016; Pedersen and Boldreel, 2016). Consequently,
80 understanding how these glacitectonic thrust complexes are initiated and evolve and the ice
81 sheet dynamics required for their formation is becoming increasingly important in aiding our
82 understanding of the evolution of major palaeo ice masses.

83 This paper focuses upon the glacitectonised sequence exposed at the Mud Buttes in
84 southern Alberta, Canada (Figure 1), where Cretaceous sandstones, siltstones and
85 mudstones are intensely folded and thrust within a large-scale (c. 2 km long, c. 800 m wide),
86 arcuate cupola hill (Hopkins, 1923; Slater, 1927; Fenton *et al.*, 1993). The Mud Buttes is one
87 of a number of large glacitectonic landforms (Neutral Hills, Misty Hills; Figure 2) in this part of
88 Alberta which are thought to have been produced the readvance of ice streams against the
89 northernmost extension of the NW-SE orientated Missouri Coteau escarpment during retreat
90 of the Laurentide Ice Sheet (Evans *et al.*, 2008). Although the Mud Buttes is acknowledged
91 as a text book site for the study of glacitectonics (e.g. Aber and Ber, 2007; Benn and Evans,
92 2010), very little detailed research has been carried out here since the pioneering work of
93 George Slater (Slater 1927). The results of the multidisciplinary study (sedimentology,
94 structural geology and geomorphology) of the Mud Buttes area presented here address this
95 shortfall. The detailed analysis of the structures developed within this thrust complex has
96 enabled the construction of a cross-section through the glacitectonised sequence and the
97 establishment of a relative chronology of deformation events that took place during its
98 construction. The factors controlling the initial detachment, transport and subsequent
99 accretion of the thrust-bound bedrock slices are discussed, with large-scale glacitectonism
100 being related to surge-type behaviour of lobate ice stream margins during the later stages of
101 ice sheet recession from Alberta.

102

103 **Methods**

104 The glacial geomorphology of the study area was mapped manually from a 15 m light
105 detection and ranging (LiDAR) bare-earth digital elevation model (DEM) and the Shuttle
106 Radar Topography Mission (SRTM, 30 m DEM). This mapping was based on the non-
107 genetic, morphometric characteristics of landforms (Figures 1b to 3) and was augmented by
108 reference to aerial photograph mosaics flown and compiled by the Alberta Department of
109 Lands and Forest in the 1950s as well as Google Earth imagery. This approach has been
110 employed previously on the Canadian prairies (Evans *et al.*, 2008, 2014; Ó Cofaigh *et al.*,
111 2010; Fenton *et al.*, 2013; Atkinson *et al.*, 2014a, b) and ensures the representation of
112 landform detail at a variety of scales appropriate to the study area being depicted. Genetic
113 terms were then applied to features on the finalized map based on the descriptive and
114 interpretative details provided below utilizing where appropriate interpretations from previous
115 research (e.g. Shetsen, 1987, 1990; Fenton *et al.*, 2013; Atkinson *et al.*, 2014a and
116 references therein).

117 The glacitectonic deformation of the glacial sediments and Cretaceous bedrock
118 exposed at the Mud Buttes has been investigated using a range of macroscale techniques.
119 The sections through the deformed bedrock were described on the basis of their macroscale
120 features, particularly lithology, type of bedding, bed geometry and structure (both
121 sedimentary and glacitectonic). The orientation of folds, foliations, and faults, as well as
122 bedding were recorded at a number of localities (Figure 4) and plotted on a series of lower
123 hemisphere stereographic projections (dip and dip-direction/azimuth) (Figures 4c to g) and
124 rose diagrams (strike/trend) (Figure 4h) using StereoStat software by Rockworks™. The
125 sense of asymmetry of various fold phases and movement on the faults, and inter-
126 relationships between the various generations of structures were established. Successive
127 generations of structures (e.g. folds F1, F2.....Fn) are distinguished using the nomenclature
128 normally used in structural geological studies (F1 earliest folds to Fn latest). However, this
129 nomenclature does not necessarily imply that these structures evolved during separate
130 deformation events (D1, D2.....Dn). A series of overlapping photographs of key sections
131 within the deformed sequence (see Figures 5 to 8) enabling the analysis of the larger-scale
132 structures and the construction of a schematic structural cross-section through the Mud
133 Buttes thrust complex.

134 Sedimentological investigations were undertaken on the Quaternary deposits that
135 form a carapace over the non-dissected parts of the Mud Buttes. Individual lithofacies are
136 described in detail from five locations based upon bedding, texture, lithology and
137 sedimentary structures and classified according to the modified scheme of Eyles *et al.*
138 (1983) proposed by Evans and Benn (2004) and Evans (in press), specifically in relation to

139 glacially diamictons and glaciectonites. In order to assess the former shearing history of
140 the sediments and potential ice flow direction, clast macrofabrics were measured based
141 upon ≈ 30 clasts per sample, because clasts were too sparsely distributed to enable larger
142 samples and at the same time ensure that data collection was confined to small areas of
143 individual sedimentary units. Additionally, the orientations of microflutes, located at the basal
144 contact of a diamicton in one exposure, were measured. The macrofabrics are based on the
145 dip and azimuth (orientation) of the clast A-axes and were measured using a compass
146 clinometer, aiming to use predominantly clasts in the range of 30-125 mm (A-axis length) to
147 allow comparison with other studies (Benn, 1994a, b; 1995; Evans, 2000b; Evans and
148 Hiemstra, 2005; Evans *et al.*, 2007). The A-axes of clasts will tend to rotate to parallelism
149 with the direction of shear in a shearing Coulomb plastic medium like till (c.f. March, 1932;
150 Ildefonse and Mancktelow, 1993; Hooyer and Iverson, 2000). Fabric data were plotted in
151 Rockware™ on spherical Gaussian weighted, contoured lower hemisphere stereographic
152 projections. Statistical analysis of fabric data was undertaken using eigenvalues ($S_1 - S_3$),
153 based on the degree of clustering around three orthogonal vectors ($V_1 - V_3$), and presented
154 in fabric shape ternary diagrams (Benn, 1994b). This identifies the three end-members of
155 predominantly isotropic ($S_1-S_2 \sim S_3$), girdle ($S_1-S_2 \gg S_3$) or cluster fabrics ($S_1 \gg S_2 \sim S_3$). Further
156 analysis of strain history involved the classification of fabric data according to five modal
157 groups (un-unimodal, su-spread unimodal, bi-bimodal, sb-spread bimodal and mm-
158 multimodal) and their plotting against isotropy (S_3/S) in a modality-isotropy template, after
159 Hicock *et al.* (1996) and Evans *et al.* (2007).

160

161 **Location of study area and geological context**

162 The Mud Buttes form part of an extensive area of glaciectonic constructional terrain that
163 comprises the core of the Neutral Hills Uplands (Pettapiece, 1986; Shetsen, 1987).
164 Geomorphologically, at 50 m high, they are not the most spectacular features in these
165 uplands (Figure 2), which include the much larger and sharper relief Neutral Hills (120 m),
166 Misty Hills (85 m) and Nose Hill (100 m), but are invaluable for interpreting landform genesis
167 because their cores are well-exposed in a badland terrain created by deglacial meltwater
168 incision and postglacial runoff. Long recognized and mapped as glaciectonised bedrock
169 (Hopkins, 1923; Slater, 1927; Kupsch, 1962; Moran *et al.*, 1980; Shetsen, 1987, 1990;
170 Evans *et al.*, 2008), this suite of landforms is large enough to form its own physiographic
171 zone at a regional scale (Bostock, 1970a, b; Pettapiece, 1986).

172 Geologically, the region is located in the south-central part of the Western Canada
173 Sedimentary Basin and is underlain by fluvial and marine deposits associated with the
174 transgression of the Western Interior Seaway during the Late Cretaceous (Mossop and
175 Shetsen, 1994). The Belly River Group outcrops throughout the Mud Buttes and comprises
176 a fluvial succession of interbedded fine to coarse-grained pale coloured (light grey to light
177 brown) sandstone, dark coloured siltstone and mudstone with minor layers of coal and
178 sideritic concretions (Hopkins, 1923; Slater, 1927; Fenton *et al.*, 1993; Prior *et al.*, 2013).
179 These are overlain by marine strata of the Bearpaw Formation, which primarily consists of
180 laminated mudstone, with minor sandstone beds and layers of bentonite concretions.
181 Although the Bearpaw Formation underlies most of east-central Alberta and outcrops in the
182 Misty Hills to the south (Slater, 1927; Fenton *et al.*, 1993; Glombick, 2010), it is absent in the
183 Mud Buttes.

184

185 **Glacial Geomorphology of the Neutral Hills Uplands and surrounding areas**

186 The Mud Buttes lie in the south-central part of the Neutral Hills Uplands, an area of complex
187 and varied glacial landforms dominated by glacitectonic compressional structures but also
188 containing expansive areas of hummocky terrain and kame and kettle topography (Figures 1
189 and 2). This area lies between the strongly streamlined trunks of the former palaeo-ice
190 streams previously identified by Evans *et al.* (2008, 2014, 2016), Ross *et al.* (2009) and Ó
191 Cofaigh *et al.* (2010) as 'flow set 1' and marked here on Figure 1b as the Central Alberta Ice
192 Stream (CAIS) and Maskwa Ice Stream. Based upon the cross-cutting relationships depicted
193 in Figure 1b (see Evans *et al.* in prep for details), it appears that the CAIS operated for
194 longer than previously thought, maintaining a N-S flow in the west of the study region
195 through ice flow phases 3-6. In the centre of the study region, the later ice streaming phases
196 formed flow sets 2 and 3, which in the Neutral Hills Uplands are manifest respectively as a
197 WNW-ESE orientated streamlined corridor that is subtle but cuts across the numerous thrust
198 masses (flow set 2) and a multi-lobate assemblage of proglacial thrust masses (3a-c) at the
199 southern limit of a NNE-SSW aligned streamlined trunk zone, hereby called the 'Prospect
200 Valley lobe' (Figure 1b). The more substantial thrust masses of the Neutral Hills and Misty
201 Hills were similarly thought by Ó Cofaigh *et al.* (2010) to have been constructed during the
202 formation of flow sets 2 and 3 when the 'elbow' of the flow set 2 ice stream was more lobate
203 and radiating to the S and SW (Figure 1b). The impinging of the eastern margin of the CAIS
204 also likely played a significant role in landform construction in the western part of the Neutral
205 Hills Uplands. Based upon cross-cutting relationships, it appears that the Prospect Valley
206 lobe created an inset sequence of thrust masses (phases/margins 3a-c), which were partially

207 streamlined by later flow phases 4 and 5 (Figure 1b). A final readvance of the Prospect
208 Valley lobe (phase 6) constructed an extensive area of kettled thrust masses to the north,
209 which also appears to be linked to the construction of a hill-hole pair on the bed of the former
210 Maskwa Ice Stream (Evans *et al.*, 2016).

211 The southernmost and hence oldest of these major thrust masses appears to be the
212 Misty Hills, which lie 25 km south of the major arc of the Neutral Hills/Nose Hill thrust
213 moraine (Figures 2 and 3). The Misty Hills form the most prominent and dissected, likely
214 more recently reactivated, part of a much larger arc of glacitectonised bedrock masses
215 which sweep ESE across the Sounding Creek valley. At their geographical centre they
216 display a variety of structural lineaments which appear to highlight individual thrust masses
217 that have been differentially displaced or slightly rotated in the horizontal plane during glacial
218 compression (Figure 3). Lineaments are the surface expression of the crests of large-scale
219 fold noses or thrust faults and are clearly related to thrust masses where their internal
220 structure is visible. Even in the absence of exposures, surface lineaments or ridges have
221 been equated to glacitectonic compression based upon their appearance as closely spaced,
222 parallel-aligned but often sinuous corrugations (e.g. Kupsch, 1962; Christiansen and
223 Whitaker, 1976; Sauer, 1978; Moran *et al.*, 1980; Bluemle and Clayton, 1984; Tsui *et al.*,
224 1989). A protocol for the differentiation of such glacitectonic ridges and visually similar
225 appearing recessional push-moraines on the prairies was developed by Evans *et al.* (2014).

226 The details of the structural lineaments identified in Figure 3 from the Misty Hills
227 reveal variously orientated linear chains of depressions (likely faults) and three prominent
228 ridge patterns of likely folded and thrust strata: (i) N-S aligned; (ii) WSW-ENE aligned; and
229 (iii) arcuate ridges. The N-S-trending ridge pattern is the most significant, especially in the
230 west of the uplands, and it continues northwards through an upland spine that separates the
231 Monitor Creek and Sounding Creek valleys. Additionally, individual thrust masses or blocks
232 can be identified where linear depressions, likely marking fault (strike/slip) traces, demarcate
233 their boundaries. For example, at the western-end of the Misty Hills, a large NNE-SSW
234 aligned linear depression forms the boundary between a thrust block comprising N-S aligned
235 ridges and another whose predominantly N-S-trending ridges have been curved into a W-E
236 alignment; this gives the impression that the northern block has been displaced to the SSW
237 along the linear depression or fault accompanied by the distortion of the ridge pattern by
238 dragging the ridges (steep fold noses) northwards. Elsewhere, arcuate ridge patterns appear
239 to lie south of domed structures that otherwise comprise WSW-ENE or N-S aligned ridges;
240 the Mud Buttes form one such dome. Although the structurally-controlled ridge patterns can
241 be traced into the eastern part of the Misty Hills, the topography in this area is more subdued
242 and the landforms more hummocky and pitted, with increasingly expansive water-filled

243 depressions in an eastward direction, culminating in the larger expanses of Misty Lake and
244 Grassy Island Lake. Sinuous ridges (eskers) are also prominent in this area and trend W-E,
245 winding their way between densely-spaced hummocks, flat-topped hills (prairie mounds) and
246 circular rimmed features (donuts) (Figure 3). This landform association, hereon named the
247 Grassy Island Moraine, is one that is traditionally related to the stagnation of debris-rich ice
248 on the prairies (Gravenor and Kupsch, 1959; Clayton and Cherry, 1967; Clayton and Moran,
249 1974; Johnson and Clayton, 2003; Clayton *et al.*, 2008; Evans *et al.*, 2014) and demarcates
250 an expansive area of former buried glacier ice on the eastern part of the Misty Hills through
251 which structural lineaments are visible in some locations. Esker networks cross Grassy
252 Island Lake, which occupies an elongate depression along the thalweg of a major preglacial
253 river that flowed along the present Monitor Creek before turning SE to flow through the Misty
254 Lake area (Carlson 1969); esker continuity indicates that eastward flowing meltwater
255 drainage was englacial, enabling water to bypass the preglacial valley, which remained
256 inundated by ice during deglaciation, explaining why such prominent ice stagnation
257 topography (Grassy Island Moraine) developed in this area. Both the draping of the Misty
258 Hills structures by eskers as well as their visibility through the hummocky terrain indicate that
259 they were overrun by glacier ice after construction.

260 The various alignments of lineaments described above and their relationships to
261 regional overprinting/streamlining (Figures 1b and 3) appear to reflect a more complex
262 constructional history for the Misty Hills than previously reported (e.g. Fenton *et al.*, 1993).
263 The N-S-aligned lineaments continue south of the Misty Hills, beyond the limit of the high
264 relief thrust features of the Sharp Hills (Figure 2), where they can be traced beneath the
265 streamlined terrain of flow phase 2 (Figures 1 and 2). Hence the N-S lineaments are
266 classified as a partially overridden or fluted thrust moraine of pre-phase 2 age. This places
267 the origins of the Misty Hills in pre-phase 2, but later modification of these lineaments
268 appears to have been initiated during phase 3a, the southern extent of which is demarcated
269 by their realignment (blue line on Figure 3). The Grassy Island Moraine (Figures 2 and 3)
270 was overprinted on the eastern Misty Hills either during this phase and/or during phase 4. A
271 more S to SSW ice flow during phase 4 was responsible for streamlining the terrain to the
272 north of the Misty Hills and the construction and overriding of the Mud Buttes (Figures 1b
273 and 3; Evans *et al.*, in prep).

274

275 **Deformation structures and structural architecture of the Mud Buttes**

276 Deformation of the Belly River Formation at the Mud Buttes is characterised by large-scale
277 thrusting and folding (Figures 5 to 14). This glacially deformed sequence of sandstones,

278 siltstones and mudstones was first described by Hopkins (1923) who stated that “*the intense*
279 *deformation of the beds observed at Mud Buttes and similar localities is entirely superficial*
280 *and without deep-seated significance and in no way connected genetically with tectonic*
281 *disturbance of the region*”. However, it was the later work of Slater (1927) that clearly
282 demonstrated that the deformation was the result of “*ice-action*” comparing the
283 glacitectorism seen at the Mud Buttes with that observed on the Isle of Mön, Denmark, the
284 Isle of Rügen, Germany, and the North Norfolk coast of eastern England. In his detailed
285 cross-sections, Slater divided the deformed sequence at the Mud Buttes into three structural
286 zones separated by major thrust planes (Figure 15a; also see figs. 1 and 2 of Slater 1927).
287 This subdivision was later revised by Fenton *et al.* (1993) who argued that the
288 glacitectorised sequence could be divided into four major thrust sheets (Figure 15b; also
289 see fig. 16 of Fenton *et al.*, 1993). Thrust sheet 1 of Fenton *et al.* (1993) (zone 1 of Slater
290 1927) occurs on the southern side of the Mud Buttes and is the structurally lowest and least
291 deformed part of the sequence (Figure 15). The structurally overlying second thrust sheet
292 (zone 2 of Slater 1927) was described as being characterised by an increase in the degree
293 of folding but without appreciable thrusting (Fenton *et al.*, 1993). The third thrust sheet (zone
294 3 of Slater 1927) occupies the central higher ground of the Mud Buttes (Figure 15) and is
295 formed of highly folded and thrust sandstones and mudstones (Fenton *et al.*, 1993). The
296 fourth thrust sheet (not represented on the cross sections of Slater 1927) occurs on the
297 northern side of the Mud Buttes (Figure 15b) and was interpreted by Fenton *et al.* (1993) as
298 having been thrust over structurally lower sheets. Fenton *et al.* (1993) concluded that the
299 deformation was the result of ice advancing from the north with minor changes in the
300 orientation of the folds being indicative of a locally radial ice flow.

301 Our re-examination of the glacitectorism at the Mud Buttes recognises that the style
302 and intensity of deformation varies from south to north within this polydeformed sequence
303 (c.f. Slater 1927; Fenton *et al.*, 1993). For ease of description the sequence has been
304 divided into four NE to SW-trending ‘structural domains’ (Figure 4b) which internally exhibit a
305 similar range of structures (folds, thrusts, fabrics and shear zones) and relative intensity of
306 deformation. The boundaries between these domains correspond to major thrusts (see
307 Figure 4b) which truncate bedding and deformation structures developed within the
308 underlying domain. Structural domains 1 and 2 broadly correspond to the structurally lower
309 three thrust sheets of Fenton *et al.* (1993) and zones 1 to 3 of Slater (1927). However a zone
310 of intense brittle-ductile shearing has been identified on the northern-side of the central
311 higher ground of the Mud Buttes (part of the third thrust sheet of Fenton *et al.*, 1993) and
312 assigned to structural domain 3 (see below). Structural domain 4 of this study corresponds

313 to the fourth thrust sheet of Fenton *et al.* (1993). The deformation structures present within
314 each of these domains are described below.

315 **Structural Domain 1**

316 Structural domain 1 occurs on the southern-side of the Mud Buttes (Figure 4b) and
317 represents the least deformed part of the glacitected sequence. The domain is
318 characterised by a gently to moderately (10° to 45°) N to NE-dipping (Figures 4c and d)
319 sequence of interbedded pale grey, fine-grained sandstones, siltstones and grey-brown
320 mudstones deformed by northerly dipping (Figures 4e and f), southerly directed thrusts
321 (Figures 5 and 6). Although repeated by thrusting, sedimentary structures (graded bedding,
322 cross-lamination) preserved within the Belly River Formation indicate that these rocks are in
323 generally the right-way-up. The thrusts are typically developed within the relatively weaker
324 mudstones, particularly close to, or immediately adjacent to the boundaries of the thicker,
325 more competent sandstones. Their orientation varies from bedding-parallel to moderately
326 dipping structures which clearly truncate bedding (Figure 5a). Small-scale and mesoscale,
327 asymmetrical, southerly verging folds are only locally developed within domain 1 occurring in
328 the hanging-walls of the thrusts where they deform 1 to 2 m thick units of thinly interbedded
329 sandstones and mudstones (Figures 5a and 5b). Northwards, across domain 1, the
330 mesoscale folds appear to tighten, with their increasingly steep southern limbs resulting in
331 the localised overturning (towards the south) of bedding (Figure 6). Small-scale thrusts are
332 locally observed within the hinge zones of the folds and deforming the overturned limbs of
333 these structures (Figures 5a and 6b). In detail these small-scale thrusts vary from discrete,
334 planar dislocations to narrow brittle-ductile shear zones possessing a well-developed S-C
335 fabric (Figure 6c). Where developed, the geometry of this asymmetrical foliation records a
336 southerly directed sense of shear.

337 **Structural Domain 2**

338 Structural Domain 2 is located immediately to the north of domain 1 and is characterised by
339 a marked increase in the complexity of both folding and thrusting within the Belly River
340 Formation (Figures 7 to 9). The overall intensity of this deformation increases from south to
341 north across domain 2 and is accompanied by a progressive increase in the angle of dip of
342 bedding and the thrusts (see Figures 8a, 8b and 8c). Although repeated by thrusting,
343 bedding within the Belly River Formation is only locally overturned on the steep limbs of
344 associated meso- and large-scale folds. Both Slater (1927) and Fenton *et al.* (1993)
345 recognised this increase in the intensity of deformation within the central part of the Mud
346 Buttes (see Figure 15). However, detailed analysis of the relationships between the various
347 generations of folds and thrusts present within domain 2 has revealed that within this part of
348 the thrust complex, the Belly River Formation has undergone a distinct polyphase

349 deformation history (see below). Domain 2 is further subdivided into: (i) domain 2a located
350 along its south side and composed of moderately inclined and thrust repeated sandstones,
351 siltstones and mudstones (Figures 4, 5 and 6a); and (ii) domain 2b occupying the central
352 higher ground of the Buttes and characterised by moderately to steeply inclined, highly
353 folded and thrustured Belly River Formation rocks (Figures 9b, 9c, 10 and 11). Although these
354 two subdomains can be broadly correlated with the second and, to a lesser extent, third
355 thrust sheets of Fenton *et al.* (1993), the progressive nature in the change in both the
356 intensity and attitude of the deformation structures from domain 2a into domain 2b indicates
357 that they share a common deformation history and are therefore considered to form part of
358 the same structural domain.

359 Immediately adjacent to the southern boundary of domain 2a are locally well-
360 developed large-scale, upright, tight to moderate to tight, 'box-like' fold structures (Figures
361 8b, 9a and 9b); the "*diapyre curve*" of Slater (see fig. 3 of Slater, 1927). The local truncation
362 of bedding on the limbs and within the hinge zones of these folds indicate that they deform a
363 set of earlier developed thrusts (T1), indicating that they are F2 in age (Figure 9a). The
364 sense of offset of bedding across these earlier developed thrusts records a southward
365 displacement during T1 thrusting. The sandstones and mudstones on the limbs of the folds
366 are also locally deformed by a set of later thrusts (T2) and more steeply inclined reverse
367 faults (Figure 9a). The sense of displacement on these relatively younger thrusts is also
368 towards the south, indicating that both the T1 and T2 phases of faulting probably resulted
369 from the same overall N-S-directed sense of shear (see Figure 9a). Locally developed
370 northerly directed thrusts close to the southern margin of domain 2a and are interpreted as
371 minor back-thrusts.

372 The dominant deformation within the remainder of domain 2a is the thrust repetition
373 and stacking of fault-bound slices of Belly River Formation (Figures 7 and 8). As noted
374 above the dip of these thrust slices progressively increases northwards across the domain
375 (Figure 8). The thrusts are once again preferentially developed within the weaker mudstones
376 immediately adjacent to the boundaries with the more competent sandstone units (see
377 Figures 8, 9a and 9b). In detail the individual thrust planes are locally marked by thin (5 to 20
378 cm thick) lenses (1 to 2 m long) to laterally more extensive (5 to 15 m) layers of a dark grey,
379 highly fissile, organic-rich mudstone with associated minor ironstone nodules (Figures 10a
380 and b), suggesting that these peaty-looking mudstones, where present, acted as a focus for
381 thrusting. Small-scale (centimetre scale) asymmetrical folds, asymmetrical S-C fabrics and
382 the offset of bedding associated with the thrusts within domain 2a similarly record a
383 consistent southerly directed sense of displacement.

384 Large-scale, moderately inclined synclines developed within the foot-walls of the
385 thrusts are truncated by these low-angle faults (Figure 7a) and possibly represent the relicts
386 of tip-folds developed in front of the propagating thrusts, which became dissected by these
387 brittle structures as thrusting continued. These folds can be seen to deform both bedding
388 and a set of earlier developed bedding-parallel thrusts (T1) (Figure 7a), indicating that large-
389 scale thrusting and imbrication within domain 2a is predominantly T2 in age. Mesoscale folds
390 within domain 2a range from relatively simple, upright to inclined, asymmetrical, south-
391 verging, structures developed within the hanging-walls of the T2 thrusts (Figures 7b and 8c)
392 to more complex structures with associated well-developed, small-scale S, M and Z shaped
393 parasitic folds (Figure 9c). These more complex fold systems are typically observed
394 deforming thinly interbedded sandstones, siltstones and mudstones, and occur within
395 discrete bands or horizons following the outcrop pattern of the more mudstone-rich, thinly
396 bedded units within the Belly River Formation. The NNE-SSW-trending folds (Figures 4g and
397 h) are non-cylindrical structures with curved axial traces which plunge (up to 20°) towards
398 the E/ENE or W/WSW. They locally exhibit a marked thickening of the hinge zone and/or
399 steeply inclined to overturned limbs, as well as attenuation (thinning) of their moderately
400 inclined upper limbs. The folds are F2 in age and were observed deforming earlier
401 developed low-angle (with respect to bedding) to bedding-parallel T1 thrusts. Small- to
402 mesoscale T2 thrusts (displacements up to 1-2 m) developed within the cores of the larger
403 F2 folds (Figure 9c) are interpreted as either accommodation structures formed in response
404 to the progressive tightening of the folds during deformation, or the propagating tips of larger
405 blind T2 thrusts. Both the folds and thrusts (both T1 and T2) record a sense of shear towards
406 the south, indicating that they probably developed during the same overall southerly directed
407 deformation event.

408 The boundary between domains 2a and 2b is gradational and marked by an increase
409 in the relative intensity and scale of the folding and thrusting (Figures 11 and 12), with the
410 largest scale (amplitude of tens of metres) occurring within the “core” of the Mud Buttes
411 (Figure 12). Units of thinly bedded sandstone and mudstone within the Belly River Formation
412 show evidence of increased amounts of shortening with well-developed south-verging,
413 asymmetrical to locally disharmonic folds and southerly directed thrusts (Figure 11). The
414 folds are tight to locally isoclinal, steeply to moderately inclined, southerly verging, non-
415 cylindrical structures which are locally dissected by moderate to steeply inclined, N/NNE-
416 dipping thrusts (Figure 12a). Ductile shearing of the limbs of the isoclinal folds during folding
417 resulted in the attenuation and localised disruption of bedding within the sandstones (see
418 Figure 12a). Small- to mesoscale folds developed on the limbs of the larger folds exhibit S,

419 M and Z geometries depending upon their position relative to the hinges of these macroscale
420 structures (Figure 12b).

421 **Structural Domain 3**

422 Structural domain 3 has been identified flanking the northern side of the higher ground within
423 the “core” of the Mud Buttes (Figure 4). This c. 40 to 80 m wide zone of relatively intense
424 brittle-ductile deformation (Figure 13a) pinches out laterally to the W and E (see Figure 4b)
425 where it appears to have been cut out at the base of the structurally overlying domain 4 (see
426 below). Domain 3, where present, is preferentially developed within a relatively mudstone-
427 rich part of the Belly River Formation (see Figure 13a). It is characterised by tight to isoclinal,
428 southerly verging, asymmetrical rootless folds deforming 0.5 to 1.5 m thick sandstone units
429 and highly foliated, fissile mudstones and siltstones (Figure 13a). The hinge zones and
430 overturned limbs of these folds are cut by a series of small-scale, northerly dipping thrusts
431 which have accommodated displacements from a few millimetres to several tens of
432 centimetres. Narrow (5 to 15 cm wide) brittle-ductile shear zones deforming the sandstones,
433 siltstones and mudstones possess a locally well-developed S-C fabric which record a
434 relatively consistent southerly directed sense of shear (Figures 10c and d).

435 The boundary between domain 3 and the structurally underlying domain 2 is marked
436 by a 5 to 10 m wide shear zone containing truncated non-cylindrical, tight to isoclinal folds
437 deforming the sandstones (Figure 13b) and intense ductile shearing within the more
438 mudstone-rich units (Figure 13c). The primary sedimentary lamination within the mudstones
439 and siltstones within this shear zone has been variably transposed by a heterogeneously
440 developed northerly dipping ($69^{\circ}\text{N}/291^{\circ}$, $66^{\circ}\text{N}/300^{\circ}$, $71^{\circ}\text{N}/292^{\circ}$) tectonic foliation,
441 responsible for the marked fissility within these rocks. Moderately to steeply inclined,
442 northerly dipping brittle thrusts within the shear zone are marked by narrow (1 to 5 cm thick)
443 shears which locally possess a variably developed S-C fabric. These asymmetrical shear
444 fabrics, where present, record a southerly directed sense of displacement. The shear zone
445 marking the southern boundary of domain 3 can be traced laterally for several tens of metres
446 across this part of the Mud Buttes where it truncates the large-scale folds (F2) within domain
447 2b. This relationship indicates that the relatively intense brittle-ductile shearing which
448 characterises domain 3 largely post-dated folding within the structurally lower parts of this
449 thrust complex.

450 **Structural Domain 4**

451 Structural domain 4 is the most northerly of the domains identified within the Mud Buttes and
452 has been thrust over the structurally underlying domains (cf. Fenton *et al.*, 1993). It is
453 composed of gently to moderately north-dipping stacked thrust-bound slices of Belly River

454 Formation (Figure 14). This domain is poorly exposed compared to the remainder of the
455 thrust complex. The structurally lower parts of domain 4, where exposed, are apparently
456 dominated by more massive, poorly bedded sandstone (Figure 14a). The relative intensity of
457 glacitectorism appears to increase structurally upwards through the domain, where the thinly
458 bedded sandstones, siltstones and mudstones are deformed by a series of south-directed
459 gently to moderately inclined, northerly dipping thrusts and southerly verging folds (Figure
460 14a); this increase may be largely lithologically controlled. To the east, domain 4 rests
461 directly upon folded and thrust sedimentary rocks assigned to domain 2, with the low-angle
462 thrust contact marking the base of domain 4 clearly truncating the underlying upright to
463 steeply inclined, large-scale (F2) folds (Figure 10e). In the central part of the Mud Buttes,
464 domain 4 rests directly upon the highly deformed mudstone dominated sequence of domain
465 3 (Figure 13a). These relationships indicate that southerly directed thrusting, leading to the
466 accretion of domain 4, occurred during the later stages of the development of this thrust
467 complex and its emplacement resulted in the truncation of the older parts of this cupola hill.

468 **Quaternary deposits at the Mud Buttes**

469 The glacitectorically deformed bedrock at Mud Buttes was likely covered by a thin
470 succession of Quaternary glacial sediment prior to their erosion into badland topography.
471 This is evident in a number of exposures through the various horizontal butte summits and
472 non-gullied margins of the badland exposures. Five stratigraphic sections (MBQ 1-5; Figure
473 4a) are reported here as representative of the Quaternary succession.

474 Section MBQ 1 (Figure 16) displays 0.92 m of clast-poor diamicton, with a sandy
475 gravel interbed, overlying pale grey silty sandstone bedrock containing gypsum nodules. The
476 lower and thicker diamicton has a dark brown clayey silt matrix but contains deformed and
477 undeformed intraclasts of sandstone, many of which appear to be rotten bedrock rafts, and
478 boudins and smudges of grey clay, likely originating from mudstone bedrock rafts. Although
479 classified as a massive diamicton (Dmm) the variably coloured matrix and rafts also comply
480 with the definition of a Type III mélange (Cowan, 1985). The interbed that separates the
481 lower and upper diamictons comprises 0.12 m of contorted and attenuated sand and fine
482 gravel lenses, whose contacts are interdigitated with the diamictons; this is indicative of a
483 shearing zone developed during emplacement of the upper diamicton. The section is capped
484 by a 0.30 m thick clay-rich, massive, matrix-supported diamicton with an indurated but
485 crumbly structure and containing numerous gypsum nodules.

486 Section MBQ 2 (Figure 17) displays a vertical continuum of well-exposed, deformed
487 and sheared mudstone capped by a poorly exposed, clay-rich diamicton. Although the
488 diamicton, which is the lateral equivalent of the diamictons identified in the other four

489 sections is not well-exposed here, this section is important in that it provides the thickest
490 exposure through the boundary zone between Cretaceous bedrock and the overlying
491 Quaternary sediments at Mud Buttes. The mudstone is sub-horizontally bedded, dipping at
492 15°-20° northwards but is characterized in its upper 1.10 m by recumbent, isoclinal and
493 rootless folds and thrust asymmetrical folds, with disharmonic folding and thrust faults
494 dominating the upper 0.40 m. This folded and thrust mudstone is truncated by the base of a
495 0.15-0.20 m thick sequence of weakly pseudo-laminated, predominantly grey mudstone
496 melange (Type IV *mélange* of Cowan, 1985), which is friable and crumbly in structure and
497 contains small boudins and lenses of yellow and pale grey (groundwater altered)
498 components that can be identified as more continuous beds in the less disturbed mudstone
499 beneath. This pseudo-lamination gives way abruptly to 1.10-1.30 m of overlying
500 structureless, extremely friable and crumbly mudstone, within which none of the sub-
501 horizontal bedding of the parent bedrock can be recognized. This massive appearance is a
502 product of homogenization, the intermediate stages of which are represented by the folded
503 and thrust mudstone and pseudo-laminated mudstone (glacitectonic foliation); this vertical
504 continuum is typical of glacitectonite-subglacial till sequences from which clay-rich and clast-
505 poor glacial diamictos (tills) are derived *in situ* from sheared bedrock (Banham, 1977;
506 Pedersen, 1989; Hiemstra *et al.*, 2007).

507 Section MBQ 3 (Figure 18) comprises 2.2 m of *mélange* and diamicton directly
508 overlying silty sandstone upon which striated shield boulders and cobbles are lodged to form
509 a discontinuous clast pavement or line, with striated facets bevelled at the same level as the
510 bedrock surface (Figure 18b ii). The surface of the bedrock is also striated, manifest as
511 prominent microfluting sole casts, which like the clast surface striae are strongly aligned
512 NNW-SSE and appear to terminate at small sandstone particles (Figure 18b iii). Directly
513 overlying the microflutings is 0.5-1.0 m of clayey-silt diamicton containing numerous rotten
514 sandstone intraclasts and deformed sand lenses or boudins (Figure 18a). In the basal 0.3 m
515 the clasts and lenses/boudins are relatively small and highly attenuated, often constituting
516 smudges of ingested material within the diamicton matrix. They also form discrete lines that
517 are spaced between 5 – 10 cm apart (Figure 18b ii), giving the impression of a Type IV
518 *mélange* (Cowan, 1985). In the upper 0.7 m the diamicton contains larger sand lenses and
519 boudins in which stratification is common but displays significant deformation (Figure 18b i),
520 giving the material the appearance of a Type III *mélange* (Cowan, 1985) but with little sense
521 of shearing direction. This *mélange* is overlain by a further 0.6 m of heterogeneous
522 diamicton comprising crudely horizontally bedded sands, sandy gravels, silts and clay with
523 layers of massive, clay matrix-supported diamicton, all of which have been well to very highly
524 deformed, comparable to a Type III–Type IV *mélange* (Cowan, 1985). The section is capped

525 by 0.6 m of clay-rich massive, matrix-supported diamicton comprising material that appears
526 mudstone-rich and blocky in structure with copious gypsum nodules. The basal 0.3 m of the
527 Type IV *mélange* is typical of highly sheared subglacial tills in which rafts have been plucked
528 or cannibalized from the bedrock substrate and then highly attenuated through shearing in
529 the subglacial traction zone and thickened incrementally to form stacked or repeated
530 diamicton units. This origin is consistent with the lodging of shield clasts and striating of the
531 clast facets and silty sandstone bedrock surface by small sandstone clasts, which created
532 sole casts as they were dragged across the substrate by ice flowing from the NNW. The
533 overlying diamictons display firstly a change to low strain deformation, manifest in the Type
534 III *mélange* and its larger scale deformed stratified sand bodies, but then back to more highly
535 attenuated, therefore sheared, materials typical of a Type IV *mélange*. A further important
536 characteristic is the increase in stratified sands and gravels up the sequence before the
537 emplacement of the massive clay-rich diamicton; this is interpreted as the down-ice
538 advection of increasing volumes of stratified sediment into an incrementally thickening
539 subglacial deforming layer forming on the northern side of the Mud Buttes. The capping clay-
540 rich diamicton records the termination of advection and the emplacement of mudstone-
541 dominated matrix, reflecting a change in subglacial source materials.

542 Section MBQ 4 (Figure 19) is a significant exposure because it contains evidence of
543 non-glacial Quaternary deposits lying between the glacitectonically deformed bedrock and
544 surficial glacial materials. These comprise 15-20 cm of weakly laminated to massive
545 clayey-silt directly overlying friable mudstone, grading into £ 40 cm of organic-rich clayey-silt.
546 Pollen extracted from the organic-rich material (Table 1) is well-preserved and of Quaternary
547 rather than older (i.e. Cretaceous) age. It is predominantly indicative of a cool environment,
548 especially in relation to the occurrence of *Artemisia*, *Chenopodiaceae*, grasses and sedges,
549 and the appearance of boreal species such as pine, spruce and tsuga, with only hazel being
550 relatively thermophilous. Based upon this evidence it appears that this stratigraphic unit is a
551 palaeosol, probably a prairie-type Chernozem. This has been developed in a weakly
552 laminated clayey-silt whose origin is uncertain but is most likely a locally derived aeolian
553 deposit. The *in situ* nature of this palaeosol is difficult to ascertain, especially as the clayey-
554 silt laminations in which it is developed appear to have been deformed, and therefore its
555 status as an isochronous surface versus a glacitectonic raft is uncertain and requires further
556 research.

557 The potential palaeosol is truncated but not significantly eroded by a 0.15-0.20 m
558 thick, clay-rich brown Dmm containing deformed but laterally continuous sand lenses as well
559 as wisps or smudges, giving the appearance of a Type II *mélange* (Cowan, 1985). This

560 grades abruptly into a 0.25 m thick, massive, matrix-supported diamicton, which has a
561 banded appearance due to numerous changes of colour from grey to brown and red-brown
562 in undulatory and discontinuous, sub-horizontal bands. This pseudo-lamination appears to
563 be a product of the attenuation and immature mixing of different clay-rich or sand-rich
564 materials in a shearing medium, likely derived from the underlying *mélange* as a result of
565 subglacial cannibalization and traction zone deformation. The section is capped by 0.55 m of
566 grey, clay matrix-supported diamicton with deformed sand lenses (Figure 19) and a fissile to
567 crumbly in texture due to the mudstone derived matrix. The measurement of a macrofabric
568 was possible in this unit because it contains a relatively high concentration of clasts. This
569 displays a strong alignment towards the NNW, with a mean lineation azimuth of 335° and an
570 S_1 eigenvalue of 0.63 (Figure 16). In terms of its shape (Figure 20a) and modality/isotropy
571 characteristics (Figure 20b), this macrofabric is spread-unimodal and compatible with
572 subglacial tills with high lodgement components. The origins of the deformed lenses are
573 unclear but are likely deformed rafts because their sandy character is unlike the clay matrix
574 of the surrounding diamicton. Together the Type II *mélange*, banded Dmm and grey Dmm
575 are interpreted as a vertical continuum typical of a glacitectorite-subglacial till sequence
576 from which a sheared clay-rich diamicton with deformed rafts and erratic clasts (subglacial
577 traction till) has been derived *in situ* from the mixing of sheared mudstone and pre-existing
578 stratified sands (Banham, 1977; Benn and Evans, 1996; Evans *et al.*, 2006; Evans in press).
579 The glacial origin of this sequence documents ice advance after a soil developed across
580 the glacitectorised bedrock of the Mud Buttes, indicating that two phases of glacial activity
581 are recorded at the site with only the second phase providing evidence that the Mud Buttes
582 were glacially overrun.

583 At Section MBQ 5 (Figure 21), 1.25 m of Quaternary sediment overlies a 0.20 m
584 deformed zone developed along the Cretaceous bedrock unconformity. This deformed zone
585 resembles a Type III *mélange* (Cowan, 1985) due to its heavily contorted stratified
586 sediments comprising laminated silts, sands and clays, along with pockets of organic
587 material and a coherent block of sandstone. Sub-rounded to sub-angular, slab-shaped
588 sandstone boulders are embedded or lodged into this deformed zone, exhibiting A/B plane
589 surfaces accordant with the boundary of the overlying diamicton; these boulders also form a
590 clast line or weakly developed pavement. This is overlain by 0.65 m of massive, matrix-
591 supported, clayey-silt diamicton with numerous rotten sand clasts and sandy lenses or
592 boudins arranged in horizontal lines, together with short, discontinuous sand stringers or
593 wisps spaced 5-10 cm apart, thereby resembling a Type III-IV *mélange*. A clast macrofabric
594 from this diamicton displays a weak cluster, dipping NW with a mean lineation azimuth of
595 347° and an S_1 eigenvalue of 0.52 (Figure 21). In terms of its shape (Figure 20a) and

596 modality/isotropy characteristics (Figure 20b), this macrofabric is multi-modal and typical of
597 low shear strains, however, the weakly developed orientation is entirely compatible with the
598 other macrofabric and microfluting/striae evidence collected from, and in association with,
599 the diamictos (tills) in other sections. The characteristics of this Type III-IV mélange are
600 similar to those of highly sheared subglacial tills in which rafts have been plucked or
601 cannibalized from the bedrock substrate and then highly attenuated through shearing in the
602 subglacial traction zone by ice flowing from the NW and then thickened incrementally to form
603 stacked or repeated diamicton units. This is consistent with the boulder line, which is likely
604 the product of clasts being dragged through stratified materials and organics before being
605 lodged in a Type III mélange or mixed sediment and bedrock glacitectorite. The capping
606 0.60 m of diamicton is poorly exposed at this site but generally comprises a clay-rich,
607 massive, matrix-supported diamicton with a fissile to blocky structure.

608 In summary, the Quaternary deposits and structures identified in the five sections
609 comprise a vertical sequence of locally preserved palaeosol and/or deformed bedrock and
610 stratified sediments overlain by glacitectorite (sediment or bedrock derived) and/or
611 subglacial traction till emplaced during glacier overriding from the NNW. A composite
612 summary of the vertical logs with genetic facies codes for the Quaternary stratigraphic
613 sequence at Mud Buttes is presented in Figure 22. In all outcrops, the clay-rich nature of the
614 capping till indicates that mudstones were being cannibalized during later stages of glacier
615 overriding, a process that is well represented by section MBQ 2, but this is in contrast to the
616 exploitation of stratified sands and rare gravels (and possibly soil/organics at MBQ 5) that
617 took place during the earlier emplacement of lower tills and glacitectorites. The distinct
618 vertical colour change from brown to grey within the tills and glacitectorites also attests to
619 the cannibalization of pre-existing stratified sediments and potentially also a more extensive
620 palaeosol during early glacier overriding. Explanations of the origins of this material and the
621 reasons for their exhaustion and replacement by local mudstone matrix during glacier
622 overriding likely lie in the appreciation of the pre-advance topography. However, it is clear
623 that the Mud Buttes were initially constructed proglacially and later overrun by glacier ice to
624 form the glacitectorite/till carapace, and hence they constitute a cupola hill (*sensu* Aber *et*
625 *al.*, 1989). Stratified sediments evident in the heavily fragmented and deformed rafts of the
626 lower glacitectorite/till were likely excavated from the proximal depression created by the
627 construction of the Mud Buttes as a hill-hole pair, a depression in which waterlain sediments
628 could have accumulated during the intervening non-glacial interval. Exhaustion of this
629 sediment supply, as well as most of the palaeosol, by glacier excavation and glacitectorite
630 construction resulted in the subglacial removal of freshly exposed mudrocks in order to
631 maintain till continuity and thereby seal the sequence with clay-rich till.

632

633 **Discussion**

634 It is clear from the above description that the deformation within all four structural domains
635 occurred in response to southerly directed shear, consistent with glacitectonism at the Mud
636 Buttes having been driven by ice advancing from the north (c.f. Fenton *et al.*, 1993). The
637 relationships between the various folds and thrusts present within domain 2 have allowed a
638 relative chronology of deformation events to be established for at least the southern and
639 central parts of the Mud Buttes. This progressive, southerly directed, polyphase deformation
640 history can be divided into three main phases. The earliest phase, D1, characterised by low-
641 angle to bedding-parallel thrusting (T1) and relatively minor folding (F1) which probably
642 resulted in the initial detachment of the thrust slices of bedrock and shortening of the
643 sedimentary sequence; Phase 2 leading to continued thrusting (T2) and the main phase of
644 folding (F2) within the Mud Buttes. D1 is thought to have been largely responsible for the
645 imbrication of the detached thrust-bound slices of Belly River Formation and the main phase
646 of “construction” within the developing composite thrust moraine. During the second phase
647 of deformation (D2), the earlier developed T1 thrusts were locally folded by the developing
648 F2 folds. Elsewhere, these T1 thrusts probably continued to move (i.e. evolving into T2
649 structures) accommodating further D2 shortening in response to compression imposed by
650 the advancing ice. The final phase, D3, led to continued thrusting within the Belly River
651 Formation. Movement along the earlier T2 thrusts resulted in their continued propagation
652 upwards through the sequence leading to deformation of F2 folds. Importantly, this
653 polyphase deformation sequence has not been recognised within domains 1 and 4; these
654 domains appear to have only encountered the equivalent to D1 in their deformation history.

655 The deformation structures which characterise structural domains 1, 2 and 3 record
656 an overall increase in the intensity of thrusting and folding northwards across the Mud
657 Buttes. This is accompanied by the progressive increase in the angle of dip of individual
658 thrust slices of the Belly River Formation, which become steeply northerly dipping within the
659 central part of this composite thrust moraine. This relationship is illustrated in Figure 23. As
660 noted above, the vergence of the folds and sense of displacement on the thrusts within all
661 four structural domains indicates that deformation resulted from ice advancing from the
662 north. The style and relative intensity of the deformation within domain 4, however, is
663 reminiscent of that observed within parts of domain 1 (see Figure 23), marking a relative
664 decrease in the intensity of deformation in the apparently ice-proximal part of the thrust mass
665 where glacitectonism would be expected to be most intense. Consequently, any model

666 explaining the structural evolution of the Mud Buttes cupola hill must take these spatial
667 variations in the complexity and relative intensity of deformation into account (see below).

668 ***Glacitectonic model for the evolution of the Mud Buttes***

669 The structural architecture of the Mud Buttes is illustrated in Figure 23 and clearly shows the
670 progressive increase and subsequent decrease in the relative intensity and complexity of
671 deformation from south to north across this glacitectonic landform. The main thrusts
672 identified in the surface exposures have been projected downward through the Belly River
673 Formation where they are thought to link into a subhorizontal or gently north-dipping
674 décollement surface. This décollement surface separates the allochthonous sequence of
675 thrust and folded sandstones, siltstones and mudstones from the structurally underlying *in*
676 *situ* (autochthonous) undeformed units of the Belly River Formation. However, the depth to
677 this basal detachment is currently unknown. The bedding-parallel to gently northerly dipping
678 nature of the earlier (T1) thrusts can be used to suggest that this basal detachment, or sole
679 thrust, also occurs at a low-angle within the Belly River Formation.

680 It is clear from Figure 23 that the overall structure of the main part of the Mud Buttes
681 (represented by domains 1, 2 and 3) is a broadly fan-shaped imbricate thrust stack. The
682 progressive increase in dip of the individual thrust-bound slices of Cretaceous bedrock from
683 south to north within this proposed imbricate stack is a direct result of the progressive
684 forward propagation of the evolving composite thrust moraine (Figure 24). This forward
685 propagation was driven by ice advancing from the north as indicated by the southerly
686 directed sense of thrusting/shear recorded by the deformed Belly River Formation. As one
687 thrust-bound segment began to “stick” the basal décollement propagated beneath it
688 eventually detaching a relatively younger, structurally lower thrust slice that accreted to the
689 base of the developing imbricate stack. Unless folded, these detached blocks of Belly River
690 Formation remained the right-way-up, younging toward the north. As the process of
691 accreting successively younger (structurally) thrust-slices to the base of the developing
692 imbricate thrust stack continued, the structurally higher and older thrust-slices are
693 progressively “back-rotated” (i.e. the sense of rotation of the detached thrust-bound slab is
694 towards the advancing Prospect Valley lobe) becoming increasingly steeper in attitude
695 (Figure 24).

696 During back-rotation, the earlier small-scale thrusts (T1) within the thrust-blocks were
697 folded (F2), and the hinges and overturned limbs of F1 folds cut by relatively later T2 thrusts,
698 leading to the observed polyphase deformation history identified within domain 2. As a direct
699 result of the forward propagation of the thrust stack, progressive back-rotation and internal
700 deformation of the detached thrust-slices, deformation within the imbricate stack becomes

701 progressively older and more complex towards the north and the margin of the advancing ice
702 sheet. As a direct consequence of this process, the polyphase deformation history recorded
703 by the Belly River Formation is diachronous, with each phase becoming progressively
704 younger towards the south (see Figure 23). D1, which is dominated by thrusting, can be
705 equated to the initial detachment and low-angle stacking of the thrust-slices. It therefore
706 migrated southwards to accompany the forward propagation of the imbricate thrust stack
707 (Figure 24). D2 folding and thrusting then took over as the detached thrust-slices back-
708 rotated and become displaced upwards as the developing imbricate thrust stack
709 accommodated further shortening of the Cretaceous bedrock (Figure 24). D2 will also
710 migrate southwards as new thrust-slices are progressively accreted to the base of the
711 developing imbricate stack and are back-rotated. As a consequence of the back-rotation and
712 up-thrusting of these detached blocks during D2, the surface topography of the evolving
713 composite thrust moraine would have become more pronounced (see Figure 24). D3 is
714 typically restricted to the core of the Mud Buttes and probably occurred as the sequence
715 attempted to accommodate further compression imposed by the advancing ice. However,
716 the restricted nature of D3 may possibly indicate that it occurred during, or shortly before the
717 cessation of the forward propagation of the imbricate thrust stack. Consequently, this stage
718 of the deformation history may record the “locking up” of the imbricate thrust stack and
719 potential localised stalling of the advance of the Prospect Valley lobe.

720 In this relatively simple forward propagating imbricate thrust stack model, the intense
721 brittle-ductile shearing that characterises structural domain 3 can be interpreted as having
722 occurred in an ice-proximal position. Furthermore, these highly deformed sedimentary rocks
723 may represent the former ice contact part of the landform. The brittle-ductile shear zone at
724 the base of domain 3 cross-cuts and modifies earlier structures within domain 2, suggesting
725 that this deformation may have post-dated the main constructional phase of the Mud Buttes
726 imbricate thrust stack and is therefore D4 in age. Consequently, it is possible that the intense
727 shearing within domain 3 records the repeated basal shear of the ice sheet up against this
728 ice contact zone whilst the ice occupied the marginal position represented by the imbricate
729 thrust stack.

730 The return to simple thrusting and folding within structural domain 4 is thought to
731 record the accretion of a relatively younger and much smaller thrust-block moraine onto the
732 up-ice side of the much larger imbricate thrust stack forming the bulk of the Mud Buttes
733 (Figure 24). Forward propagation and evolution of this moraine would have been impeded by
734 the presence of the much larger glacitectonic landform immediately down ice. The tight, box-
735 like folding observed at the southern margin of domain 2a may have occurred during the
736 accretion of domain 4 onto the up-ice side of the earlier formed imbricate thrust stack. Shear

737 transmitted into the imbricate during the over-thrusting of domain 4 may have led to the
738 localised tightening of earlier developed folds and renewed (minor) movement along pre-
739 existing thrusts, thereby representing D5 within the main part of the Mud Buttes composite
740 thrust moraine. This postulated minor “reactivation” of D1/D2 structures within the earlier
741 formed imbricate thrust stack was apparently focused along the boundary between domains
742 1 and 2a (see Figures 23 and 24).

743 In summary, the construction of the Mud Buttes requires at least two phases of
744 south-directed ice sheet advance separated by a period of retreat (Figure 24). The first
745 phase of advance was responsible for the construction of the large imbricate thrust stack
746 (domains 1 and 2) which underlies the main part of the Mud Buttes. Minor oscillations of the
747 ice margin whilst it occupied this position may have locally resulted in the brittle-ductile
748 shearing of the Cretaceous bedrock (domain 3) immediately adjacent to the ice contact part
749 of the mass. The Prospect Valley lobe subsequently retreated northwards, only to readvance
750 southwards once again, accreting a much smaller thrust block (domain 4) onto the up-ice
751 side of the earlier formed (phase 1) and much larger glaciectonic landform. The presence of
752 a palaeosol separating the glaciectonised bedrock from the overlying carapace of subglacial
753 traction till and glaciectonite which mantles the entire Mud Buttes, if it is *in situ*, clearly
754 indicates that these subglacial deposits record a separate (younger) ice advance across this
755 feature (Figure 24). Alternatively, the palaeosol may itself have been emplaced as a raft and
756 hence the stratigraphic integrity of this material in the region requires further study.
757 Stratified sediments within the heavily fragmented and deformed rafts of the lower
758 glaciectonite/till were likely excavated from the proximal depression created by the
759 construction of the Mud Buttes as a hill-hole pair, a depression in which waterlain sediments
760 accumulated during the intervening non-glacial interval. Removal of these sediments, as well
761 as at least most of the palaeosol, occurred during the later ice advance which resulted in the
762 modification of the morphology of the pre-existing composite thrust moraine and the
763 formation of a dome-like cupola-hill accompanied by the formation of the carapace of
764 glaciectonite and till beneath the overriding ice.

765 ***Regional glaciological context of the Mud Buttes and factors controlling thrusting of***
766 ***the Cretaceous bedrock***

767 As noted above, the Mud Buttes along with the Neutral Hills, Misty Hills and Nose Hill form
768 part of a large, regionally extensive assemblage of glaciectonic landforms (Figures 1 and 2)
769 relating to ice stream marginal readvance in southern Alberta (Evans *et al.*, 2008; Ó Cofaigh
770 *et al.*, 2010). The Misty Hills form the southernmost and oldest of these thrust masses
771 (Figure 2). Fenton *et al.* (1993) suggested that initial detachment of the glaciectonised units
772 of the Bearpaw Formation during the construction of the Misty Hills occurred in response to

773 thrusting along the sharp lithostratigraphic boundary between this mudstone-rich marine
774 sequence and the underlying Belly River Group (Mossop and Shetsen, 1994) (see fig. 14 of
775 Fenton *et al.*, 1993). This would have resulted in the effective “stripping” of the younger
776 Bearpaw Formation from the top of the bedrock sequence, exposing the underlying (older)
777 Belly River Group which was glacitectonically “excavated” during the construction of the Mud
778 Buttes. The proglacial nature of the deformation at Mud Buttes indicates that development of
779 this thrust complex occurred in response to a separate, relatively younger readvance(s) to
780 that responsible for the Misty Hills, the latter having been constructed by W-E flowing ice
781 during a pre-2 flow phase (Figures 1b and 3). This indicates that the Misty Hills and Mud
782 Buttes thrust masses have exploited the same substrate conditions and hence the factors
783 governing the initial detachment and subsequent removal of the thrust-bound slabs of
784 bedrock remained (or were reinstated) in approximately the same geographical area during
785 subsequent phases of ice sheet readvance. Sedimentary evidence presented here clearly
786 demonstrates that the Mud Buttes thrust complex was constructed and subsequently
787 overridden by an entirely separate and much younger readvance (flow phase 4; Figures 1b
788 and 3). **If** the palaeosol is *in situ* rather than a raft then the inundation of the Mud Buttes by
789 this later ice flow was preceded by a prolonged interval during which vegetation of a pre-Late
790 Wisconsinan glaciated land surface was accompanied by soil development (Figure 24).

791 Although the Bearpaw Formation-Belly River Group boundary was the most likely
792 focus for thrusting during the construction of the Misty Hills, the factors controlling the
793 development of a major décollement surface associated with the development of the Mud
794 Buttes remain uncertain. It is clear that the force being generated by the advancing ice sheet
795 margin was being transmitted deep into the Belly River Group, with thrusting being
796 partitioned into the weaker mudstones (Figures 5, 7, 8). Thin lenses of peaty looking
797 mudstone exposed along the thrust planes (Figures 10a and b) suggest that thrust
798 propagation may have facilitated along these highly fissile sedimentary rocks. Although
799 some early models argued for the detachment and transport of bedrock blocks (rafts) as a
800 result of their being frozen to the base of the advancing (cold-based) ice (Banham, 1975;
801 Aber, 1988), the structural architecture of the Mud Buttes clearly indicates that they formed
802 as a result of proglacial to ice-marginal thrusting (Figure 24).

803 A number of studies have argued that proglacial to ice marginal thrusting, including
804 the detachment of bedrock rafts in the sandstone of North Dakota (Bluemle and Clayton,
805 1984) and the chalk of North Norfolk, UK (Vaughan-Hirsch *et al.*, 2011, 2013), can be
806 facilitated by the introduction of pressurized meltwater along evolving thrust planes (Bluemle
807 and Clayton, 1984; Ruszczynska-Szenajch, 1987, 1988; Phillips *et al.*, 2008; Phillips and
808 Merritt, 2008; Burke *et al.*, 2009). It has been demonstrated that the periodic over-

809 pressurization of subglacial meltwater systems can lead to hydrofracturing and the
810 introduction of pressurized meltwater (and sediment) into the substrate (Rijsdijk *et al.*, 1999;
811 van der Meer *et al.*, 1999; Kjaer *et al.*, 2006; Phillips *et al.*, 2012). However, hydrofracturing
812 on a scale required to promote the large-scale thrusting observed at Mud Buttes (and
813 elsewhere within the Misty Hills, Neutral Hills and Sharp Hills) would have resulted in
814 significant disruption of the Cretaceous bedrock, evidence of which is not apparent in the
815 field (Figures 5 to 14). Alternatively, Vaughan-Hirsch and Phillips (2016) suggested that the
816 décollement surface at the base of 5 to 6 km wide (maximum thickness 100 to 120 m)
817 imbricate thrust stack which deforms the Aberdeen Ground Formation of the central North
818 Sea formed in response to over-pressurisation of the groundwater system during rapid ice
819 sheet advance (surge-type behaviour). This would result in a marked increase in the
820 hydrostatic gradient, forcing groundwater from beneath the ice sheet (higher overburden
821 pressure) into its forefield (lower pressure) (Boulton and Caban, 1995). A similar model
822 could potentially be applied to the Mud Buttes where surge-type behaviour could lead to a
823 rapid readvance of parts of the Laurentide Ice Sheet margin (Prospect Valley lobe; Figure
824 1b) and pressurisation of groundwater within the underlying Cretaceous bedrock. The
825 resultant increase in water pressure within the Belly River Group could have led to fracturing
826 of the relatively weaker mudstones, lowering their cohesive strength, leading to failure and
827 the potential propagation of several water-lubricated detachments out into the forefield. Once
828 formed, these detachments (bedding-parallel thrusts) would have represented ideal fluid
829 pathways, helping to further transmit pressurized water into the forefield, thereby facilitating
830 the forward propagation of the developing imbricate thrust-stack.

831

832 **Conclusions**

833 The Mud Buttes is one of a number of large-scale glacetectonic landforms (Neutral Hills,
834 Misty Hills) located in southern Alberta, Canada which formed as a result of deformation
835 occurring during ice stream marginal readvance during the overall retreat of the Laurentide
836 Ice Sheet. This large-scale (c. 2 km long, c. 800 m wide) arcuate cupola hill is composed of
837 intensely folded and thrustured sandstones, siltstones and mudstones of the Cretaceous Belly
838 River Formation. A detailed study of the geomorphological setting, structural geology and
839 sedimentology of the Quaternary sediments which overlie the Mud Buttes have revealed that
840 glacetectonism responsible for the evolution of this internally complex landform occurred at
841 the margin of the newly defined Prospect Valley glacier lobe of the Laurentide Ice Sheet.

842 Analysis of the structures within the Mud Buttes clearly indicate that glacetectonism
843 responsible for its construction involved at least two phases of south-directed ice sheet

844 advance separated by a period of retreat. The first phase of advance led to the construction
845 of a large, forward propagating imbricate thrust stack which underlies the main part of the
846 Mud Buttes. The polyphase deformation history recorded by the Belly River Formation within
847 this imbricate stack is diachronous, with each phase becoming progressively younger
848 towards the south. Low-angle to bedding-parallel D1 thrusting during the early stage of ice
849 sheet advance led to the detachment of the thrust-bound bedrock slices and initial
850 shortening of the Belly River Formation. As successively younger (structurally) thrust-slices
851 were accreted to the base of the developing imbricate stack, the structurally higher and older
852 thrust-slices were progressively “back-rotated” (tilted). This tilting was accompanied by D2
853 thrusting and the main phase of folding to have affected the Belly River Formation.
854 Continued thrusting during D3 was restricted to the core of the Mud Buttes as the deforming
855 sequence attempted to accommodate further compression imposed by the advancing ice.
856 Minor oscillations of the ice margin led to localised brittle-ductile shearing (D4) of the
857 Cretaceous bedrock on the ice contact part of the thrust stack. The second phase of ice
858 sheet advance was responsible for the accretion (D5) of the relatively simple thrust and
859 folded sequence of Belly River Formation onto the northern side of Mud Buttes. This was
860 accompanied by the localised reactivation of the earlier developed thrusts and minor box-like
861 folding within the earlier formed imbricate thrust stack.

862 The glacetectonic landform left by these earlier phases of ice advance was
863 subsequently overridden by the Prospect Valley lobe advancing from the NNW. The
864 presence of a palaeosol (if *in situ*) separating the glacetectonised bedrock from the overlying
865 carapace of subglacial traction till and glacetectonite may tentatively be used to suggest that
866 these subglacial deposits record a separate (younger) ice advance. Rafts of stratified
867 sediments the lower glacetectonite/till are thought to have been excavated from the proximal
868 depression created by the construction of the Mud Buttes as a hill-hole pair, a depression in
869 which waterlain sediments accumulated during the intervening interval. Removal of these
870 sediments, as well as at least most of the palaeosol, occurred during the later ice advance
871 which resulted in the modification of the morphology of the pre-existing thrust block moraine
872 and the formation of a dome-like cupola-hill.

873

874 **Acknowledgements**

875 ERP publishes with the permission of the Executive Director of the British Geological
876 Survey, Natural Environmental Research Council. Thanks to Jim Innes in the Geography
877 Department, Durham University for identifying the pollen in the palaeosol at Mud Buttes and
878 Ben Hathway (Alberta Geological Survey) for advice on the regional bedrock stratigraphy.

879

880 **References**

881 Aber, J.S. 1988. Ice-shoved hills of Saskatchewan compared with Mississippi Delta
882 mudlumps - implications for glaciotectionic models. In: Croot, D. (Ed.), *Glaciotectionics:*
883 *Forms and Processes*. Balkema, Rotterdam, 1-9.

884 Aber, J.S., Ber, A. 2007. *Glaciotectionism*. *Development in Quaternary Science* 6, Elsevier,
885 Amsterdam.

886 Aber, J.S., Croot, D.G., Fenton, M.M. 1989. *Glaciotectionic Landforms and Structures*.
887 Kluwer, Dordrecht.

888 Andersen, L.T., Hansen, D.L., Huuse, M. 2005. Numerical modelling of thrust structures in
889 unconsolidated sediments: implications for glaciotectionic deformation. *Journal of Structural*
890 *Geology* 27, 587-596.

891 Atkinson, N., Utting, D.J., Pawley, S.P. 2014a. *Glacial Landforms of Alberta*. Alberta
892 Geological Survey, AER/AGS Map 604.

893 Atkinson, N., Utting, D.J., Pawley, S.P. 2014b. Landform signature of the Laurentide and
894 Cordilleran ice sheets across Alberta during the last glaciatiion. *Canadian Journal of Earth*
895 *Sciences* 51, 1067-1083.

896 Banham, P.H. 1975. Glaciotectionic structures: a general discussion with particular reference
897 to the contorted drift of Norfolk. In: Wright, A.E., Moseley, F. (Eds.), *Ice Ages: Ancient and*
898 *Modern*. Seel House Press, Liverpool, 69-84.

899 Banham, P.H. 1977. Glaciotectionites in till stratigraphy. *Boreas* 6, 101-105.

900 Benn, D.I. 1994a. Fluted moraine formation and till genesis below a temperate glacier:
901 Slettmarkbreen, Jotunheimen, Norway. *Sedimentology* 41, 279–292.

902 Benn, D.I. 1994b. Fabric shape and the interpretation of sedimentary fabric data. *Journal of*
903 *Sedimentary Research A* 64, 910–915.

904 Benn, D.I. 1995. Fabric signature of till deformation, Breiðamerkurjökull, Iceland.
905 *Sedimentology* 42, 735–747.

906 Benn, D.I., Evans, D.J.A. 1996. The interpretation and classification of subglacially-deformed
907 materials. *Quaternary Science Reviews* 15, 23–52.

- 908 Benn, D.I., Evans, D.J.A. 2010. *Glaciers and Glaciation*. Hodder Education, London.
- 909 Bluemle, J.P., Clayton, L. 1983. Large-scale glacial thrusting and related processes in North
910 Dakota. *Boreas* 13, 279-299.
- 911 Bostock H.J.1970a. Physiographic regions of Canada. Geological Survey of Canada Map
912 1254A, scale 1:5 000 000.
- 913 Bostock H.J. 1970b. Physiographic subdivisions of Canada. In: Douglas R.J.W. (ed.),
914 *Geology and Economic Minerals of Canada*. Geological Survey of Canada, Economic
915 Geology Report 1, 11-30.
- 916 Boulton, G.S. and Caban, P. 1995. Groundwater flow beneath ice sheets, part II; It's impact
917 on glacier tectonic structures and moraine formation. *Quaternary Science Reviews* 14, 563-
918 587.
- 919 Burke, H., Phillips, E., Lee, J.R., Wilkinson, I.P. 2009. Imbricate thrust stack model for the
920 formation of glaciotectionic rafts: an example from the Middle Pleistocene of north Norfolk,
921 UK. *Boreas* 38, 620-637.
- 922 Carlson, V.A. 1969. Bedrock topography of the Oyen map area NTS 72M, Alberta. Research
923 Council of Alberta, 1:250,000 scale map.
- 924 Christiansen, E.A., Whitaker, S.H. 1976. Glacial thrusting of drift and bedrock. In Leggett, R.
925 F. (ed.): *Glacial Till*, 121–130. Royal Society of Canada, Special Publication 12.
- 926 Clayton, L., Cherry, J.A. 1967. Pleistocene superglacial and ice walled lakes of west-central
927 North America. *North Dakota Geological Survey, Miscellaneous Series* 30, 47–52.
- 928 Clayton, L., Moran, S.R. 1974. A glacial process-form model. In: Coates, D.R. (ed.): *Tills and*
929 *Glaciotectonics*, 183–195. A. A. Balkema, Rotterdam.
- 930 Clayton, L., Attig, J.W., Ham, N.R., Johnson, M.D., Jennings, C.E., Syverson, K.M. 2008.
931 Ice-walled-lake plains: implications for the origin of hummocky glacial topography in middle
932 North America. *Geomorphology* 97, 237–248.
- 933 Cowan, D.S. 1985. Structural styles in Mesozoic and Cenozoic mélanges in the western
934 Cordillera of North America. *Geological Society of America Bulletin* 96, 451-462.
- 935 Croot, D.G. 1987. Glaciotectonic structures: a mesoscale mode of thin-skinned thrust
936 sheets? *Journal of Structural Geology* 9, 797, 808.

937 Dahlen, F., Suppe, J., Davis, D., 1984. Mechanics of fold-and-thrust belts and accretionary
938 wedges: Cohesive Coulomb theory. *Journal of Geophysical Research* 89, 10087–10101.

939 Davis, D., Suppe, J., Dahlen, F.A. 1984. Mechanics of fold-and-thrust belts and accretionary
940 wedges: Cohesive Coulomb theory. *Journal of Geophysical Research* 89, 10087-10101.

941 Evans, D.J.A., 2000. Quaternary geology and geomorphology of the Dinosaur Provincial
942 Park area and surrounding plains, Alberta, Canada: the identification of former glacial lobes,
943 drainage diversions and meltwater flood tracks. *Quaternary Science Reviews* 19, 931–958.

944 Evans, D.J.A. 2007. Glacitectonic structures and landforms. *Encyclopaedia of Quaternary
945 Science*, Elsevier Publishing, Oxford, 831-838.

946 Evans, D.J.A. In press. *Till: A Glacial Process Sedimentology*. Wiley Blackwell, Chichester.

947 Evans, D.J.A., Benn, D.I. 2004. Facies description and the logging of sedimentary
948 exposures. In: Evans, D.J.A., Benn, D.I. (Eds.), *A Practical Guide to the Study of Glacial
949 Sediments*. Arnold, London, pp. 11-51.

950 Evans, D.J.A., Hiemstra, J.F., 2005. Till deposition by glacier submarginal, incremental
951 thickening. *Earth Surface Processes and Landforms* 30, 1633-1662.

952 Evans, D.J.A., Phillips, E.R., Hiemstra, J.F., Auton, C.A. 2006. Subglacial till: formation,
953 sedimentary characteristics and classification. *Earth Science Reviews* 78, 115-176.

954

955 Evans, D.J.A., Clark, C.D., Rea, B.R., 2008. Landform and sediment imprints of fast glacier
956 flow in the southwest Laurentide Ice Sheet. *Journal of Quaternary Science* 23, 249–272.

957

958 Evans, D.J.A., Hiemstra, J.F., Ó Cofaigh, C., 2007. An assessment of clast macrofabrics in
959 glaciogenic sediments based on A/B plane data. *Geografiska Annaler* A89, 103-120.

960

961 Evans, D.J.A., Young, N.J., Cofaigh, C., 2014. Glacial geomorphology of terrestrial
962 terminating fast flow lobes/ice stream margins in the southwest Laurentide ice sheet.
963 *Geomorphology* 204, 86–113.

964

965 Evans, D.J.A., Storrar, R.D., Rea, B.R. 2016. Crevasse-squeeze ridge corridors: Diagnostic
966 features of late-stage palaeo-ice stream activity. *Geomorphology* 258, 40-50.

967

- 968 Evans, D.J.A., Atkinson, N., Phillips, E.R. In prep. Glacial geomorphology of the Neutral Hills
969 Uplands, Alberta, Canada: on the process-form imprints of dynamic ice streams and ice
970 lobes. *Geomorphology*.
- 971 Eyles, N., Eyles, C.H., Miall, A.D. 1983. Lithofacies types and vertical profile models; an
972 alternative approach to the description and environmental interpretation of glacial diamict
973 and diamictite sequences. *Sedimentology* 30, 393-410.
- 974 Fenton, M.M., Langenberg, W., Pawlowicz, J. 1993. Glacial deformation phenomena of east-
975 central Alberta in the Stettler-Coronation region. Field trip B-1, Guidebook. Geological
976 Association of Canada, Mineralogical Association of Canada, pp 46.
- 977 Fenton, M.M., Waters, E.J., Pawley, S.M., Atkinson, N., Utting, D.J., McKay, K. 2013.
978 Surficial geology of Alberta. Alberta Geological Survey, AER/AGS Map 601.
- 979 Gehrmann, A., Hüneke, H., Meschede, M., Phillips, E. 2016. 3D microstructural architecture
980 of deformed glacial sediments associated with large-scale glaciectonism, Jasmund
981 Peninsula (NE Rügen), Germany. *Journal of Quaternary Science* DOI: 10.1002/jqs.2843.
- 982 Glombick P. 2010. Top of the Belly River Group in the Alberta Plains: subsurface
983 stratigraphic picks and modelled surface. Energy Resources Conservation Board,
984 ERCB/AGS Open File 2010-10, pp 27.
- 985 Gravenor, C.P., Kupsch, W.O. 1959. Ice disintegration features in western Canada. *Journal*
986 *of Geology* 67, 48–64.
- 987 Harris, C., Brabham, P., Williams, G.D. 1995. Glaciotectonic structures and their relation to
988 topography at Dinas Dinlle, Arvon, northwest Wales. *Journal of Quaternary Science* 10,
989 397–399.
- 990 Harris, C., Williams, G., Brabham, P., Eaton, G., McCarroll, D. 1997. Glaciotectonized
991 Quaternary sediments at Dinas Dinlle, Gwynedd, North Wales, and the bearing on the style
992 of deglaciation in the eastern Irish Sea. *Quaternary Science Reviews* 16, 109-127.
- 993 Hiemstra, J.F., Evans, D.J.A., Ó Cofaigh, C. 2007. The role of glaciectonic rafting and
994 comminution in the production of subglacial tills: examples from SW Ireland and Antarctica.
995 *Boreas* 36, 386–399.
- 996 Hicock, S.R., Goff, J.R., Lian, O.B., Little, E.C. 1996. On the interpretation of subglacial till
997 fabric. *Journal of Sedimentary Research* 66, 928–934.

- 998 Hopkins, O.B., 1923. Some structural features of the plains area of Alberta caused by
999 Pleistocene glaciation. *Bulletin of the Geological Society of America* 34, 419–430.
- 1000 Hooyer, T.S., Iverson, N.R. 2000. Diffusive mixing between shearing granular layers:
1001 constraints on bed deformation from till contacts. *Journal of Glaciology* 46, 641–651.
- 1002 Huuse, M., Lykke-Andersen, H. 2000. Overdeepened Quaternary valleys in the eastern
1003 Danish North Sea: morphology and origin. *Quaternary Science Reviews* 19, 1233-1253.
- 1004 Ildefonse, B., Mancktelow, N.S. 1993. Deformation around rigid particles: the influence of
1005 slip at the particle/matrix interface. *Tectonophysics* 221, 345–359.
- 1006 Johnson, M.D., Clayton, L. 2003. Supraglacial landsystems in lowland terrain. In: Evans,
1007 D.J.A. (Ed.), *Glacial Landsystems*. Arnold, London, 228–251.
- 1008 Kjær, K.H., Larsen, E., van der Meer, J.J.M., Ingólfsson, Ó., Krüger, J., Benediktsson, Í.Ö.,
1009 Knudsen, C.G., Schomacker, A. 2006. Subglacial decoupling at the sediment/bedrock
1010 interface: a new mechanism for rapid flowing ice. *Quaternary Science Reviews* 25, 2704-
1011 2712.
- 1012 Lee, J.R., Phillips, E., Booth, S.J., Rose, J., Jordan, H.M., Pawley, S.M., Warren, M., Lawley,
1013 R.S. 2013. A polyphase glacetectonic model for ice-marginal retreat and terminal moraine
1014 development: the Middle Pleistocene British Ice Sheet, northern Norfolk, UK. *Proceedings of*
1015 *the Geologists Association*, 124. 753-777.
- 1016 Lee, J.R., Phillips, E., Rose, J., Vaughan-Hirsch, D. 2016. The Middle Pleistocene glacial
1017 evolution of northern East Anglia, UK: a dynamic tectonostratigraphic–parasequence
1018 approach. *Journal of Quaternary Science* DOI: 10.1002/jqs.2838.
- 1019 March, A. 1932. Mathematische Theorie der Regelung nach der Korngestalt bei affiner
1020 Deformation. *Zeitschrift für Kristallographie* 81, 285-297.
- 1021 Moran, S.R., Clayton, L., Hooke, R., Fenton, M.M., Andriashek, L.D. 1980. Glacier-bed
1022 landforms of the prairie region of North America. *Journal of Glaciology* 25, 457-473.
- 1023 Mossop, G.D., Shetsen I. 1994. *Geological Atlas of the Western Canada Sedimentary Basin*.
1024 Canadian Society of Petroleum Geologists and Alberta Research Council, Special Report,
1025 510 p.
- 1026 Mulugeta, G., Koyi, H. 1987. Three-dimensional geometry and kinematics of experimental
1027 piggyback thrusting. *Geology* 15, 1052–1056.

- 1028 Nieuwland, D.A., Leutscher, J.H., Gast, J., 2000. Wedge equilibrium in fold-and thrust belts:
1029 prediction of out-of-sequence thrusting based on sandbox experiments and natural
1030 examples. *Geologie en Mijnbouw/Netherlands Journal of Geosciences* 79, 81–91.
- 1031 Ó Cofaigh, C., Evans, D.J.A., Smith, I.R. 2010. Large-scale reorganization and
1032 sedimentation of terrestrial ice streams during late Wisconsinan Laurentide ice sheet
1033 deglaciation. *Geological Society of America Bulletin*, 122: 743–756.
- 1034 Pedersen, S.A.S. 1987. Comparative studies of gravity tectonics in Quaternary sediments
1035 and sedimentary rocks related to fold belts. In: Jones, M.E., Preston, R.M.F. (Eds.),
1036 *Sediment Deformation Mechanisms*. Geological Society of London, Special Publication 29,
1037 pp. 43–65.
- 1038 Pedersen, S.A.S., 1989. Glaciotectonite: brecciated sediments and cataclastic sedimentary
1039 rocks formed subglacially. In: Goldthwait, R.P., Matsch, C.L. (Eds.), *Genetic Classification of*
1040 *Glacigenic Deposits*. Balkema, Rotterdam, pp. 89–91.
- 1041 Pedersen, S.A.S. 2005. Structural analysis of the Rubjerg Knude Glaciotectonic Complex,
1042 Vendsyssel, northern Denmark. *Geological Survey of Denmark and Greenland Bulletin* 8,
1043 192 pp.
- 1044 Pedersen, S.A.S. 2014. Architecture of Glaciotectonic Complexes. *Geosciences* 2014, 4,
1045 269-296.
- 1046 Pedersen, S.A.S., Boldreel, L.O. 2016. Glaciotectonic deformations in the Jammerbugt and
1047 the glaciodynamic development in the eastern North Sea. *Journal of Quaternary Science* (in
1048 press).
- 1049 Pettapiece, W.W. 1986. Physiographic subdivisions of Alberta. *Agriculture and Agri-Food*
1050 *Canada, Ottawa, Ontario*.
- 1051 Phillips, E., Merritt, J. 2008. Evidence for multiphase water-escape during rafting of shelly
1052 marine sediments at Clava, Inverness-shire, NE Scotland. *Quaternary Science Reviews* 27,
1053 988-1011.
- 1054 Phillips, E., Lee, J.R., Burke, H. 2008. Progressive proglacial to subglacial deformation and
1055 syntectonic sedimentation at the margins of the Mid-Pleistocene British Ice Sheet: evidence
1056 from north Norfolk, UK. *Quaternary Science Reviews* 27, 1848-1871.

- 1057 Phillips, E., Everest, J., Reeves, H. 2012. Micromorphological evidence for subglacial
1058 multiphase sedimentation and deformation during overpressurized fluid flow associated with
1059 hydrofracturing. *Boreas*, 42, 395–427.
- 1060 Prior, G.J., Hathway, B., Glombick, P.M., Paná, D.I., Banks, C.J., Hay, D.C., Schneider,
1061 C.L., Grobe, M., Elgr, R., Weiss, J.A. 2013. Bedrock geology of Alberta. Alberta Energy
1062 Regulator, AER/AGS Map 600, scale 1:1 000 000.
- 1063 Rijdsdijk, K.F., McCarroll, D., Owen, G., van der Meer, J.J.M., Warren, W.P. 1999. Clastic
1064 dykes in glacial diamicts: Evidence for subglacial hydrofracturing from Killiney Bay,
1065 Ireland. *Sedimentary Geology* 129, 111-126.
- 1066 Roberts, D.H., Dackombe, R.V., Thomas, G.S.P. 2006. Palaeo-ice streaming in the central
1067 sector of the British-Irish Ice Sheet during the Last Glacial Maximum: evidence from the
1068 northern Irish Sea Basin. *Boreas* 36, 115-129.
- 1069 Ross, M., Campbell, J.E., Parent, M., Adams, R.S. 2009. Palaeo-ice streams and the
1070 subglacial landscape mosaic of the North American mid-continental prairies. *Boreas* 38,
1071 421–439.
- 1072 Rotnicki, K., 1976. The theoretical basis for and a model of glaciotectionic deformation.
1073 *Quaestiones Geographicae* 3, 103–139.
- 1074 Ruszczynska-Szenajch, H. 1987. The origin of glacial rafts: Detachment, transport,
1075 deposition. *Boreas* 16, 101-112.
- 1076 Ruszczynska-Szenajch, H. 1988. Glaciotectionics and its relationship to other glaciogenic
1077 processes. In Croot, D.G. (ed.): *Glaciotectionic Forms and Processes*, 191–193. Balkema,
1078 Rotterdam.
- 1079 Sauer, E.K. 1978. The engineering significance of glacier ice thrusting. *Canadian*
1080 *Geotechnical Journal* 15, 457–472.
- 1081 Shetsen, I. 1987. Quaternary geology, southern Alberta. Alberta Geological Survey, Map
1082 207.
- 1083 Shetsen, I. 1990. Quaternary geology, central Alberta. Alberta Geological Survey, Map 213.
- 1084 Slater, G. 1927. Structure of the Mud Buttes and Tit Hills in Alberta. *Bulletin of the*
1085 *Geological Society of America* 38.

- 1086 Slater, G. 1931. The structure of the Bride Moraine, Isle of Man. Proceedings of the
1087 Liverpool Geological Society 14, 186-196.
- 1088 Steinich, G. 1972. Endogene Tektonik in den Unter-Maastricht-Vorkommen auf Jasmund
1089 (Rügen). In: Geologie 20, Beiheft 71/72, S. 1 - 207. Berlin.
- 1090 Thomas, G.S.P., Chiverrell, R.C. 2007. Structural and depositional evidence for repeated
1091 ice-marginal oscillation along the eastern margin of the Late Devensian Irish Sea Ice
1092 Stream. Quaternary Science Reviews 26, 2375-2405.
- 1093 Thomas, G.S.P., Chiverrell, R.C. 2011. Styles of structural deformation and syntectonic
1094 sedimentation around the margins of the Late Devensian Irish Sea Ice Stream: the Isle of
1095 Man, Llyn Peninsula and County Wexford. In Phillips, E., Lee, J.R., Evans, H.M. (Eds.).
1096 2011. Glacitectonics – Field Guide. Quaternary Research Association.
- 1097 Thomas, G.S.P., Chiverrell, R.C., Huddart, D., Long, D., Roberts, D.H. 2006. The Ice Age In:
1098 Chiverrell RC and Thomas GSP (eds.). A New History of the Isle of Man: Volume 1 Evolution
1099 of the natural landscape. Liverpool University Press, 126-219.
- 1100 Tsui, P.C., Cruden, D.M., Thomson, S. 1989. Ice thrust terrains and glaciotectionic settings in
1101 central Alberta. Canadian Journal of Earth Sciences 26, 1308-1318.
- 1102 van Gijssel, K. 1987. A lithostratigraphic and glaciotectionic reconstruction of the Lamstedt
1103 Moraine, Lower Saxony (FRG). In: J.J.M. van der Meer (ed.). Tills and Glaciotectionics.
1104 Balkema, Rotterdam, 145-155.
- 1105 van der Meer, J.J.M., Kjær, K.H., Krüger, J., Rabassa, J., Kilfeather, A.A., 2009. Under
1106 pressure: clastic dykes in glacial settings. Quaternary Science Reviews. 28, 708-720.
- 1107 van der Wateren, F.M. 1985. A model of glacial tectonics, applied to the ice-pushed ridges in
1108 the central Netherlands. Bulletin of the Geological Society of Denmark 34, 55-77.
- 1109 van der Wateren, F.M. 1987. Structural geology and sedimentology of the Dammer Berge
1110 push moraine, FRG. In: J.J.M. van der Meer (ed.). Tills and Glaciotectionics. Balkema,
1111 Rotterdam, 157-182.
- 1112 van der Wateren, F.M. 1995. Structural geology and sedimentology of push moraines.
1113 Mededelingen Rijks Geologische Dienst 54. PhD, University of Amsterdam.

- 1114 van der Wateren, F.M. 2005. Ice-marginal terrestrial landsystems: Southern Scandinavian
 1115 Ice Sheet Margin. In: Evans, D.J.A. (Ed.), *Glacial Landsystems*. Hodder Arnold, London, pp.
 1116 166–203.
- 1117 Vaughan-Hirsch, D., Phillips, E., 2016. Mid-Pleistocene thin-skinned glaciotectonic thrusting
 1118 of the Aberdeen Ground Formation, Central Graben region, central North Sea. *Journal of*
 1119 *Quaternary Science* (in press)
- 1120 Vaughan-Hirsch, D.P., Phillips, E.R., Lee, J.R., Burke, H.F. Hart, J.K. 2011: Glacitectonic
 1121 rafting of chalk bedrock: Overstrand. In Phillips, E., Lee, J. R. & Evans, H. M. (eds.):
 1122 *Glacitectonics – Field Guide*. Quaternary Research Association, Pontypool. 198–217.
- 1123 Vaughan-Hirsch, D.P., Phillips, E., Lee, J.R., Hart, J.K. 2013. Micromorphological analysis of
 1124 poly-phase deformation associated with the transport and emplacement of glaciotectonic
 1125 rafts at West Runton, north Norfolk, UK. *Boreas* 42, 376–394.
- 1126 Williams, G., Brabham, P., Eaton, G., Harris, C., 2001. Late Devensian glaciotectonic
 1127 deformation at St Bees, Cumbria: a critical wedge model. *Journal of the Geological Society*
 1128 158, 125–135.

1129

1130 **Figures**

1131 **Figure 1. (a)** DEM showing place names referred to in text and major geomorphological
 1132 features of the study area and its regional context. Inset shows the surficial geology of the
 1133 study area (from Fenton *et al.*, 2013. E: aeolian deposits; LG: glaciolacustrine deposits; FG:
 1134 glaciofluvial deposits; M: undifferentiated moraine (diamict); MS: stagnation moraine; MF:
 1135 fluted moraine; MT: ice thrust moraine); and **(b)** Features identified on the DEM include
 1136 major glacitectonic thrust masses (green shade) and the margins and flow directions (circled
 1137 numbers and arrows) of the main ice flow phases including, from oldest to youngest, 1
 1138 (white), 2 (pink), 3 (blue), 4 (black), 5 (red) and 6 (yellow). Major moraines (from Evans *et*
 1139 *al.*, in prep) include: HM – Handel Moraine of Evans *et al.* (2016); AM – Altario Moraine; VM
 1140 – Veteran Moraine; GIM – Grassy Island Moraine; MB – Mud Buttes.

1141 **Figure 2.** Annotated DEM of the field area, showing major moraines and other major glacial
 1142 landforms (from Evans *et al.*, in prep). Also outlined are areas of major glacitectonically
 1143 thrust masses (green outline), significant hummocky terrain (blue outline) and fluted thrust
 1144 moraine (black outline).

1145 **Figure 3.** Annotated DEM of the Misty Hills and associated landforms. The Misty Hills thrust
 1146 structures are outlined in pink and the direction of ice flow related to their original

1147 construction is designated by the pre-2 ice flow phase arrows. Subsequent ice lobe margins
1148 and flow phases are identified by blue lines and arrows (phase 3a and 3b) and black arrows
1149 for phase 4, during which the Mud Buttes and a further cupola hill to the north were
1150 constructed and overrun.

1151 **Figure 4. (a)** Annotated aerial image (Google Earth) of the Mud Buttes, SW Monitor, Alberta,
1152 Canada; **(b)** Structural geology map of the Mud Buttes thrust complex (inset showing the
1153 location of the Mud Buttes); **(c)** to **(g)** Lower hemisphere stereographic projections showing
1154 the structural data - **(c)** and **(d)** bedding (dip and dip-direction), **(e)** and **(f)** thrusts/faults (dip
1155 and dip-direction), **(g)** folds (plunge); and **(h)** Rose diagram showing trend of fold axes.

1156 **Figure 5. (a)** and **(b)** Large-scale thrusting and repetition of Belly River Formation
1157 sandstones, siltstones and mudstones within structural domain 1 of the Mud Buttes thrust
1158 complex [UTM 0531208 5743775].

1159 **Figure 6. (a)** Large-scale thrusting and repetition of Belly River Formation sandstones,
1160 siltstones and mudstones within structural domain 1 of the Mud Buttes thrust complex; **(b)**
1161 Asymmetrical, inclined asymmetrical anticline-syncline fold pair (see Figure 3a for location of
1162 fold) [UTM 0530927 5743980]; **(c)** Detail of asymmetrical S-C fabric developed within thrust
1163 indicating a southerly directed sense of shear on this structure [UTM 0530927 5743980].

1164 **Figure 7.** Large-scale thrusting and repetition of Belly River Formation sandstones,
1165 siltstones and mudstones within structural domain 2a of the Mud Buttes thrust complex: **(a)**
1166 Large-scale synclines developed within the foot-walls of two prominent northerly dipping
1167 thrusts [UTM 0531021 5744096]; and **(b)** Folding and thrusting characteristic of structural
1168 domain 2a [UTM 0531294 5743835].

1169 **Figure 8. (a)** to **(c)** Large-scale thrusting and repetition of Belly River Formation sandstones,
1170 siltstones and mudstones within structural domain 2a of the Mud Buttes thrust complex. Note
1171 the progressive increase in the angle of dip of the thrust slices from south to north across the
1172 domain [(a) UTM 0531285 5743922; (b) UTM 0531399 5743894; (c) UTM 0531320
1173 5743983].

1174 **Figure 9. (a)** Large-scale, upright 'box-like' anticline deforming not only bedding within the
1175 Belly River Formation but also a set of earlier developed low-angle (relative to bedding) to
1176 bedding-parallel (T1) thrusts [UTM 0530992 5744093]; **(b)** Large-scale, upright, M-shaped
1177 'box-like' anticline developed adjacent to the southern margin of structural domain 2a; and
1178 **(c)** Parasitic minor folds developed upon a mesoscale south-verging anticline and syncline
1179 fold pair. Note that the folds deform a set of earlier developed (T1) thrusts and a later set of

1180 small-scale, southerly directed (T2) thrusts developed within the core of the anticline [UTM
1181 0531385 5744105].

1182 **Figure 10. (a) and (b)** Large-scale thrusting of the Belly River Formation within domain 2a.
1183 The prominent thrust planes are preferentially developed within the weaker mudstones
1184 immediately adjacent to the bases of the more competent sandstones. The thrust planes are
1185 marked by thin lenses of fissile, organic-rich mudstones [UTM 0531320 5743983]; **(c)** and
1186 **(d)** Well-developed, asymmetrical S-C fabrics developed within narrow brittle-ductile shear
1187 zones cutting the Belly River Formation sandstones and siltstones in structural domain 3 [(c)
1188 [UTM 0531205 5744179]; (d) UTM 0531212 5744159]; and **(e)** Large-scale, upright fold in
1189 domain 2b truncated by a gently north-dipping thrust interpreted as marking the base of
1190 structural domain 4 [UTM 0531510 5744107].

1191 **Figure 11.** Large-scale folding and thrusting of structural domain 2b [UTM 0530992
1192 5744174]. Note the zone of complex folding and thrusting developed within the unit of thinly
1193 interbedded sandstones, siltstones and mudstones.

1194 **Figure 12.** Large-scale folding and thrusting within the core of the Mud Buttes thrust
1195 complex and characteristic of structural domain 2b: **(a)** Steeply inclined, tight to isoclinal,
1196 southerly verging folds deforming the sandstones of the Belly River Formation [UTM
1197 0531078 5744120]. Note that the very tight to isoclinal fold toward the centre of the
1198 photograph is deformed by a number of brittle thrusts; and **(b)** Large-scale southerly verging
1199 folds deforming a 2 to 3 m thick sandstone unit within the Belly River Formation [UTM
1200 0531221 5744112].

1201 **Figure 13. (a)** Photograph showing the zone of intense brittle-ductile shearing which
1202 characterises structural domain 3 of the Mud Buttes thrust complex [UTM 0531212
1203 5744159]; **(b)** Truncated, non-cylindrical, isoclinal folds deforming the sandstones within the
1204 shear zone marking the southern boundary of structural domain 3 [UTM 0531385 5744105];
1205 and **(c)** Intense ductile shearing within a more mudstone-rich unit exposed adjacent to the
1206 southern margin of structural domain 3 [UTM 0531385 5744105].

1207 **Figure 14. (a) and (b)** Large-scale folding and thrusting characterising structural domain 4
1208 located on the northern side of the Mud Buttes thrust complex [(a) UTM 0531267 5744288;
1209 (b) UTM 0531178 5744379].

1210 **Figure 15.** Previously published structural cross-sections through the Mud Buttes thrust
1211 complex: **(a)** Slater (1927) (fig. 1 of Slater 1927); and **(b)** Fenton *et al.* (1993) (fig. 16 of
1212 Fenton *et al.*, 1993).

1213 **Figure 16.** Lithological log and field photograph of the section through the Quaternary
1214 sediments overlying the glacitected bedrock exposed in section MBQ 1.

1215 **Figure 17. (a) to (c)** Photographs showing the vertical continuum of well-exposed, deformed
1216 and sheared mudstone capped by a poorly exposed, clay-rich diamicton exposed within
1217 section MBQ 2.

1218 **Figure 18. (a)** Lithological log and field photograph of the section through the Quaternary
1219 sediments overlying the glacitected bedrock exposed in section MBQ 3; and **(b)** to be
1220 added by Dave.

1221 **Figure 19.** Lithological log and field photograph of the section through the Quaternary
1222 sediments overlying the glacitected bedrock exposed in section MBQ 4. Also shown is
1223 spherical Gaussian weighted, contoured lower hemisphere stereographic projection of the
1224 clast macrofabric data obtained from the diamicton exposed the top of this sequence.

1225 **Figure 20. (a)** Ternary diagram of $I = S_3/S_1$ versus $E = 1-(S_2/S_1)$ for the clast macrofabrics at
1226 sections MBQ 4 and MBQ 5. Also shown are the fields defined by clasts macrofabrics from
1227 the glacitected continuum (Evans *et al.*, 1988), subglacial till (Evans and Hiemstra, 2005)
1228 and lodged clasts (Evans and Hiemstra, 2005); and **(b)** Graph showing the variation in clast
1229 macrofabric modality versus S_3/S_1 isotropy.

1230 **Figure 21.** Lithological log and field photograph of the section through the Quaternary
1231 sediments overlying the glacitected bedrock exposed in section MBQ 5. Also shown is
1232 spherical Gaussian weighted, contoured lower hemisphere stereographic projection of the
1233 clast macrofabric data obtained from the diamicton exposed at this locality.

1234 **Figure 22.** Composite vertical logs with genetic facies codes for the Quaternary stratigraphic
1235 sequences exposed at Mud Buttes.

1236 **Figure 23.** Schematic cross-section through the Mud Buttes showing the structural
1237 architecture of this glacitectonic thrust complex (see text for details) (see Figure 1b for the
1238 approximate location of the line of section).

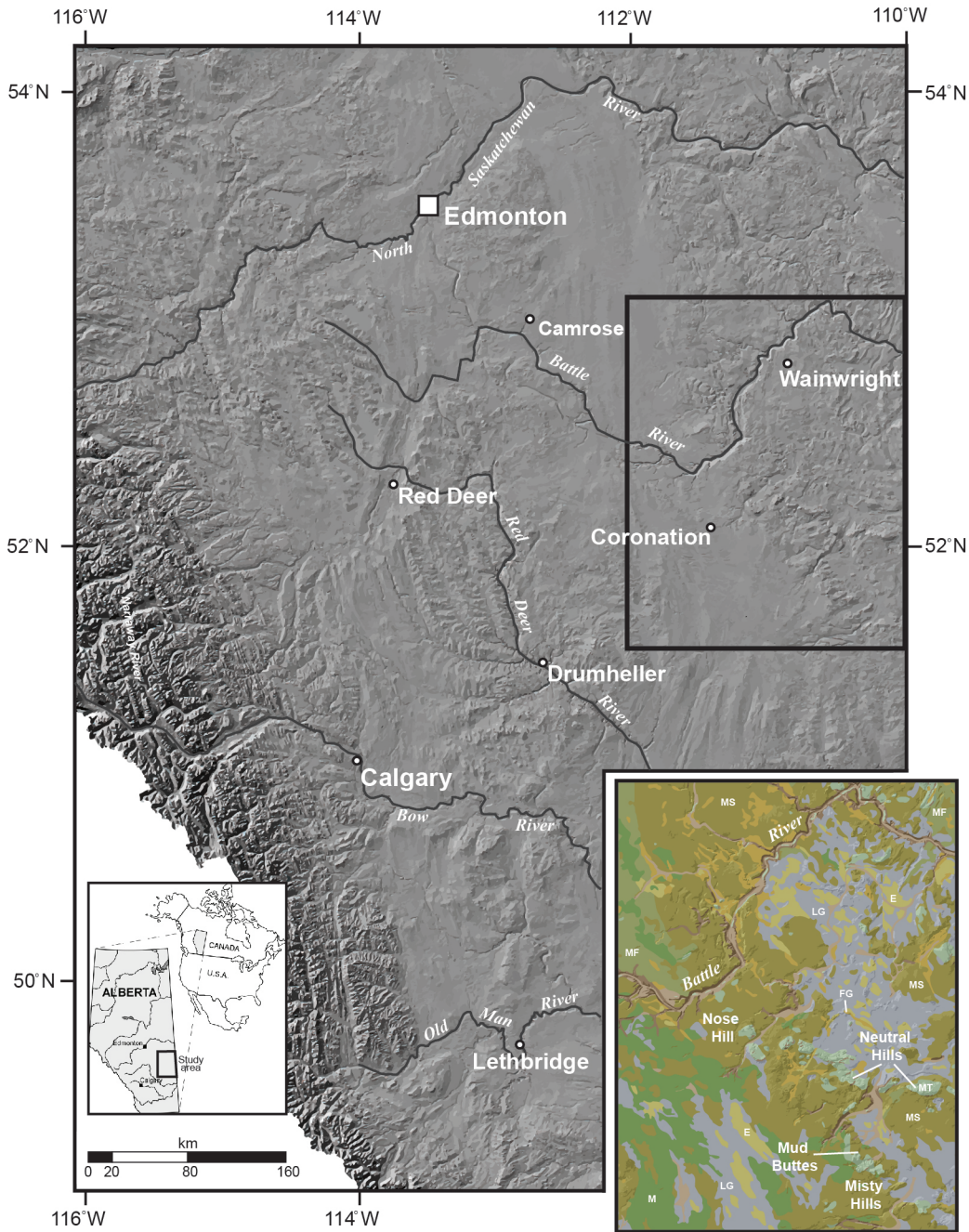
1239 **Figure 24. (a) to (h)** Cartoon showing the evolution of the Mud Buttes thrust complex as a
1240 result of proglacial deformation and this landform being subsequently overridden by ice
1241 during a later readvance to form a dome-like cupola hill (see text for details).

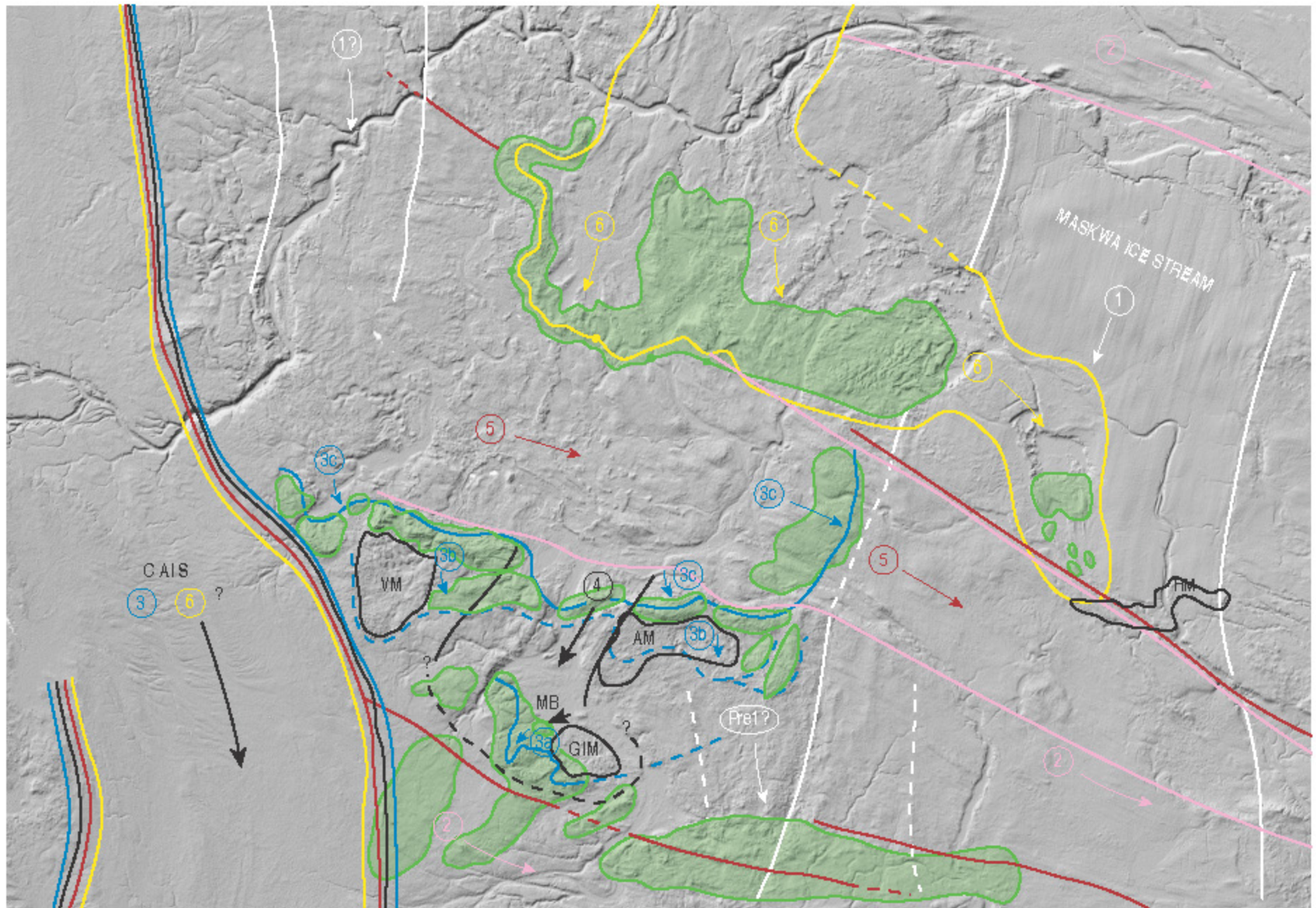
1242

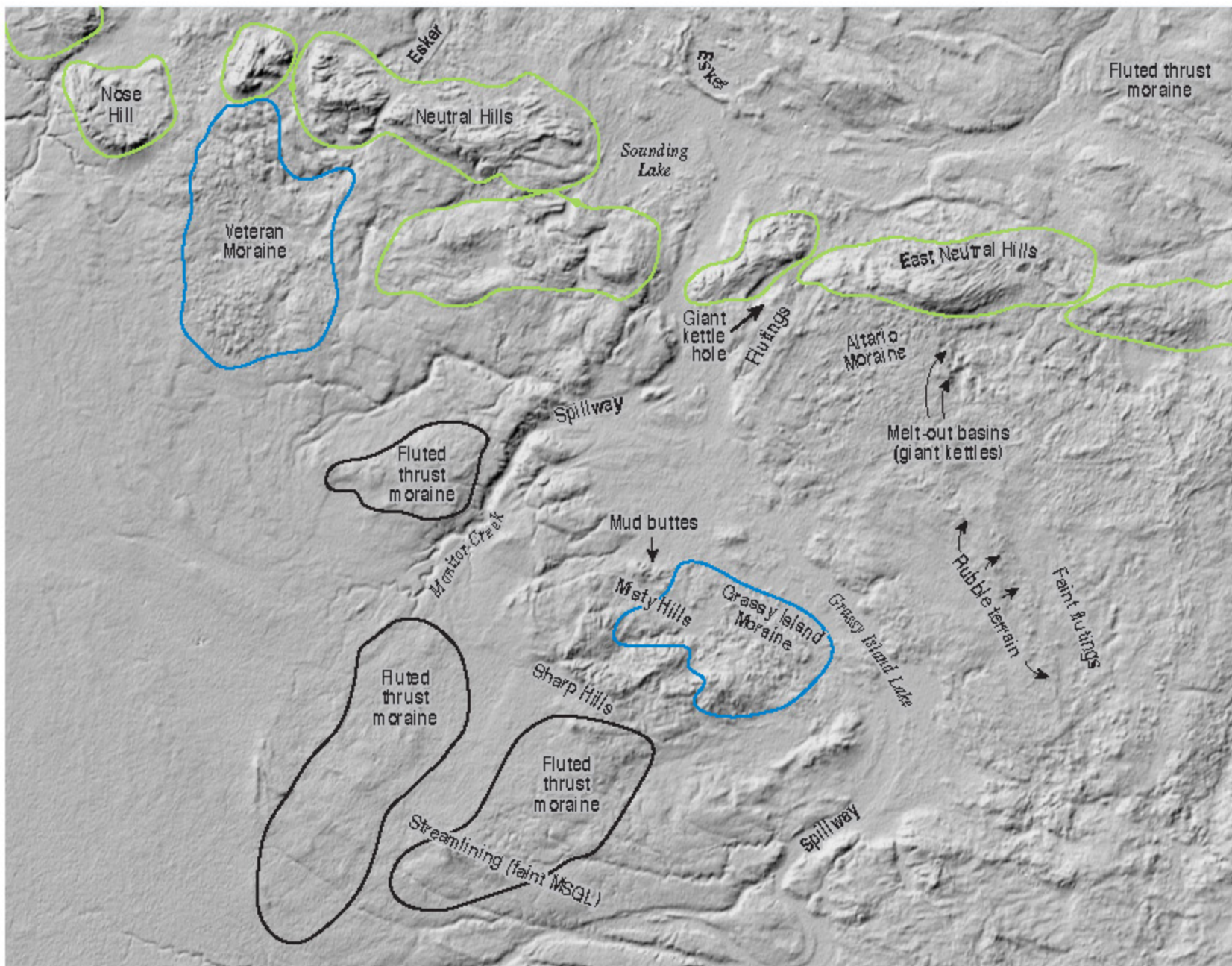
1243 **Table 1.** Pollen types detected in the organic-rich clayey-silt exposed at Section MBQ 4

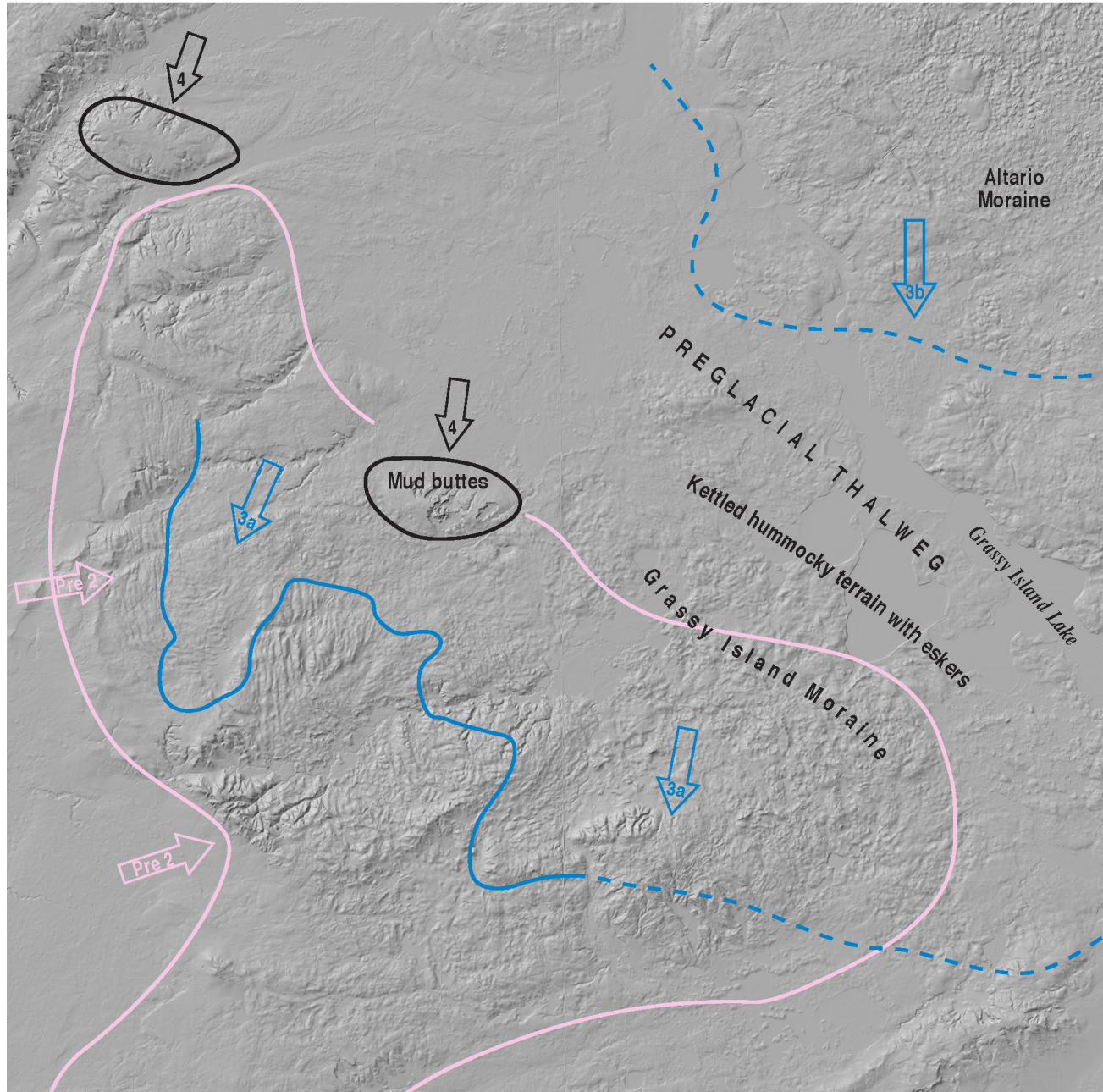
Species	Sample 15008/1	Sample 15008/2 upper	Sample 15008/2 lower
Pine	1		
Hazel	1		
Grass	1		
Artemisia	2		1
Spruce/fir		1	
Tsuga		1	
Sedges		3	
Rumex		1	
<i>Scrophulariaceae</i>		2	
<i>Chenopodiaceae</i>			1

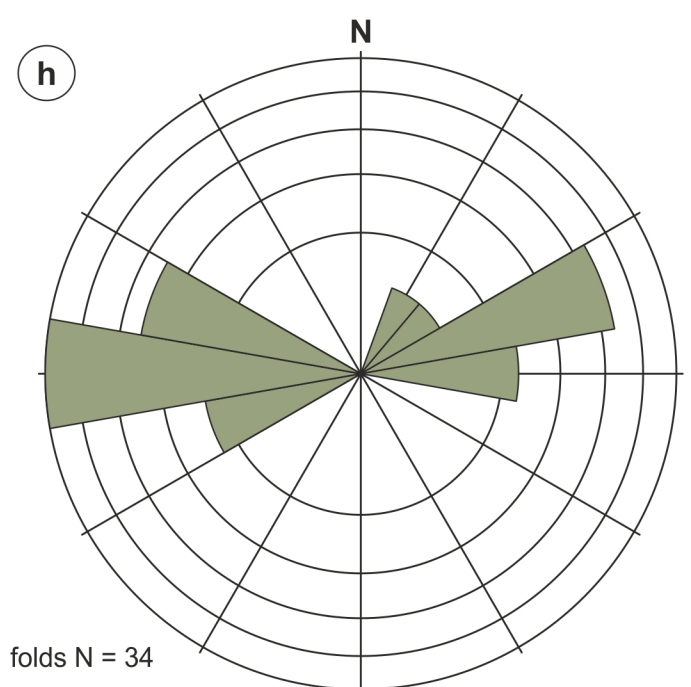
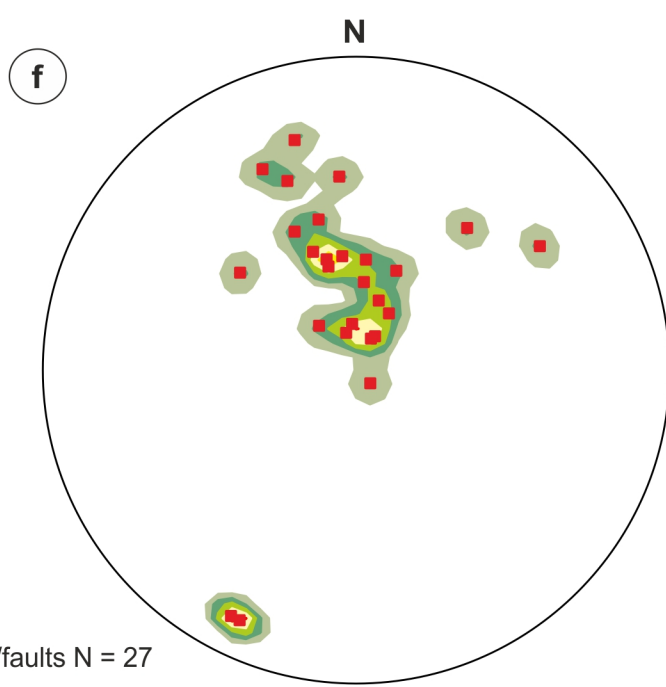
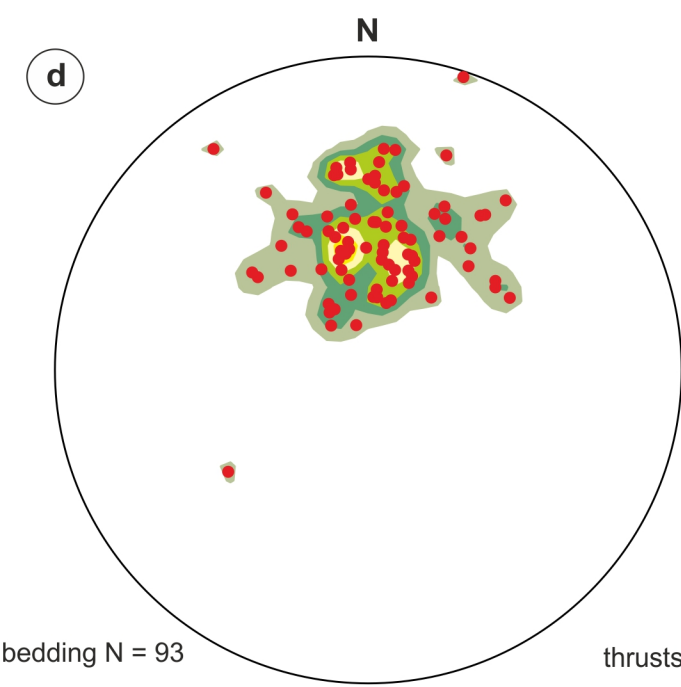
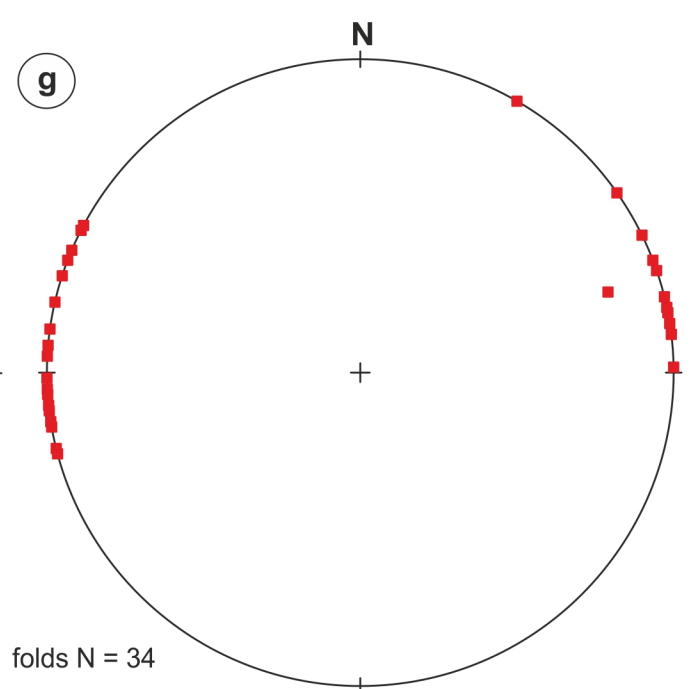
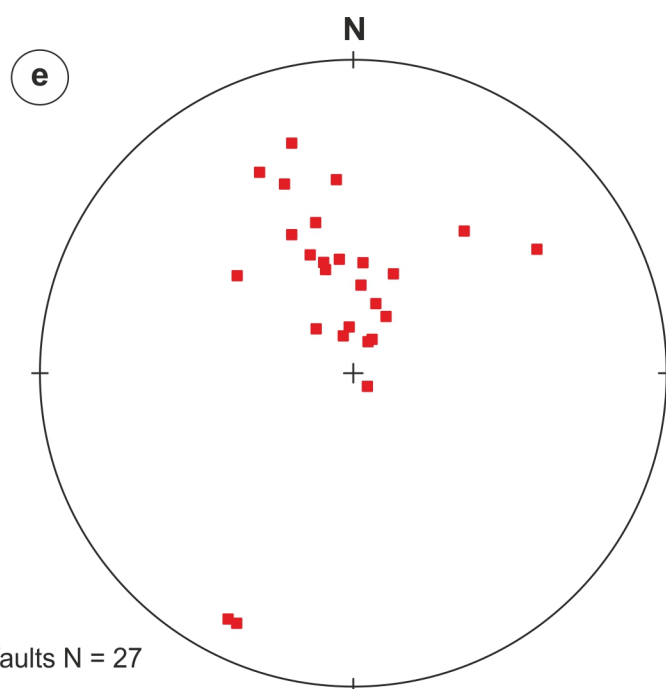
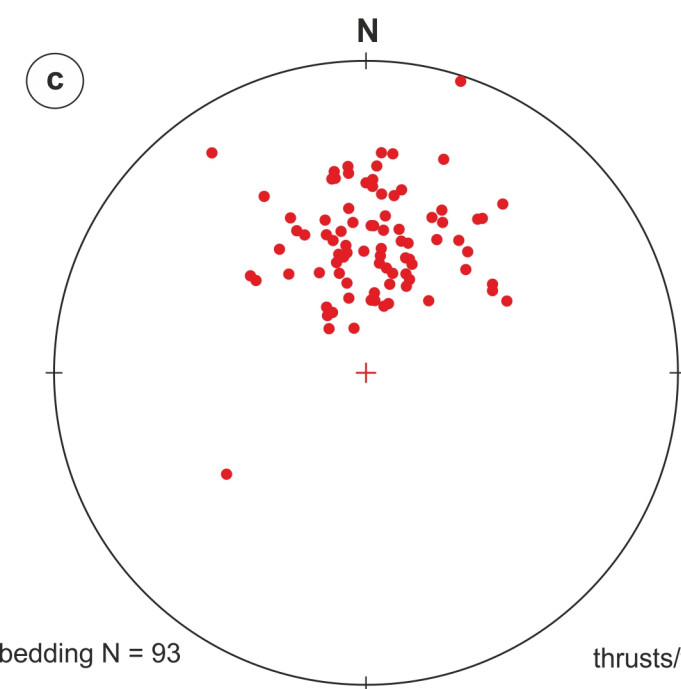
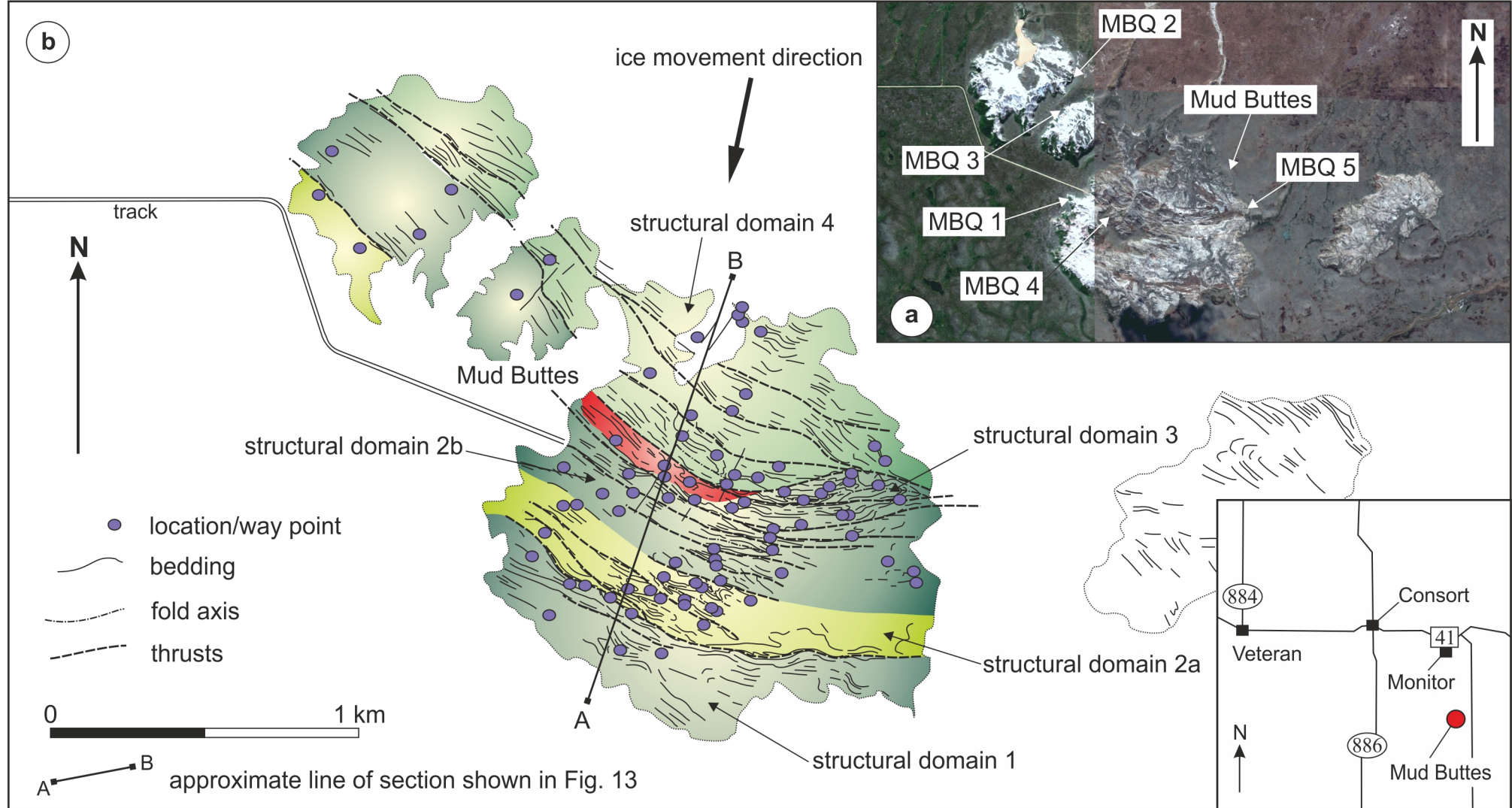
1244

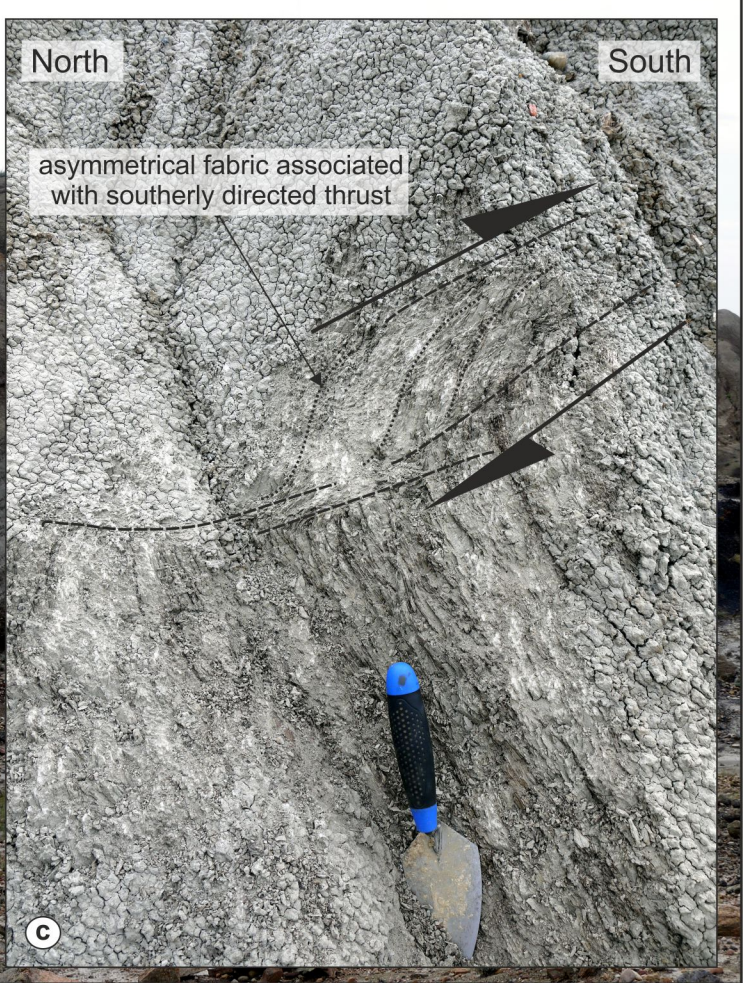
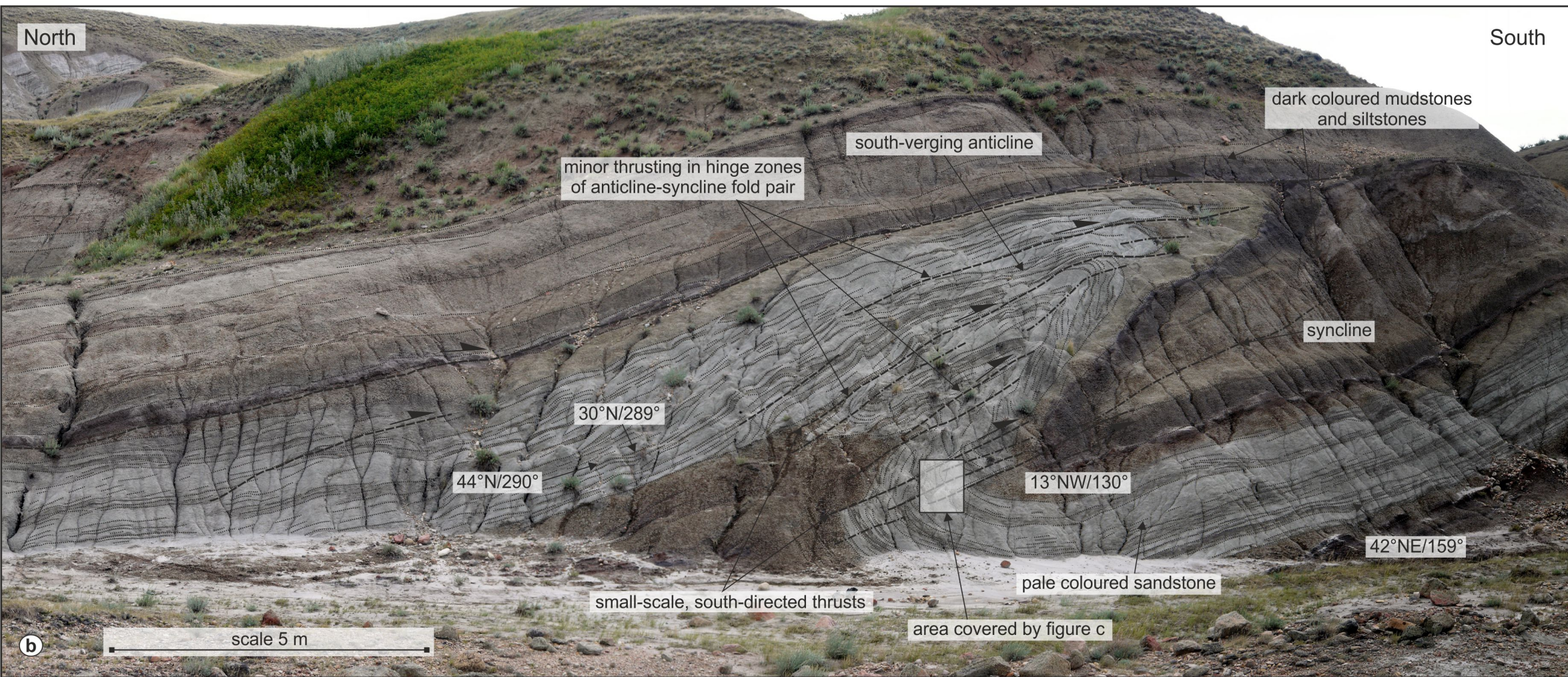
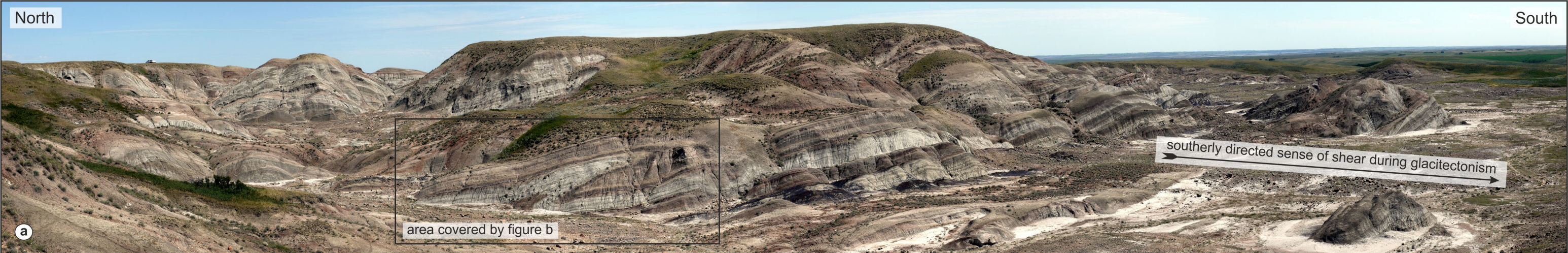




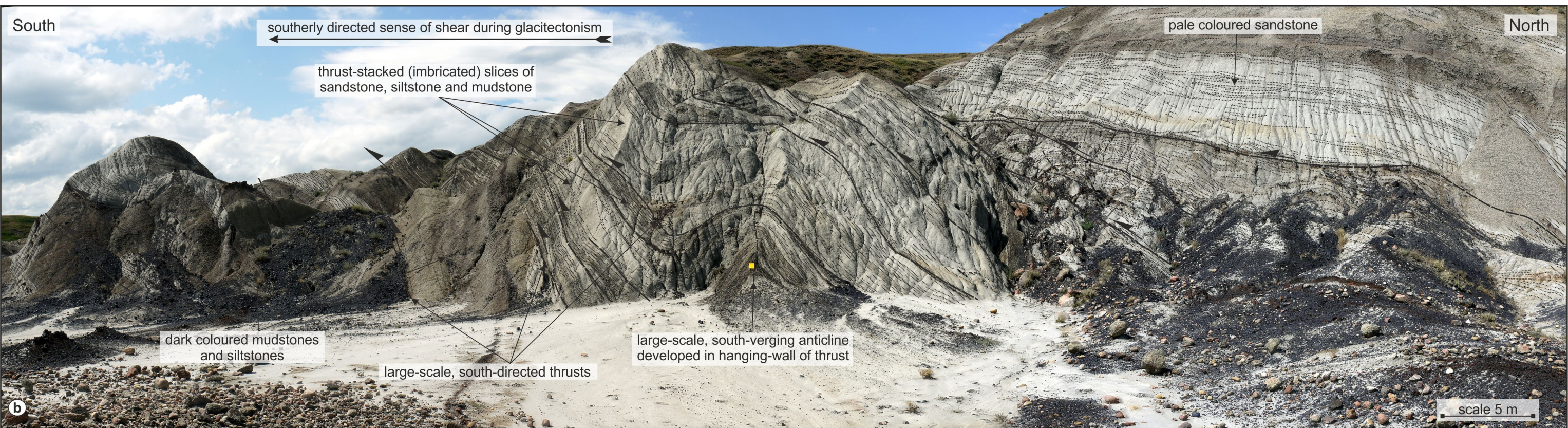
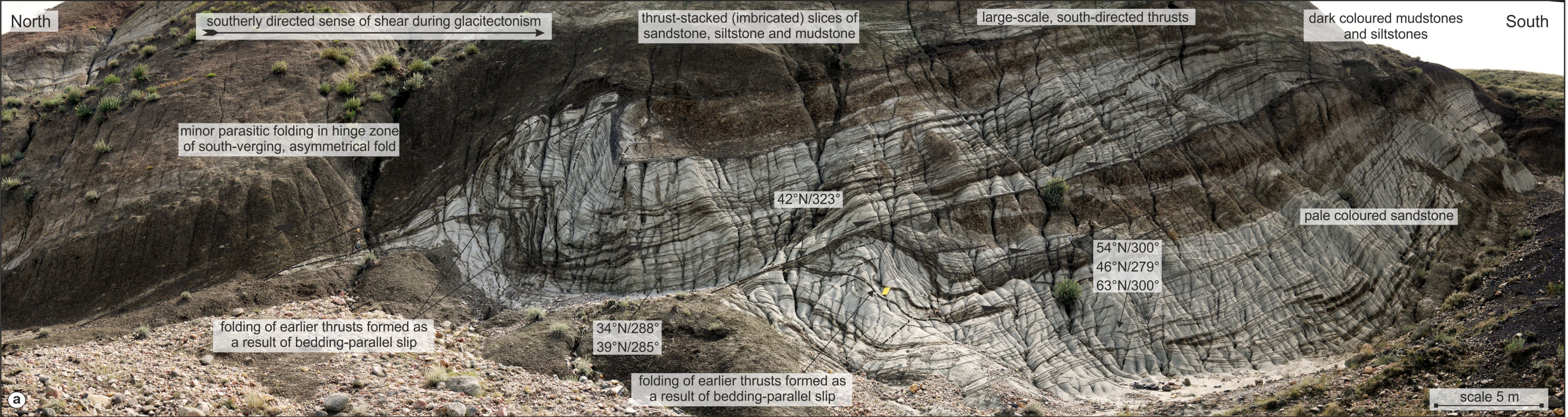




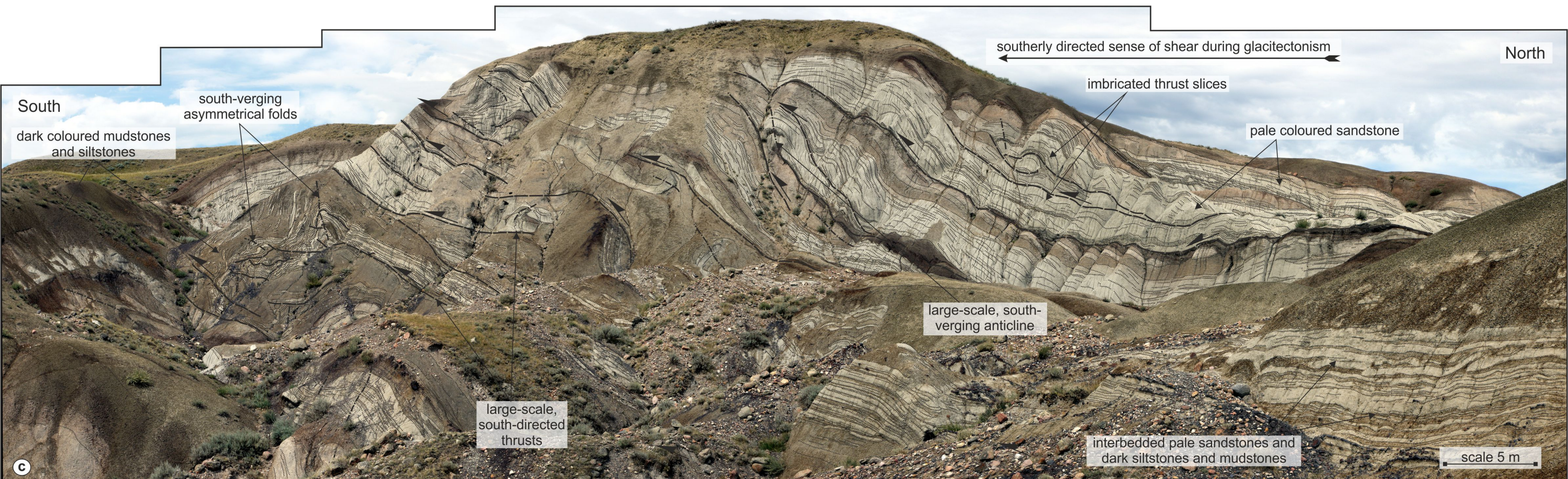
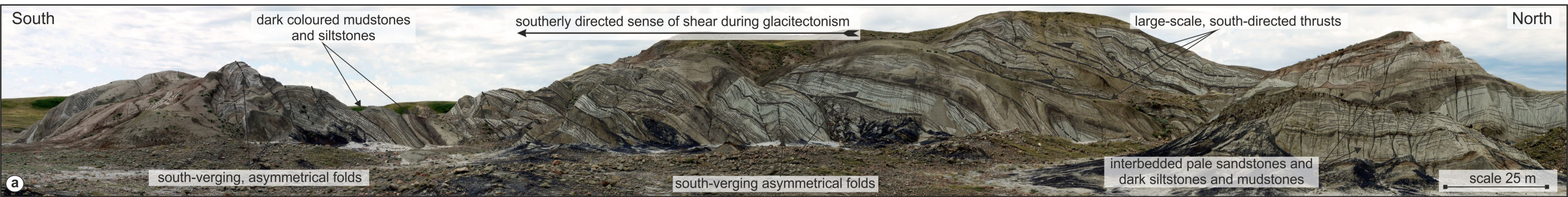




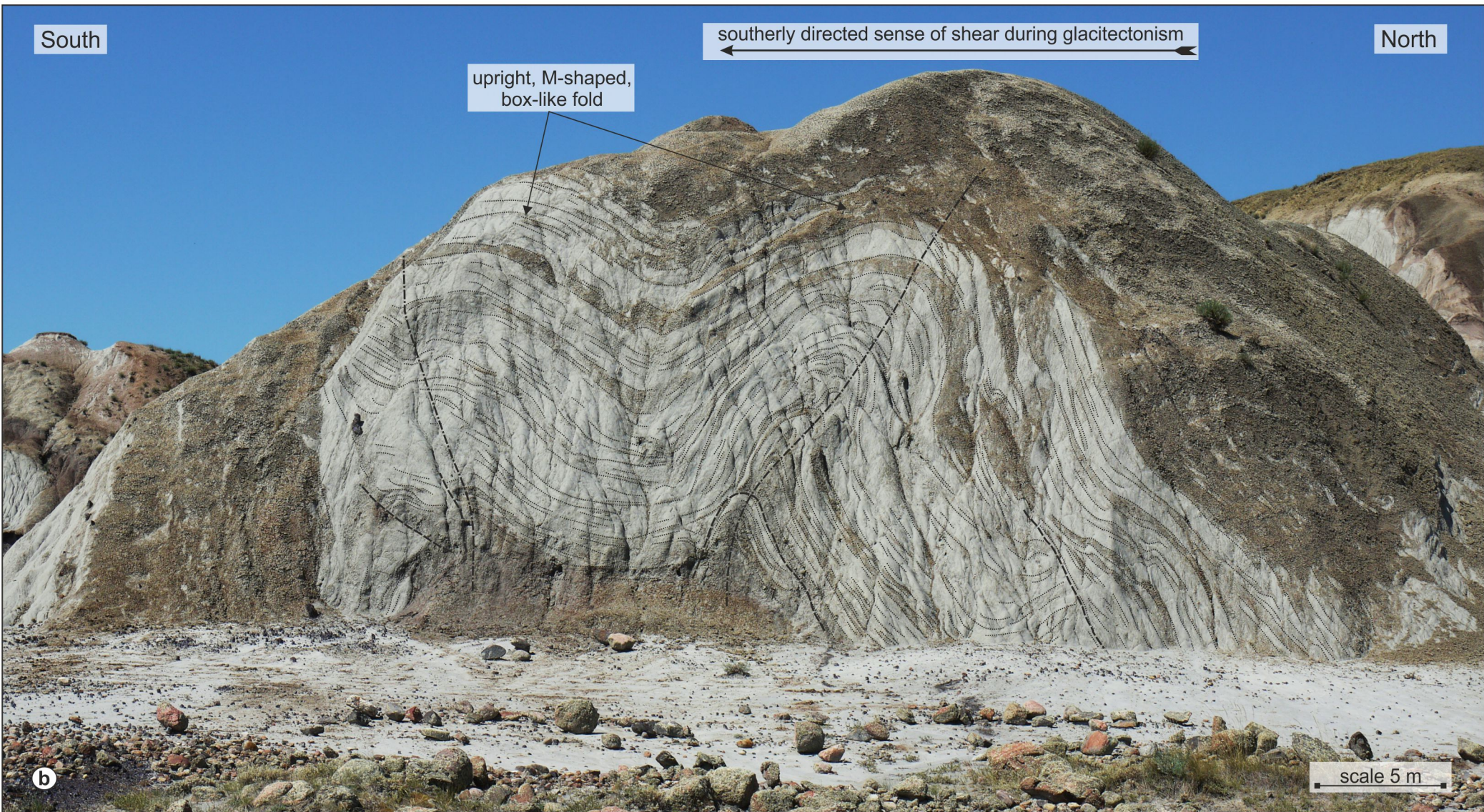
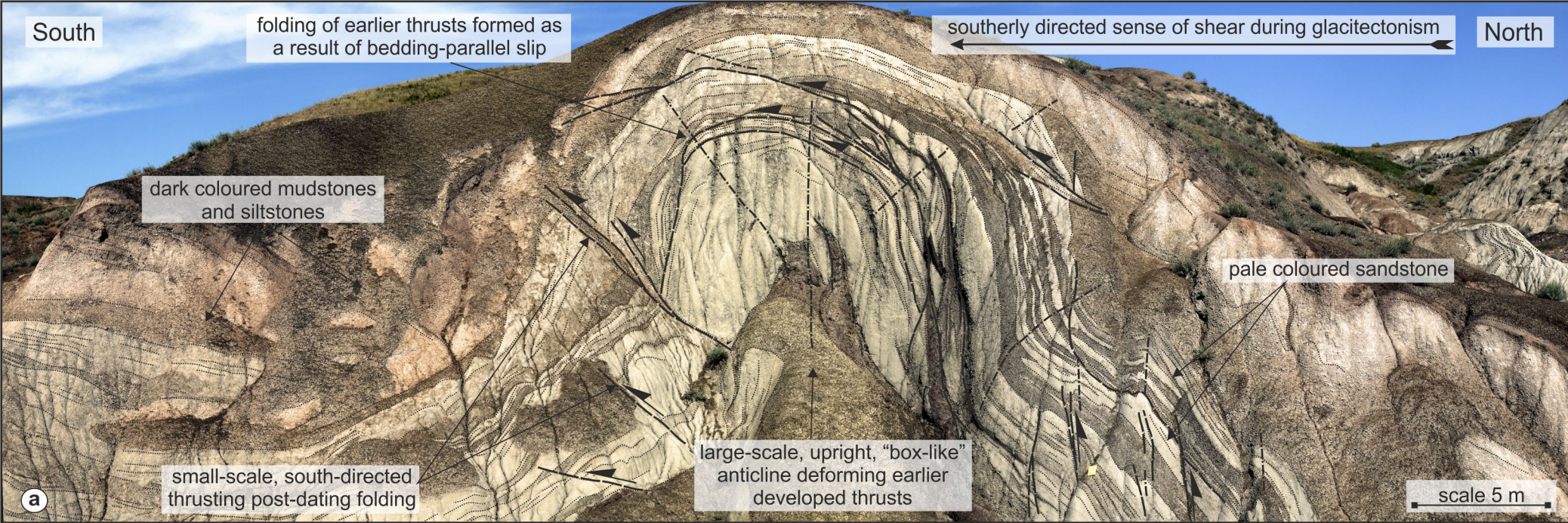
----- thrusts - - - - - fold axes bedding ◀ sense of shear/displacement



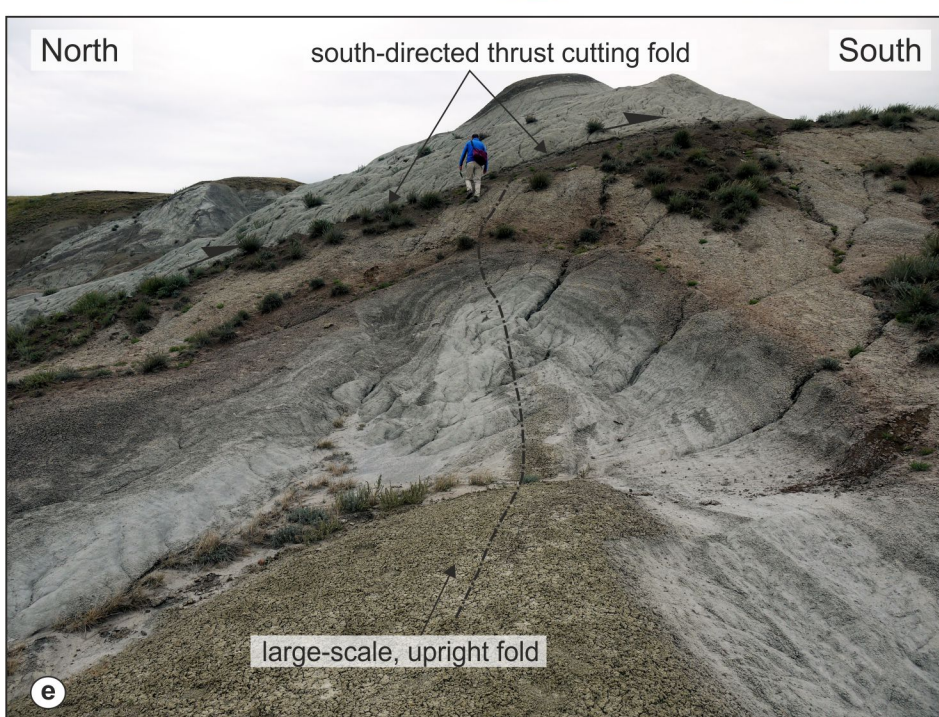
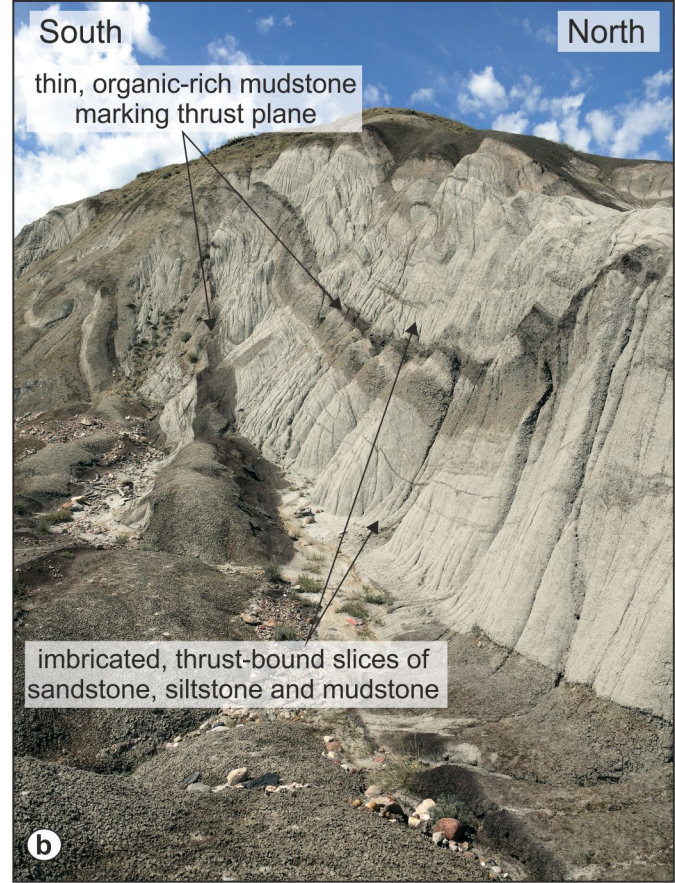
----- thrusts - - - - - fold axes bedding ◀ sense of shear/displacement



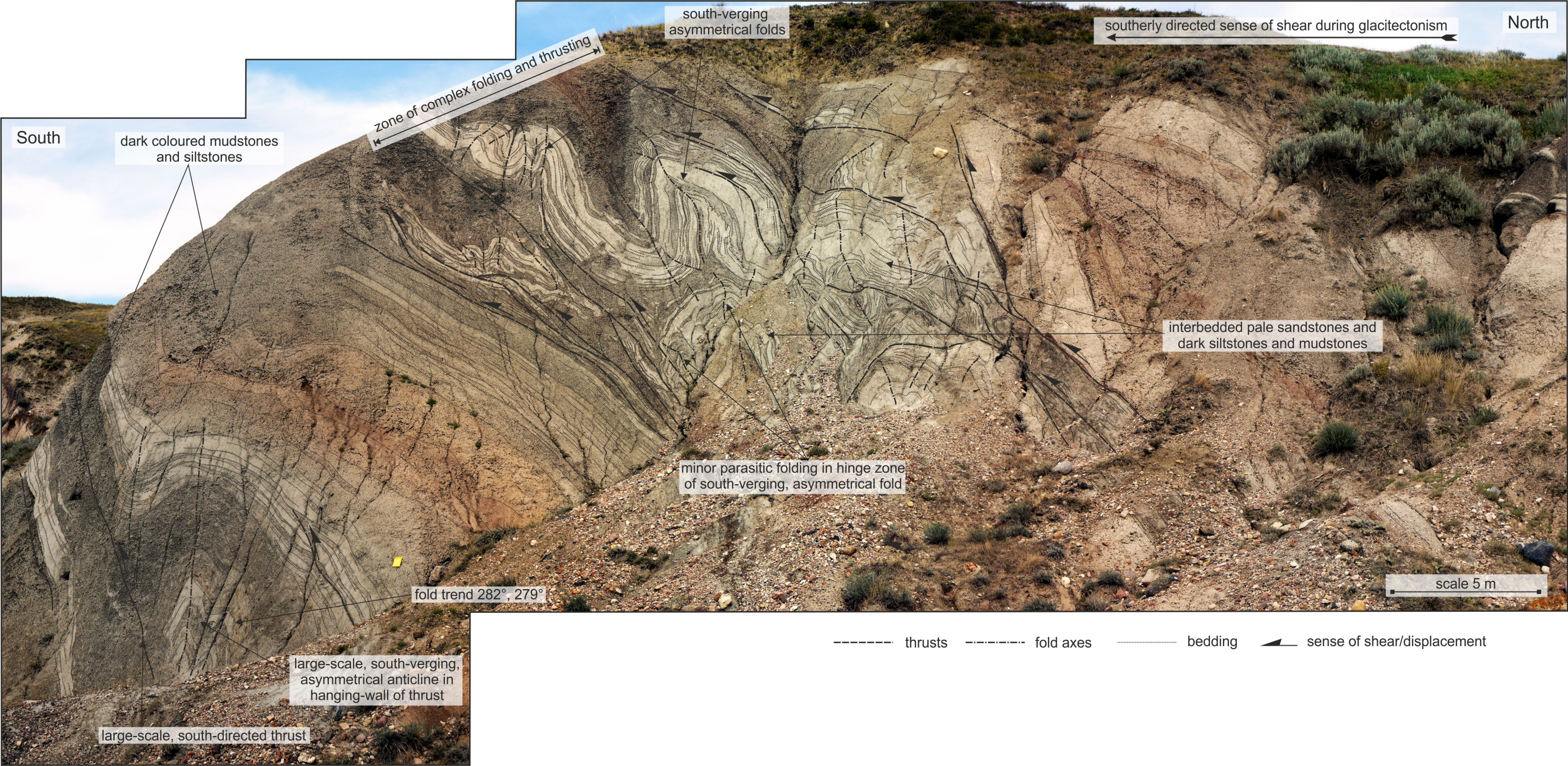
----- thrusts - - - - - fold axes bedding ◀ sense of shear/displacement



- - - - - thrusts - - - - - fold axes - - - - - bedding ◀ sense of shear/displacement



----- fold axes ◀ sense of shear/displacement



North

southerly directed sense of shear during glacitectonism

south-verging asymmetrical folds

zone of complex folding and thrusting

South

dark coloured mudstones and siltstones

interbedded pale sandstones and dark siltstones and mudstones

minor parasitic folding in hinge zone of south-verging, asymmetrical fold

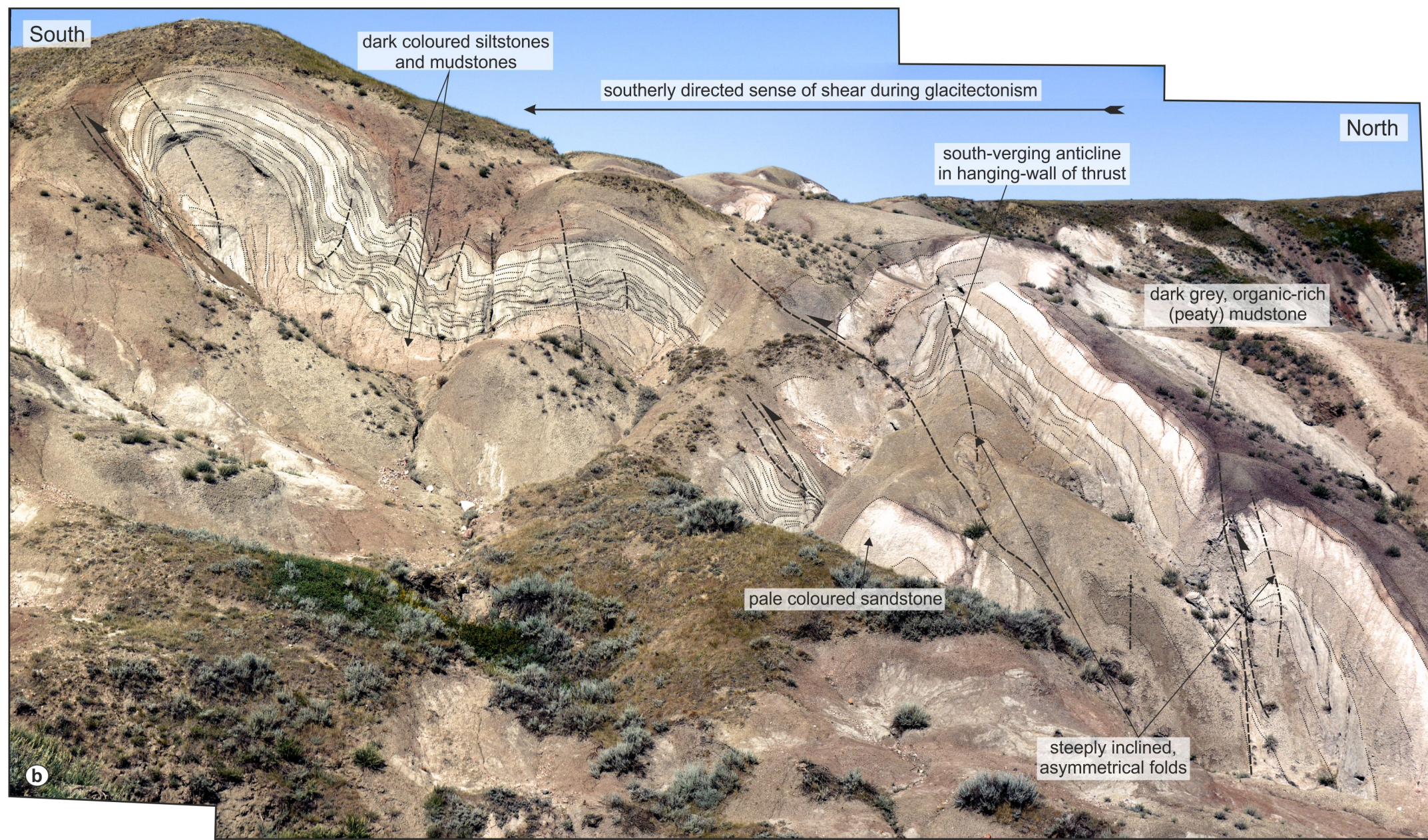
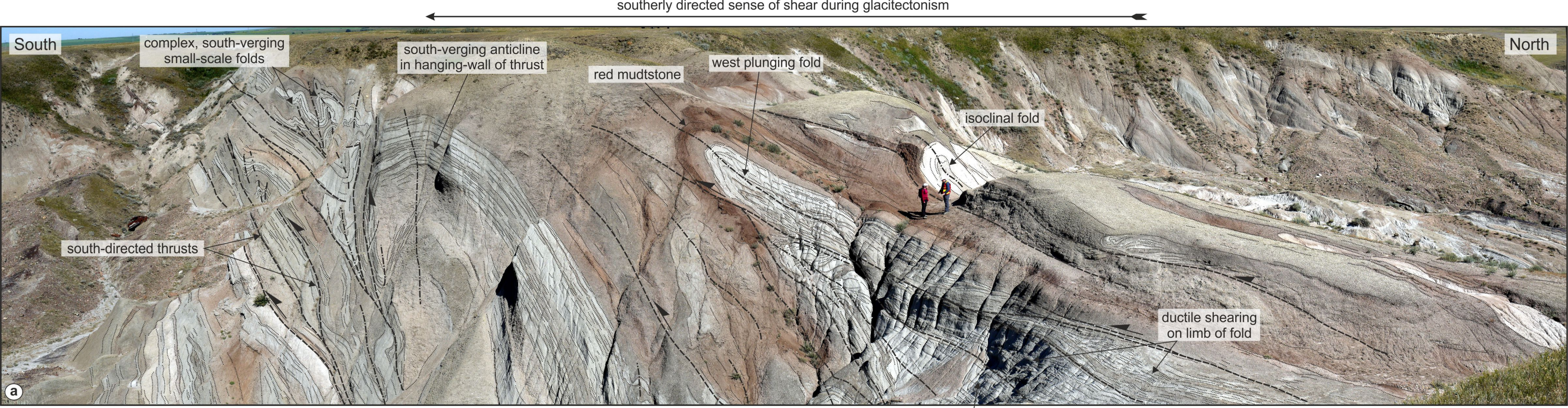
fold trend 282°, 279°

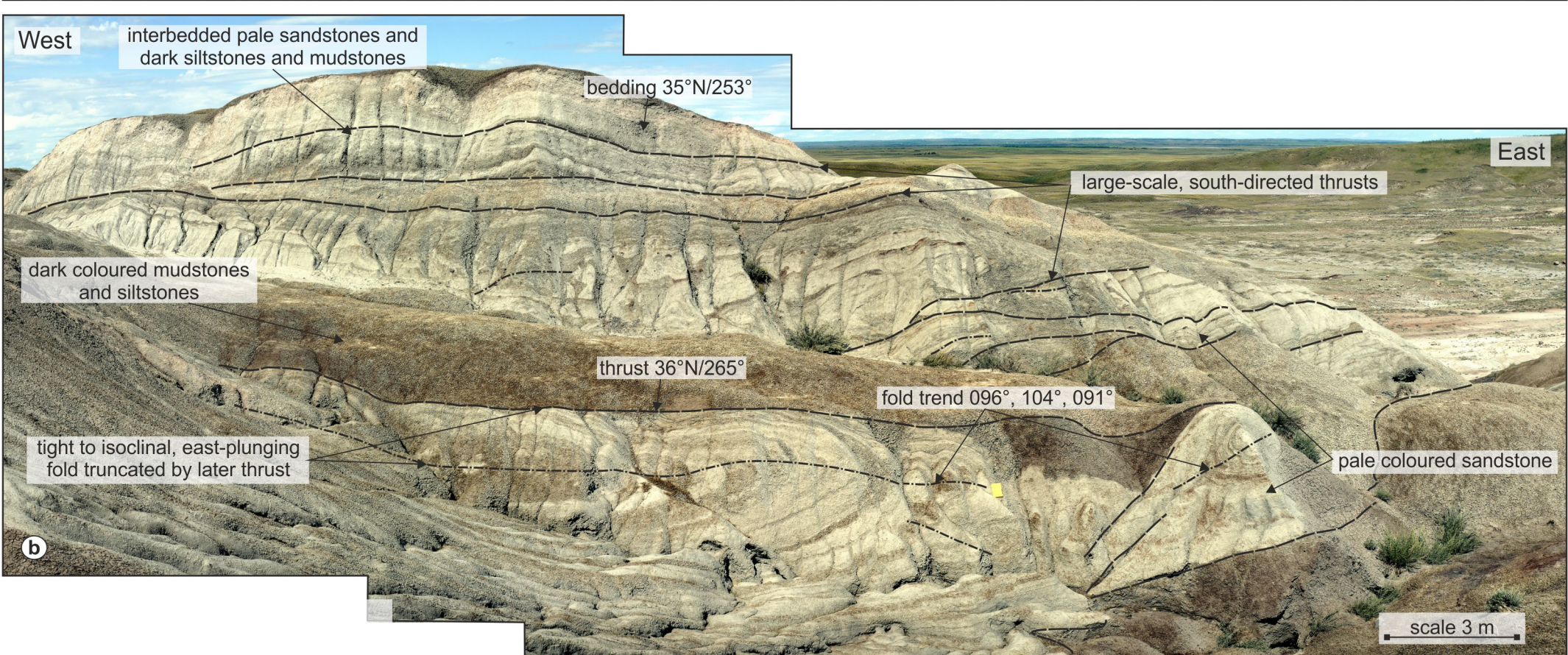
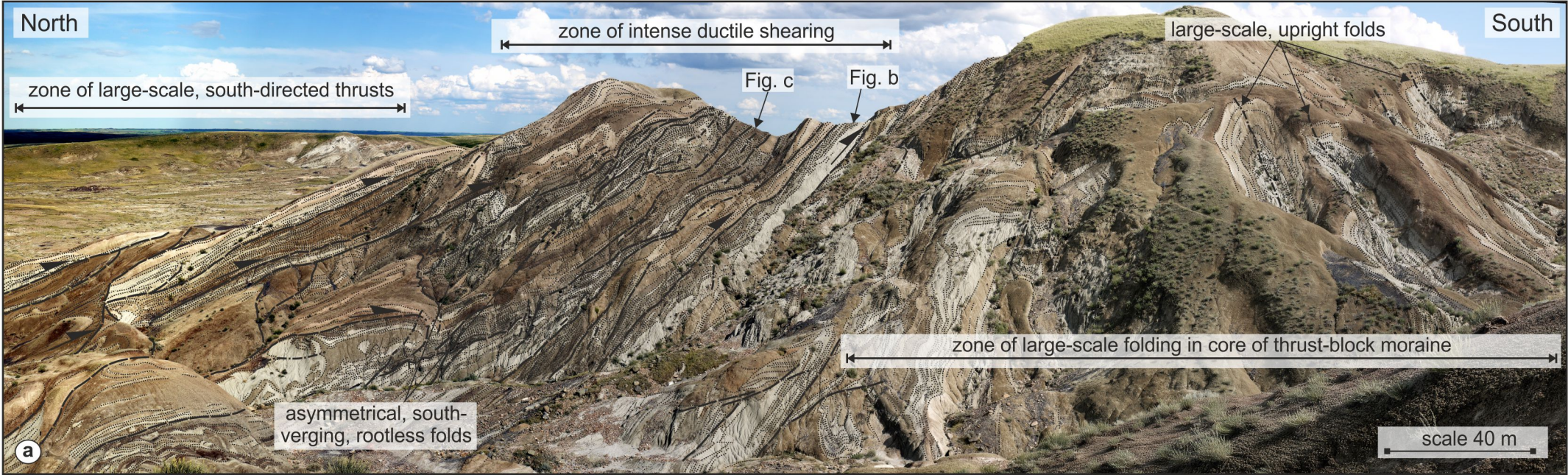
scale 5 m

large-scale, south-verging, asymmetrical anticline in hanging-wall of thrust

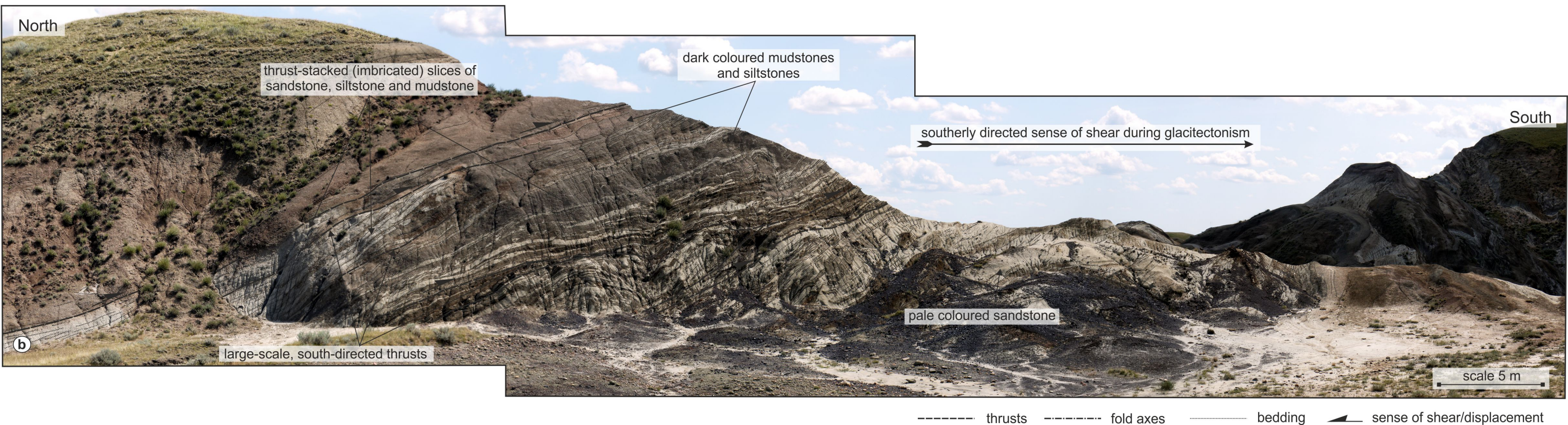
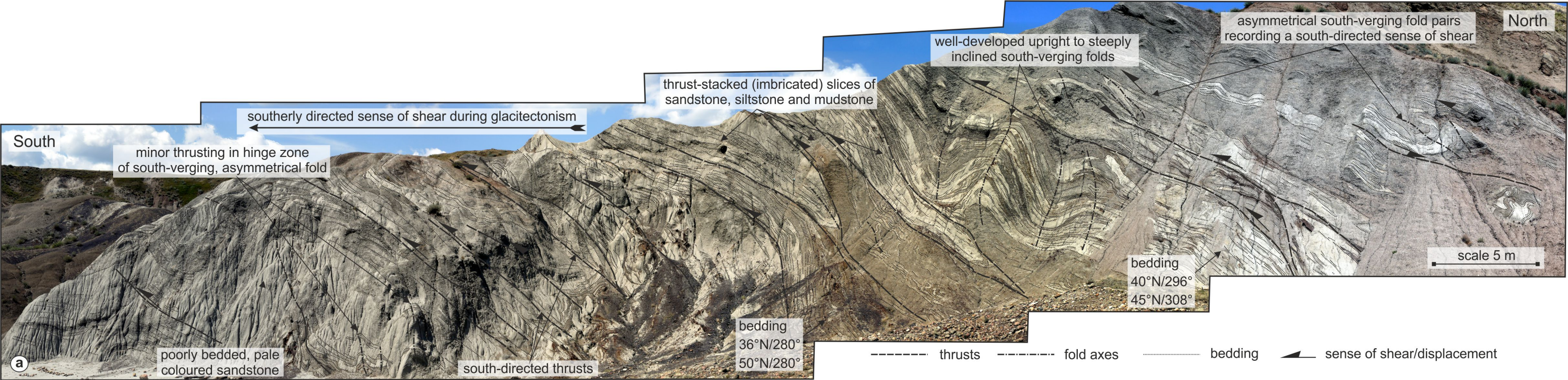
large-scale, south-directed thrust

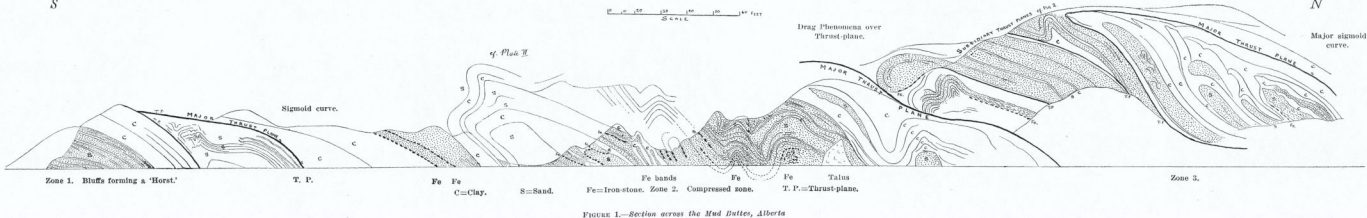
----- thrusts - - - - - fold axes bedding ▲ sense of shear/displacement



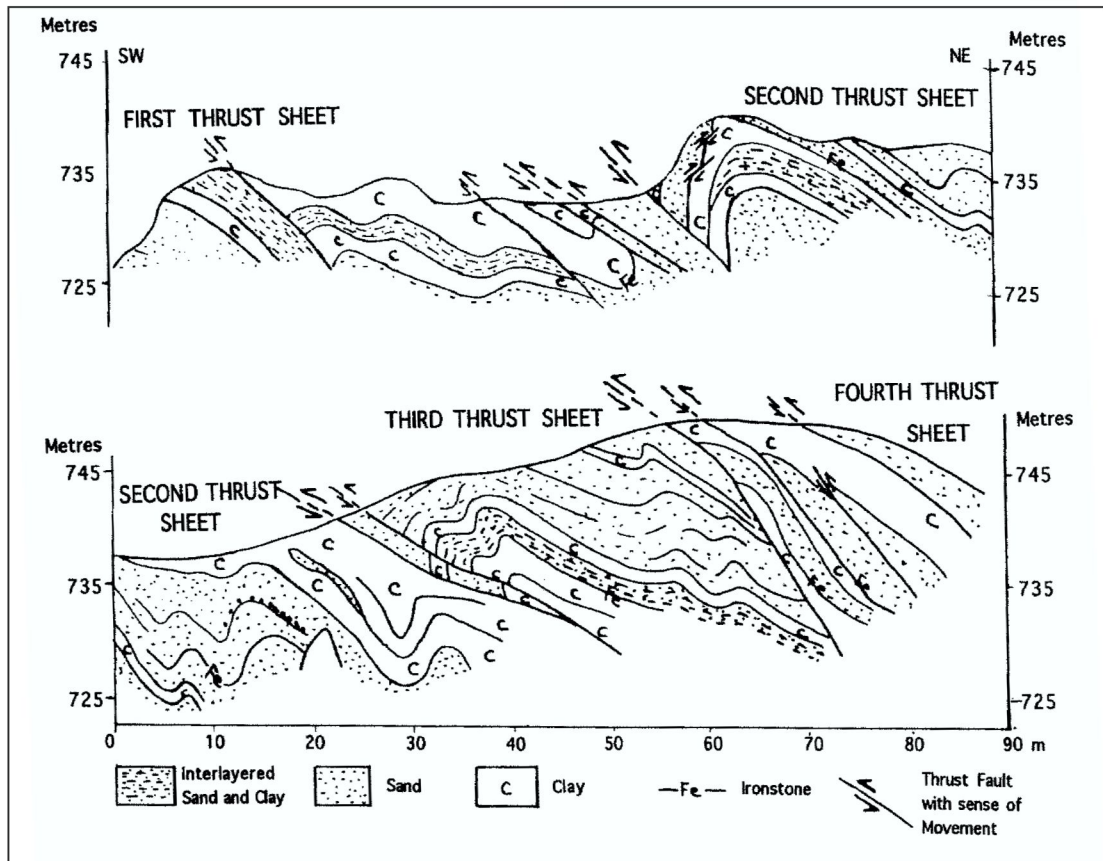


- - - - - thrusts - - - - - fold axes bedding ◀ sense of shear/displacement





a



b

Section MBQ 1

Clay-rich Dmm with indurated crumbly structure & numerous gypsum nodules

Contorted & attenuated sand & sandy, fine gravel lenses (interdigitated with overlying & underlying Dmm)

Clayey silt Dmm + numerous rotten sandstone clasts, clay intraclasts & smudged intraclasts (Type III melange)

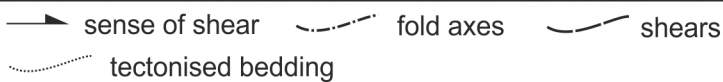
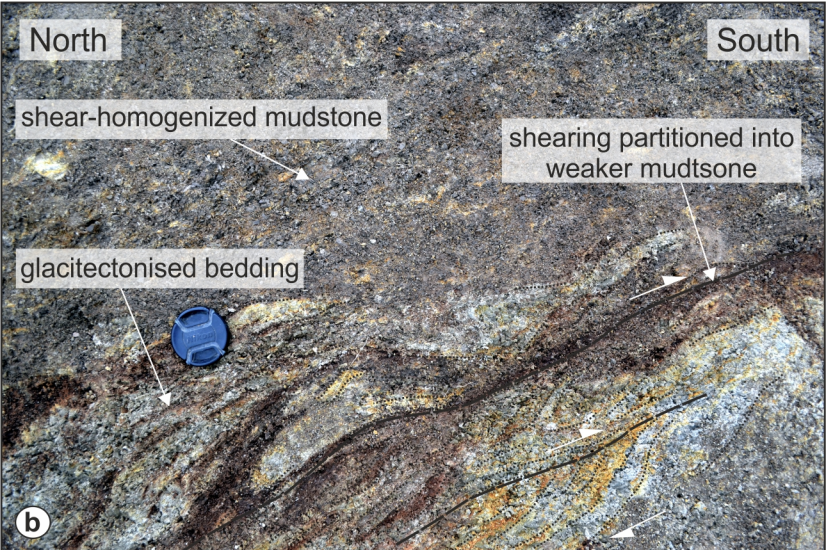
Pale grey silty sandstone + gypsum nodules (bedrock)

30cm

42cm

92cm



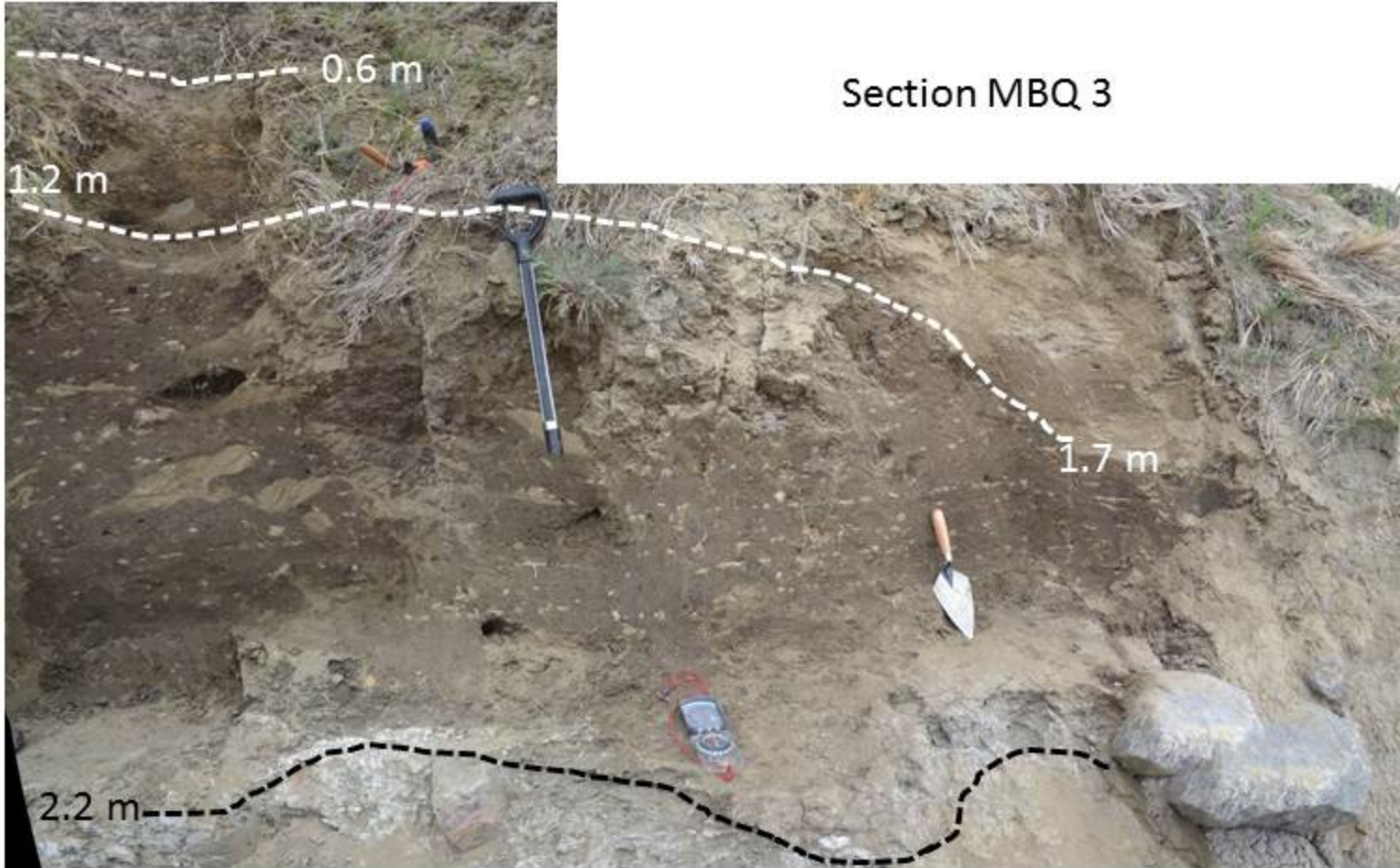


Clay rich Dmm (massive blocky structure & gypsum nodules)

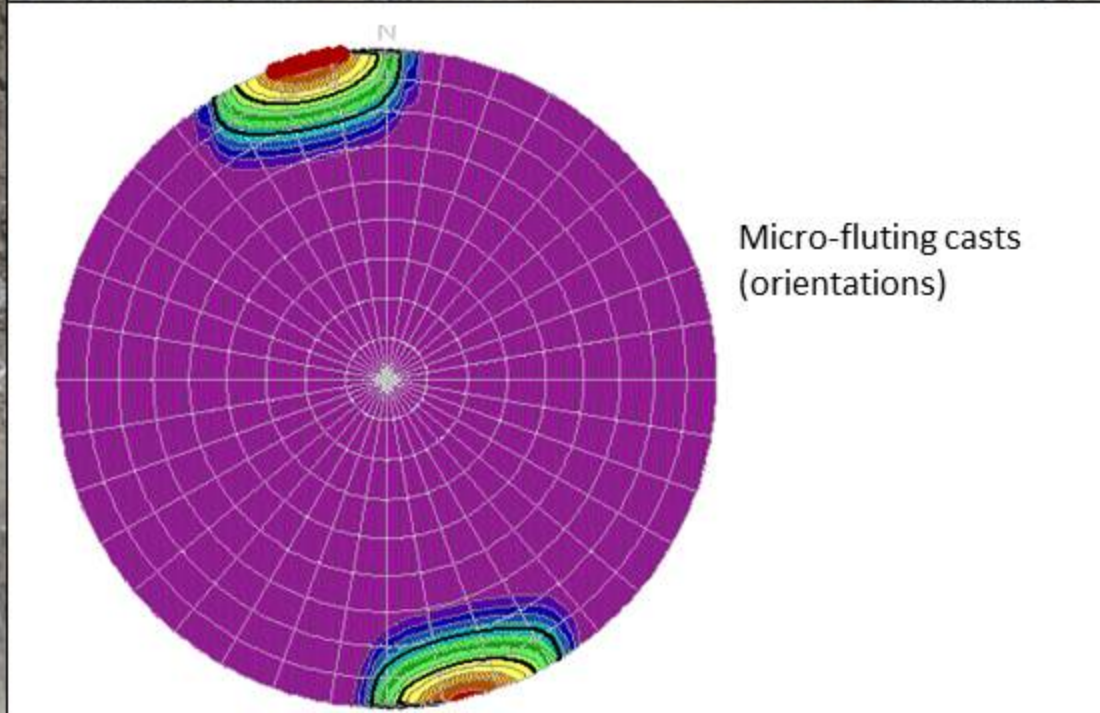
Heterogeneous diamicton (crudely bedded horizontal sands, sandy gravel, silts and clay + Dmm). Well to very highly deformed (Type III-IV melange).

0.5-1m of clayey-silt Dmm with rotten sandstone clasts (in discrete lines in basal 50cm) + sandstone boudins with deformed laminated (fine sand to silt) bedding (Type III & IV melange)

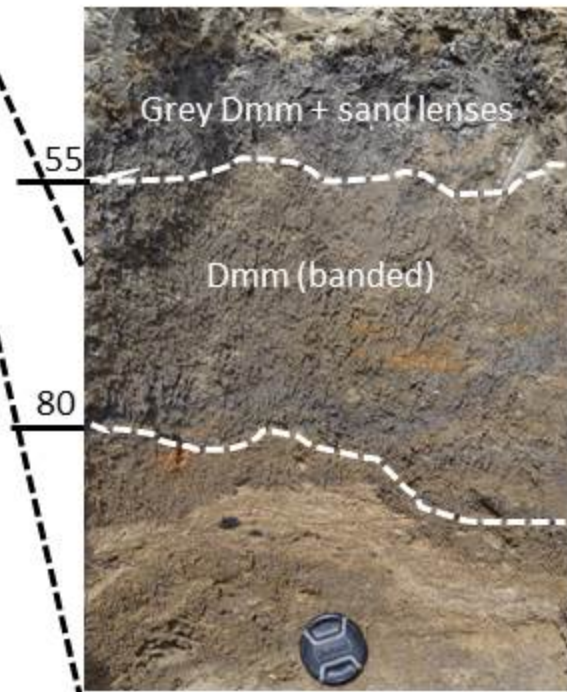
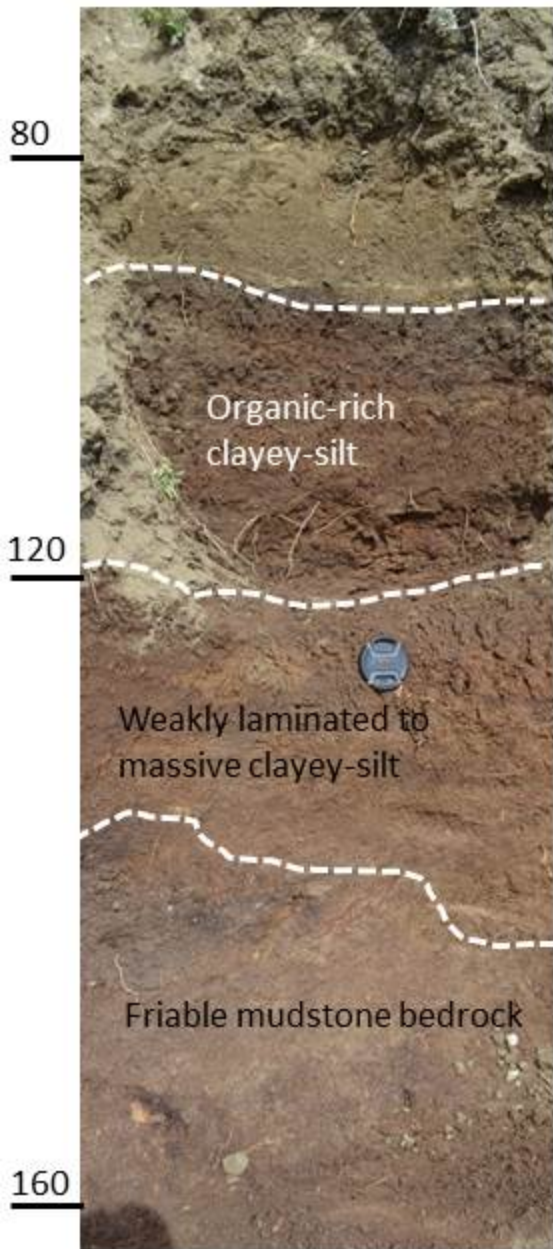
Silty sand bedrock & discontinuous boulder pavement + microfluting sole casts



Section MBQ 3

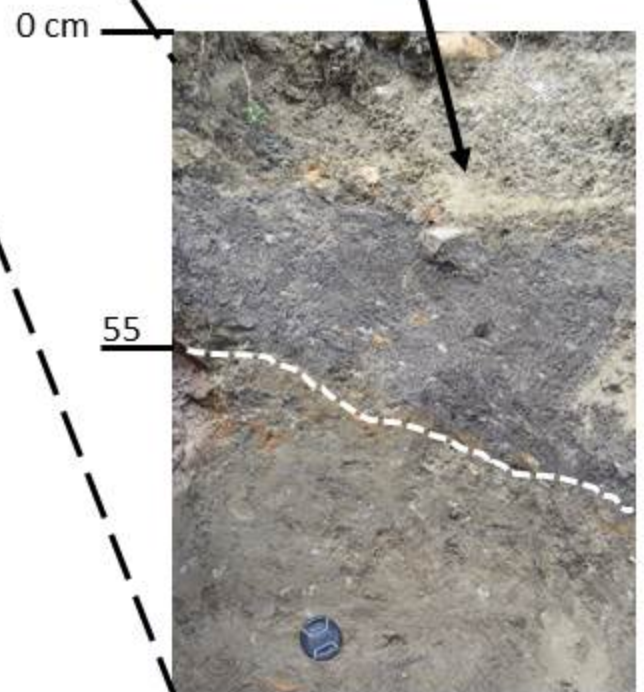
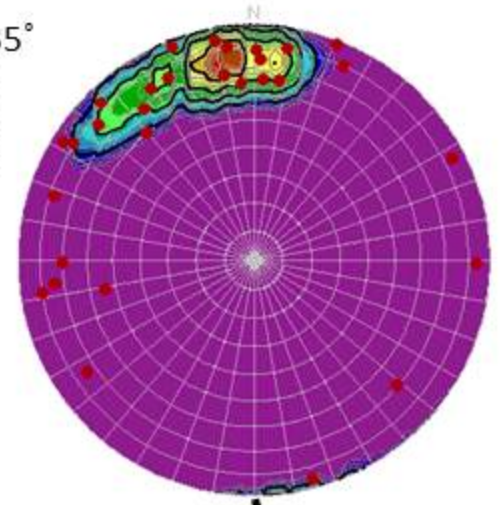


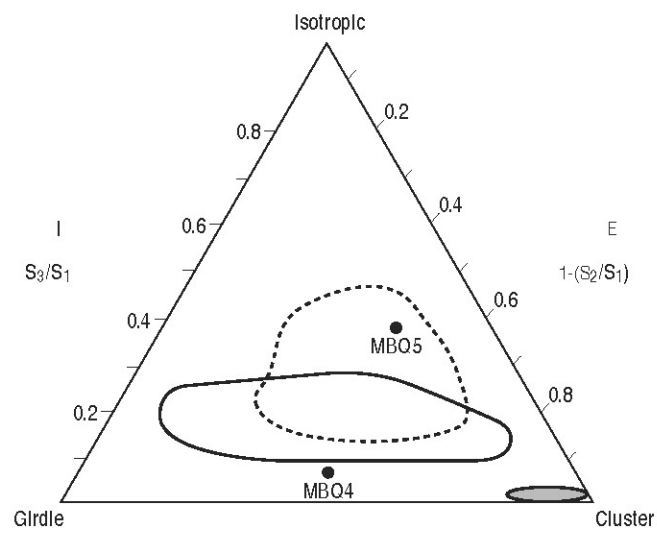
Section MBQ 4



Clay-rich brown Dmm + deformed sand lenses & wisps (Type II melange)

MLA = 335°
 $S_1 = 0.63$
 $S_2 = 0.33$
 $S_3 = 0.04$



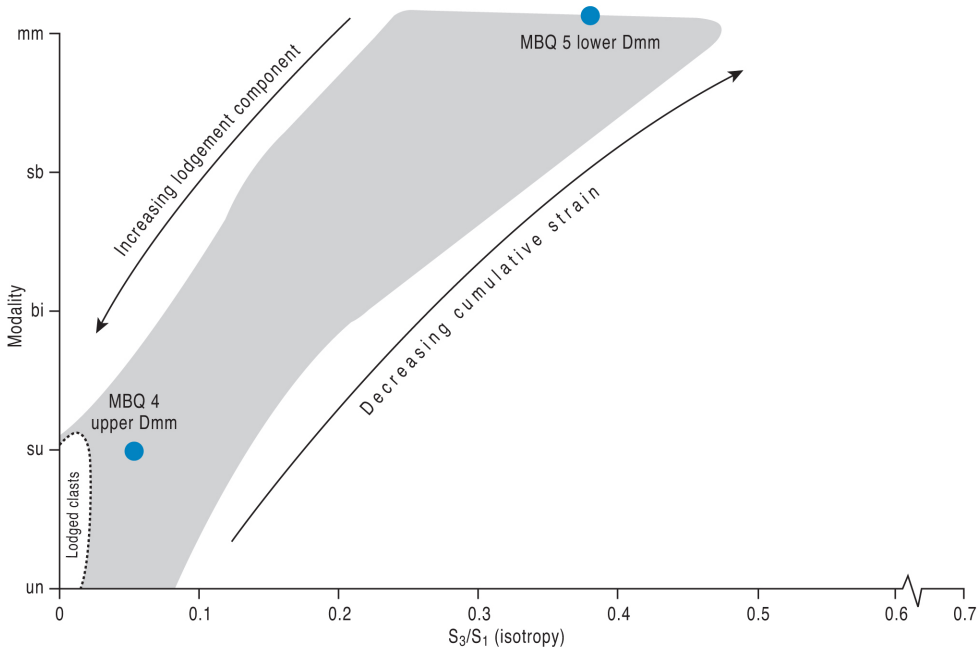


— Glactectonite continuum (Evans et al 1998)

- - - Subglacial till (Evans and Hlemstra 2005)

○ Lodged clasts (Evans and Hlemstra 2005)

A-axes



Clay-rich Dmm with blocky structure (0 - 60 cm)

60 cm

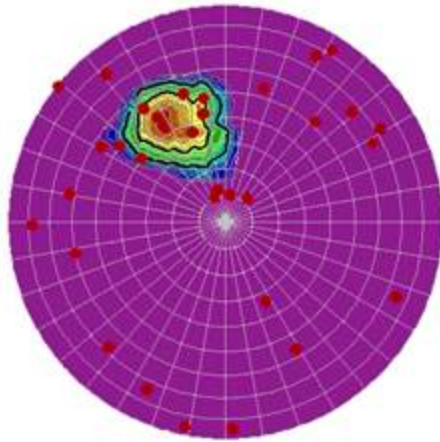
Clayey silt Dmm with rotten sand clasts and lenses (boudins) occurring in discrete horizontal lines + short, discontinuous sandy stringers

MLA = 347°

$S_1 = 0.52$

$S_2 = 0.29$

$S_3 = 0.19$



125 cm

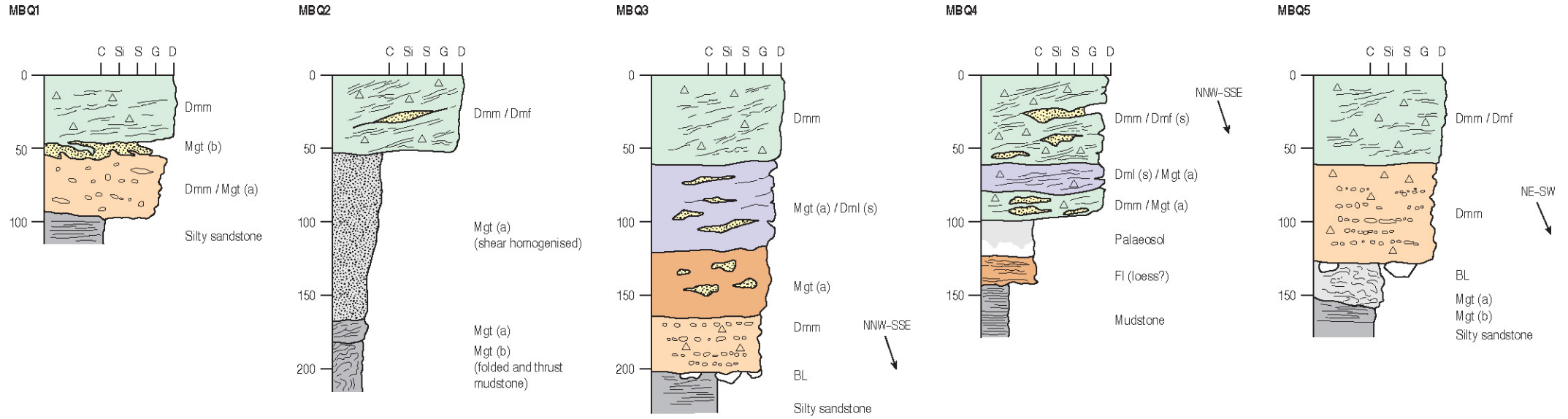
Contorted Cretaceous strata (including folded silt, sand & clay laminae & organic units & less deformed, coherent sandstone blocks). Type III melange surrounding lodged boulders that form a clast line/pavement

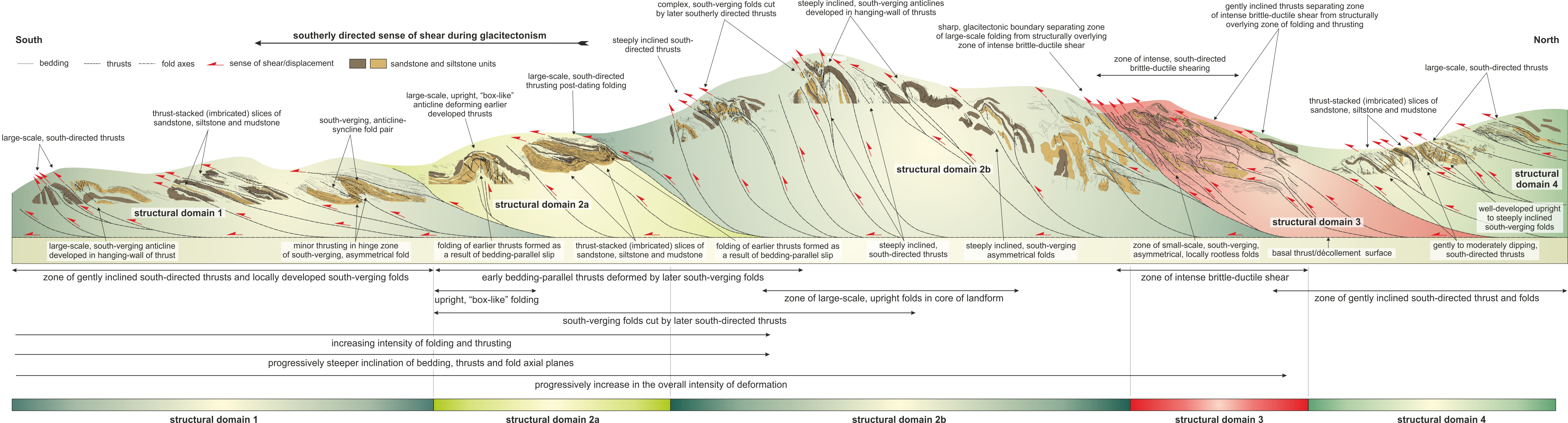
145 cm

Section MBQ 5

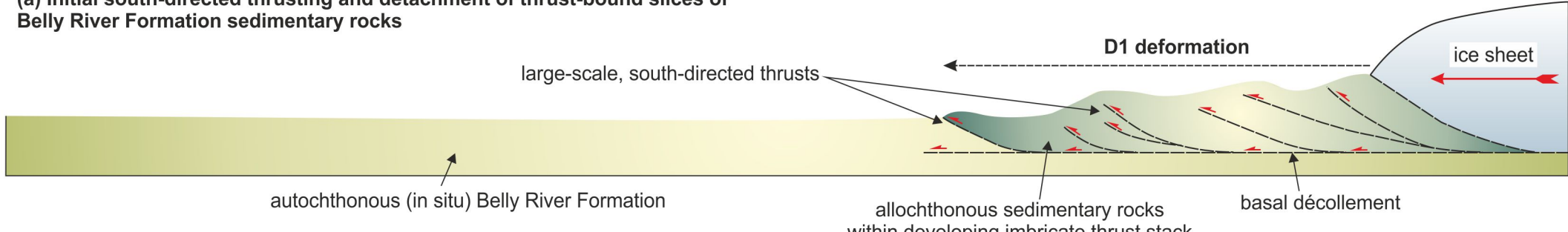


Figure Q7

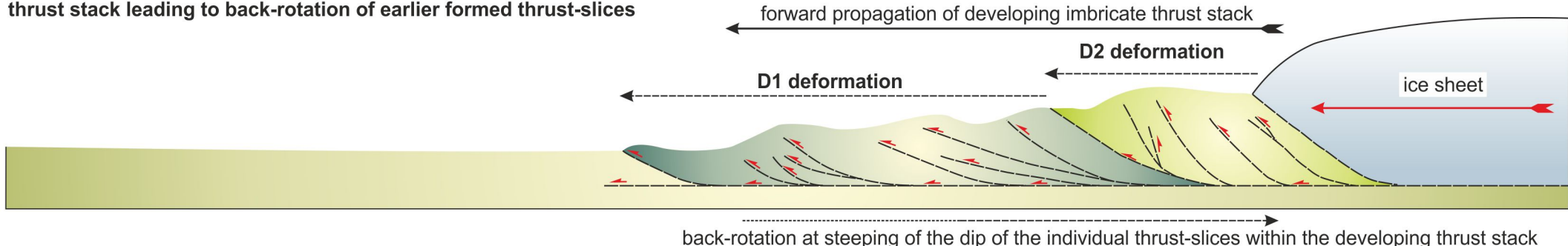




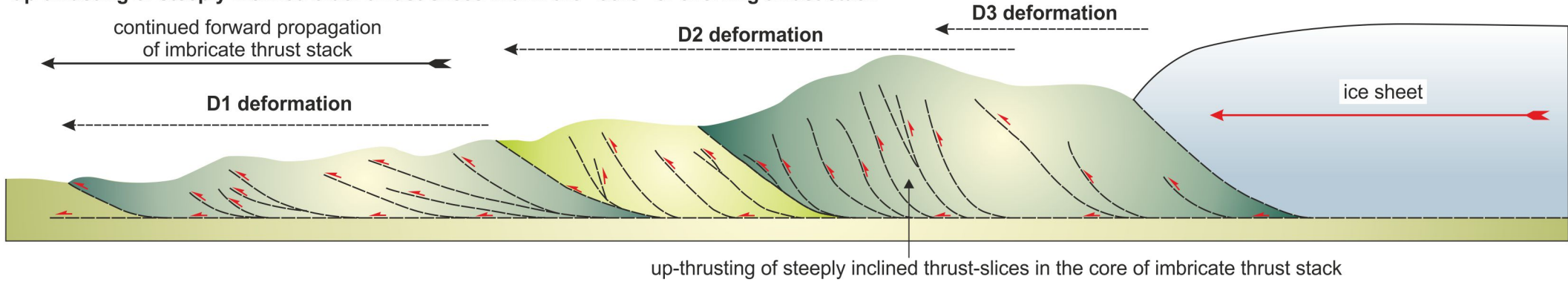
(a) Initial south-directed thrusting and detachment of thrust-bound slices of Belly River Formation sedimentary rocks



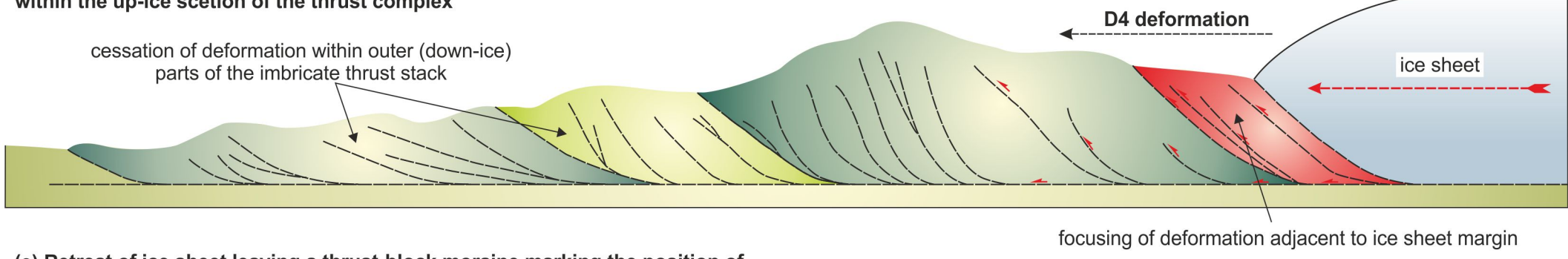
(b) Continued south-directed thrusting and forward propagation of imbricate thrust stack leading to back-rotation of earlier formed thrust-slices



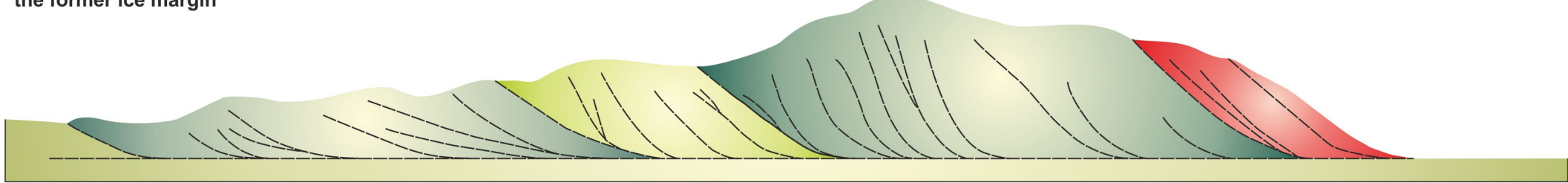
(c) Continued south-directed thrusting and forward propagation of imbricate thrust stack, up-thrusting of steeply inclined older thrust-slices within the "core" of evolving thrust stack



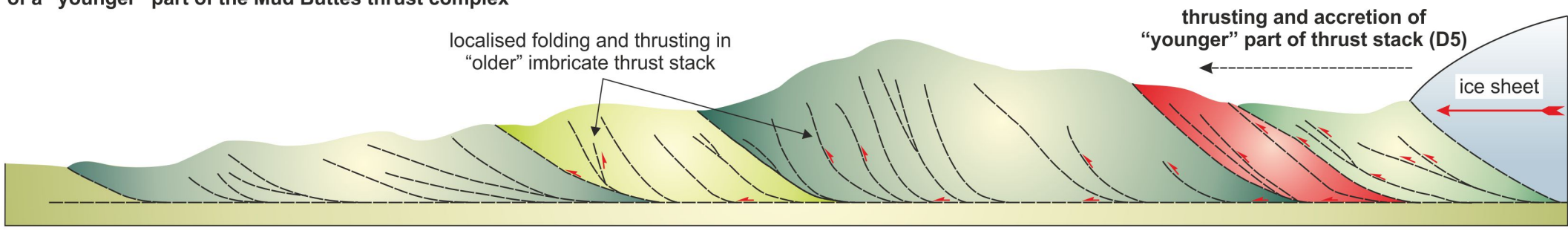
(d) "Locking up" of imbricate thrust stack with the focusing of deformation within the up-ice section of the thrust complex



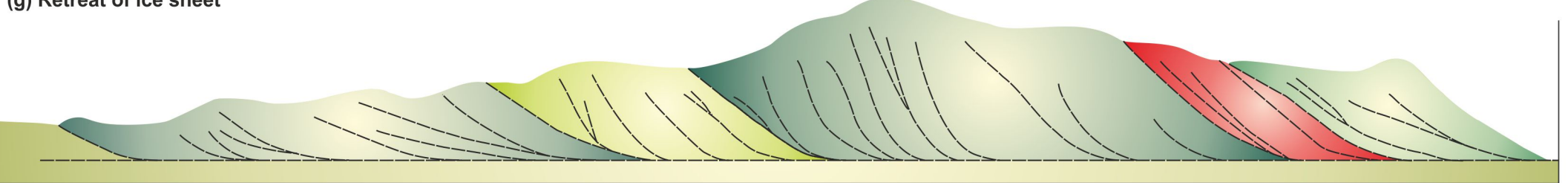
(e) Retreat of ice sheet leaving a thrust-block moraine marking the position of the former ice margin



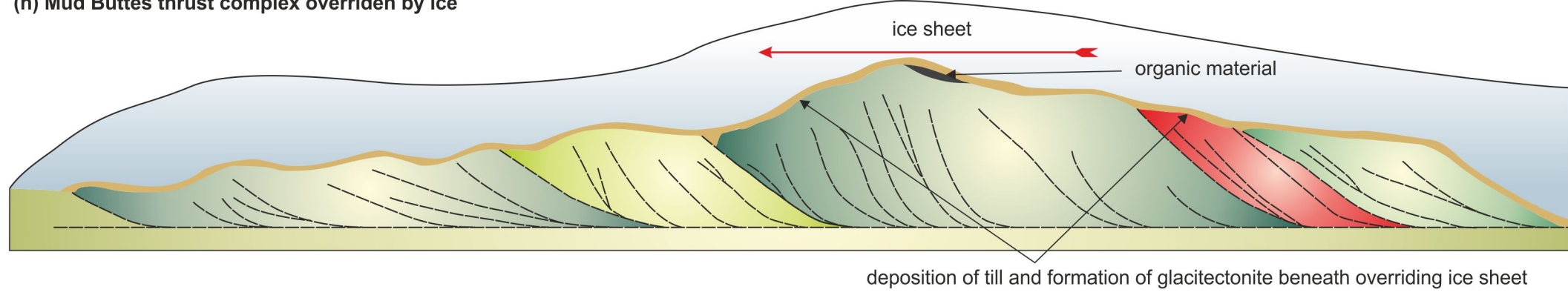
(f) Later readvance of the ice sheet leading to later phase of thrusting and accretion of a "younger" part of the Mud Buttes thrust complex



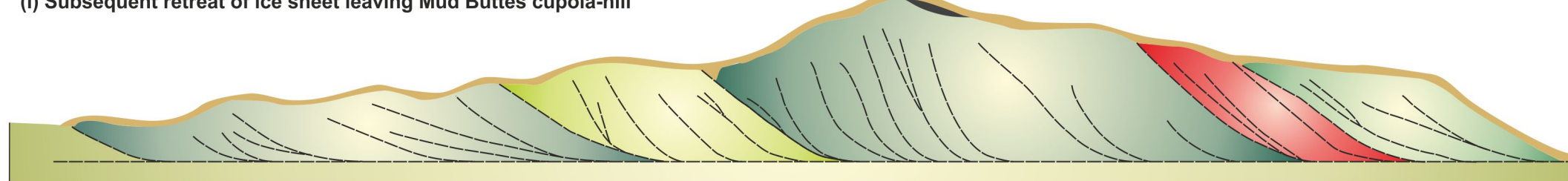
(g) Retreat of ice sheet





(h) Mud Buttes thrust complex overridden by ice



(i) Subsequent retreat of ice sheet leaving Mud Buttes cupola-hill



----- thrusts  sense of displacement on thrusts  ice movement direction